



**Development of a self-assembling modular catalyst and
its application in the Morita-Baylis-Hillman reaction.**

Andrew Holohan, B. Sc. (hons)

Under the supervision of Dr. Christopher O'Brien

A thesis presented to Dublin City University
for the degree of Master of Science

School of Chemical Sciences

Dublin City University

January 2014

Acknowledgments

I would like to thank my supervisor, Dr. Christopher O'Brien for giving me this opportunity to work and study in his research group. I thank him for his motivation, enthusiasm, and immense knowledge, coupled with his ability to get the best out of me as a chemist.

I want to thank my lab mates Bryan and Steve for endless laughter, friendship and unique generosity throughout the whole process.

Emma and Florie for their constant advice, support and encouragement during my time in the lab.

The NMR studies would not have been possible without the help of Bing Wu and Dr. Dermot Brougham, thank you both for your constant support.

I would also like to thank all the technical staff in the School of Chemical Sciences at DCU for their constant assistance.

I also want to thank my family for the constant encouragement and sacrifices made over the years for me.

Abstract

The Morita-Baylis-Hillman (MBH) reaction is one of most synthetically versatile carbon-carbon bond-forming reactions. It has been used to generate building blocks for synthesis of many heterocycles, drug molecules and natural products. This reaction facilitates the coupling of an aldehyde (or activated ketone) with an electron deficient alkene, catalysed by nucleophilic bases (tertiary amines or phosphines). Each MBH adduct contains several functional groups with the potential to undergo a variety of organic transformations involving regio- and stereochemical control.

Recently, considerable efforts have been dedicated to the development of asymmetric MBH/aza-MBH reactions. Significant progress have been made in the design and synthesis of new chiral catalysts based on the concept of bi/ multifunctionality achieving high enantioselectivity.

However, as of yet there is no single catalyst which is capable of tolerating a broad range of substrates. Thus, the development of effective catalysts for the asymmetric MBH/aza-MBH reactions that are applicable to all or at least to most of the commonly used activated alkenes and electrophiles is of the utmost importance.

The primary objective of this project was to realise the development of an effective stereoselective MBH catalyst. In our novel system, a Catalytic Module, CM (with both a catalytic centre and a component at which hydrogen-bonding can occur), and a Selectivity Inducing Module, SIM (consisting of both hydrogen-bonding scaffold and a site through which selectivity, such as enantioselectivity, may be induced), were bound through hydrogen-bonding interactions to give a modular catalyst.

The focus of this research was on the design and preparation of this system. Computational modelling was used in the design of the module predicting its interaction. Following design of the modules, they were synthesised using robust organic syntheses to produce both modules. Following synthesis, the catalyst was applied in test MBH reactions for initial catalysis screening.

Table of Contents

ACKNOWLEDGMENTS	I
ABSTRACT	II
TABLE OF CONTENTS.....	III
ABBREVIATIONS	V
1. INTRODUCTION.....	1
1.1. Organocatalysis	1
1.1.2. Lewis Base Catalysis	4
1.1.3. Brønsted Acid Catalysis	6
1.1.4. Bifunctional Acid-Base Catalysis.....	8
1.2. Morita-Baylis-Hillman Reaction.....	9
1.2.1. General Aspects.....	9
1.2.2. Origin and Development	9
1.2.3. Mechanism	11
1.2.4. Catalysis of the Morita-Baylis-Hillman Reaction	17
1.1.3. Aza-Morita-Baylis-Hillman Reaction.....	23
1.3.1. General Aspects.....	23
1.3.2. Mechanism	24
1.3.3. Catalysis of the aza- Morita-Baylis-Hillman Reaction	29
1.4. Self-assembling catalysts	34
1.5. Research Objectives.....	36
References (i)	38
2. Results and Discussion.....	42
2.1. General considerations	42
2.2. Computational studies	43
2.3. Synthetic strategy	45
2.3.1. Synthesis of the CM	46
2.3.3. Synthesis of SIM	50
2.4. Assessment of assembly event	51
2.4.1. Dosy Test.....	52
2.4.2. TV NMR Test.....	53
2.4.3. Simple Chemical Shift Demonstration Test	54
2.4.4. Hydrogen bonding equilibrium disturbing test by NMR	55

2.5. Catalytic rate studies.....	56
2.6. Conclusion.....	59
2.6.1. Outlook.....	59
References (ii)	60
EXPERIMENTAL	61
General.....	61
Preparation of the CM and SIM modules.....	61
Catalytic studies.....	69
References (iii)	90

Abbreviations

Ac	Acetyl
ACN	Acetonitrile
Å	Ångstrom
aq.	Aqueous
Ar	Aryl
BINOL	1, 1'-Bi-2-naphthol
B3LYP	Becke, 3-parameter, Lee-Yang-Parr
Bn	Benzyl
Bu	Butyl
Cat.	Catalyst
conv.	Conversion
CPME	Cyclopentyl methyl ether
D	Deuterium
DABCO	1, 4-Diazabicyclo [2.2.2] octane
DBU	1, 8-Diazabicyclo [5.4.0] undec-7-ene
DCM	Dichloromethane
DFT	Density functional theory
DMAP	4-(Dimethylamino) pyridine
DMF	Dimethylformamide
DMSO	Dimethyl sulfoxide
ee	Enantiomeric excess
ESI-MS/MS	Electron spray ionisation with tandem mass spectrometry
eq.	Equivalent
Et	Ethyl
EVK	Ethyl vinyl ketone
EWG	Electron-withdrawing group
GC	Gas chromatography
HRMS	High-resolution mass spectrometry
<i>i</i> Pr	<i>iso</i> -Propyl
IR	Infrared
J	Coupling constant
K	Kelvin

KIE	Kinetic isotope effects
LA	Lewis acid
LUMO	Lowest unoccupied molecular orbital
MBH	Morita-Baylis-Hillman
Me	Methyl
MP2	Møller-Plesset perturbation theory
MVK	Methyl vinyl ketone
NBS	<i>N</i> -Bromosuccinimide
RDS	Rate determining step
rt	Room temperature
sat.	Saturated
TADDOL	$\alpha, \alpha, \alpha', \alpha'$ -Tetraaryl-1, 3-dioxolan-4, 5-dimethanol
TEA	Triethylamine
THF	Tetrahydrofuran
TLC	Thin layer chromatography
TMS	Tetramethylsilane
TS	Transition state
UV	Ultraviolet

1. Introduction

1.1. Organocatalysis

Nature utilises weak non covalent interactions like hydrogen bonds, in the construction of three-dimensional biologically active structures, such as DNA, proteins and enzymes. Chemical transformations catalysed by enzymes are central to biology, with these greatly accelerating both the rate and specificity of a reaction. Chemists have interpreted a great deal from the mechanisms of action of enzymes and have applied these principles in the development of new synthetic strategies, inspiring the use of organic molecules as catalysts for organic reactions.

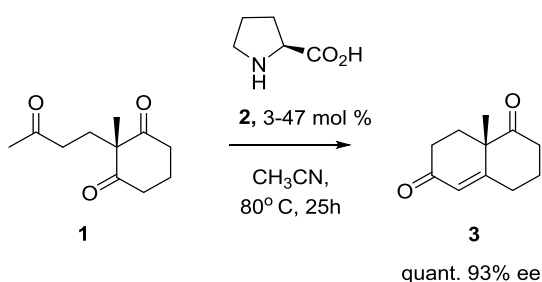
In recent years, it has been established that small organic molecules can be highly selective and efficient catalysts. A new concept has emerged in which metal-free organic molecules are used as catalysts in organic reactions.^[1,2] Bifunctional organocatalysis combine hydrogen bond donors and Lewis bases, within a single compound to accelerate organic reactions, while also providing selectivity. Hydrogen bonding is a key contributor and plays an important role in stabilising the reactive intermediates and in modulating the reactivity.

As a result, organocatalysis is gaining more and more recognition from the scientific community, thus becoming an important research area in asymmetric synthesis, complementing bio- and metal-catalysis. The term organocatalysis was introduced by MacMillan in 2000,^[3] and is used to describe the acceleration of chemical reactions with a substoichiometric amount of a small organic compound which does not contain a metal atom.^[1] This field was driven by the necessity to develop environmentally friendly methodology that can eliminate the need for potentially toxic metal-based catalysts.

Organocatalytic reactions show great resemblance to metal- and enzyme catalysed reactions in selectivity and performance, but present some potential advantages.^[2] They are inexpensive, readily available in a range of quantities, suitable for industrial-scale reactions and they are often more stable than enzymes or other bioorganic catalysts. Due to their robustness they generally do not require demanding reaction conditions like inert gas atmosphere, special reaction vessels, or ultra-dry reagents and solvents.

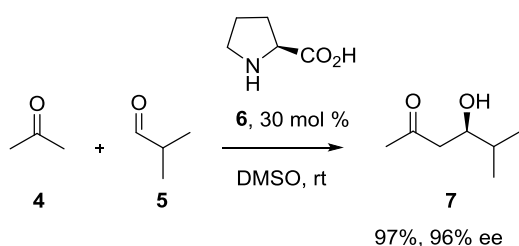
Organocatalytic reactions look back on a long history. Pizarrello and Weber proposed that this metal free type of catalysis played a key role in the formation of chiral prebiotic key building blocks for life, such as sugars, and thus allowed the introduction and spread of homochirality in living organisms.^[4]

According to this hypothesis, it was proposed that enantiomerically enriched amino acids, such as alanine and isovaline, were present with up to 15% ee in carbonaceous meteorites that landed onto earth in its early history. These natural amino acids catalyse the asymmetric synthesis of sugar derivatives with significant enantiomeric excess from glycolaldehyde and formaldehyde.



Scheme 1: The Hajos-Parrish-Eder-Sauer-Wiechert reaction.

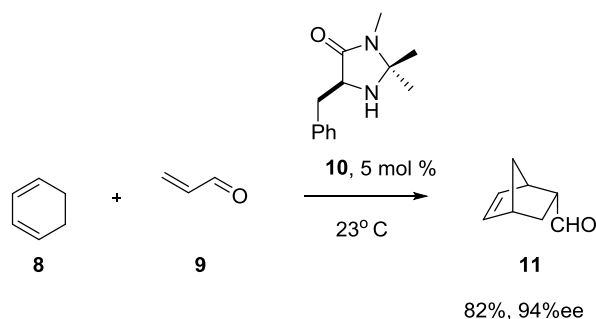
In the early 1970s, proline as an organocatalyst was explored for the first time in the intramolecular aldol reaction by the industrial groups of Eder, Sauer and Wiechert at Schering,^[5] and Hajos and Parrish at Hoffmann-La Roche.^[6] The Hajos-Parrish-Eder-Sauer-Wiechert reaction was probably the most famous small organic molecule-catalysed asymmetric reaction until the early 1990s (Scheme 1).



Scheme 2: L-Proline-catalysed intermolecular aldol reaction reported by Barbas and

List

Despite this early success it took some time for the scientific community to acknowledge this research area. It wasn't until the promising potential of organocatalytic transformations were highlighted in two publications, which appeared almost simultaneously. In 2000, List and Barbas discussed their studies on the enamine catalysis of intermolecular asymmetric aldol reactions (Scheme 2) [7] with the other from the MacMillan et al. on iminium catalysis of enantioselective Diels-Alder reactions (Scheme 3). [3]



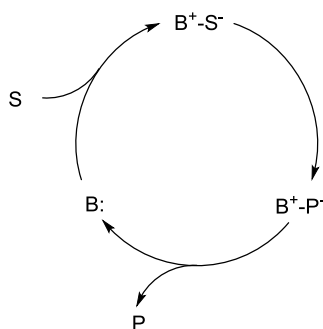
Scheme 3: First enantioselective organocatalytic Diels-Alder reaction reported by MacMillan et al.

Due to the large amount of organocatalytic reactions reported in literature in recent years, a division will be adopted in this discussion that mirrors the classification for organocatalytic processes which was introduced by List. [8] It categorises Lewis base and Brønsted acid catalysis into groups according to their mechanisms. Not all organocatalytic processes can be described with these general reaction mechanisms, but this division can give a brief overview of the large diversity of asymmetric organocatalytic reactions reported in literature.

These catalysts initiate their catalytic cycles by either providing or removing electrons or protons from a substrate or a transition state. Most of the organocatalysts published to date work via a Lewis base mechanism (Scheme 4), although the use of Brønsted acid catalysts has recently grown. [9] Incorporation of both a Lewis base and Brønsted acid has led to a new class of bifunctional catalysts which are expected to ultimately deliver extremely active catalysts that can rival the efficiency of enzymes. A bifunctional catalyst contains two distinct functionalities within the same molecule; activating either the electron donor or the acceptor thus speeding up the overall rate of the reaction.

1.1.2. Lewis Base Catalysis

The general catalytic cycle for reactions catalysed by Lewis bases ($B:$) is shown in Scheme 4. The cycle starts with a nucleophilic addition of Lewis base ($B:$) to substrate S , which is converted into adduct B^+-S^- . This adduct then undergoes a transformation to form the intermediate species B^+-P^- , from which the product (P) is released. The catalyst is regenerated and re-enters the catalytic cycle for further turnover.

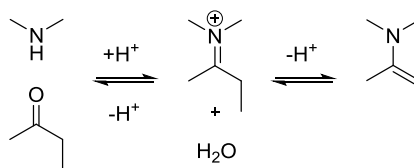


Scheme 4: General mechanism for Lewis base-catalysed reactions.

The majority of organocatalysts tend to react as heteroatom-centered N, O-, P-, and S-Lewis bases, which transform substrates into typical reactive intermediates such as iminium ions, enamines, acyl ammonium ions, and ammonium enolates.

In iminium catalysis, the active species is an iminium ion formed by the reversible reaction of an amine catalyst with a carbonyl substrate (Scheme 5). In the first iminium catalysis reaction, MacMillan reported the reaction of α, β -unsaturated aldehydes and ketones with dienes, using the chiral imidazolidinone catalyst (Scheme 3). The condensation of the α, β -unsaturated aldehyde with the enantiopure amine catalyst forms a reactive iminium ion with lowered LUMO energy, which reacts with the diene leading to a Diels–Alder cycloaddition. With lower LUMO energy, the iminium ions are more electrophilic than the corresponding aldehydes or ketones, and thereby more effectively activate the adjacent C–C–double bond for 1, 4-addition or pericyclic reactions.

This concept of activating unsaturated aldehydes into more reactive intermediate iminium ions, has been used in reactions such as [3+2]-cycloaddition reactions ^[10] and Mukayama-Michael reactions.^[11]



Scheme 5: Formation of iminium and enamine intermediates.

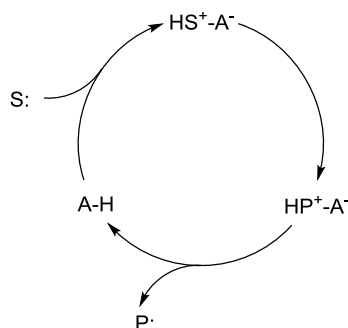
Enamine catalysis involves an enamine intermediate formed via deprotonation of an iminium ion, which can react with various electrophiles or undergo pericyclic reactions. The first example of asymmetric enamine catalysis was the Hajos–Parrish–Eder–Sauer–Wiechert reaction (Scheme 1). Proline and a carbonyl compound condense to form a nucleophilic enamine. The incoming electrophile is directed by hydrogen bonding to proline's carboxylic acid.

List and Barbas described the first intermolecular aldol reaction, shown in Scheme 2 that proceeds through the enamine intermediate. This then undergoes an aldol-type addition with aldehyde to give the product.

The Enamine catalysis concept has been further extended to other reactions like the Mannich-,^[12] and the Michael reaction.^[13] Other Lewis base-catalysed processes mainly proceed through acyl-ammonium ^[14] and ammonium-enolate intermediates ^[15] such as the Morita-Baylis-Hillman (MBH) reaction (see in chapter 1.2).

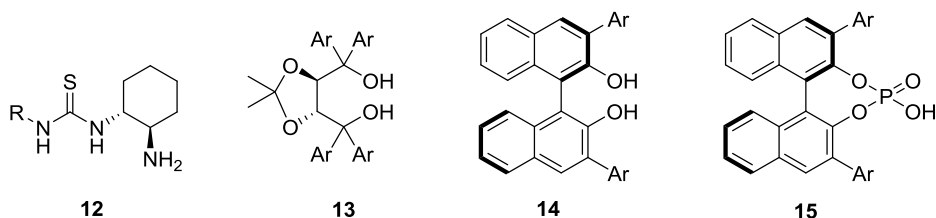
1.1.3. Brønsted Acid Catalysis

Brønsted acid-catalysed reactions are initiated with (partial) protonation of the substrate (S:). The resulting adduct HS^+A^- is converted into the adduct HP^+S^- , which undergoes an elimination reaction to release the product (P) and the catalyst (A-H) (Scheme 6).



Scheme 6: General mechanism of Brønsted acid catalysis.

Generally chiral Brønsted acids can be classified into two categories. Weakly acidic Brønsted acids, such as thiourea, (**12**) and TADDOL (**13**) derivatives, ($\text{pK}_a > 10$) and stronger Brønsted acids, such as BINOL (**14**) derivatives and phosphoric acid (**15**) ($\text{pK}_a < 10$).



Scheme 7: Examples of chiral Brønsted acid catalysts.

Jacobsen and co-workers used urea- and thiourea compounds (**12**) as chiral Brønsted acids to activate carbonyl- and imine groups in a variety of reactions like the Mannich-^[16] and Strecker reactions.^[17]

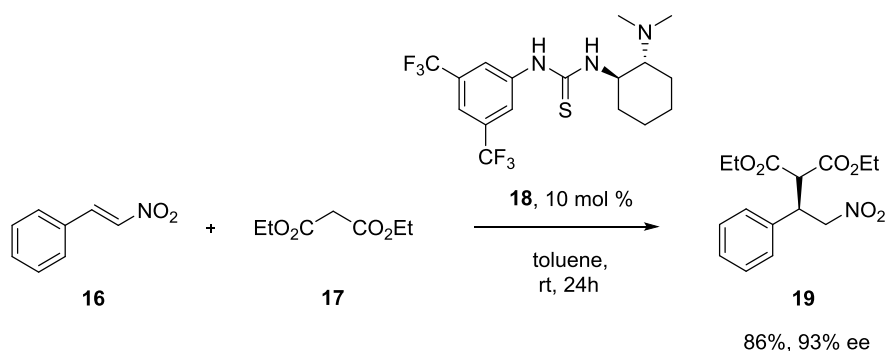
Rawal et al. reported the use of TADDOL derivative **13** as chiral catalysts for the enantioselective hetero-Diels-Alder reaction of aldehydes with dienes.^[18] They reacted benzaldehyde and diene in the presence of TADDOL to form the cycloadduct as a single diastereomer, which was converted to dihydropyrone on treatment with acetyl chloride. Protecting one or both hydroxy-groups leads to a decrease in activity and selectivity, indicating the involvement of both OH groups in the activation of the aldehyde.

The Japanese groups of Akiyama et al. and Terada et al. discovered that strong acids can be efficient asymmetric catalysts alone.^[19] As compared to hydrogen-bonding type Brønsted acid catalysis, protonation of the substrates is likely to occur in these cases. This series of chiral phosphoric acids has been applied to a variety of reactions such as the Pictet-Spengler-^[20] and aza-Diels- Alder reaction.^[21]

1.1.4. Bifunctional Acid-Base Catalysis

Recently, several groups have shown that the incorporation of a basic and an acidic moiety in one chiral molecule can facilitate a synergistic interaction speeding up the overall rate of the reaction, while also providing selectivity. Bifunctional catalysts have enabled effective transformations, which cannot be achieved by a single functional catalyst.

Shibasaki et al. developed the concept of multifunctional catalysis, employing catalysts containing both Lewis acidity and Brønsted basicity, using lanthanide complexes.^[22] An early example of a bifunctional chiral organocatalyst was reported by the group of Takemoto et al, activating nitro compounds for the enantioselective aza-Henry and Michael reactions.^[23] They used catalyst **18** which contains an amine moiety and a thiourea group, both needed for high yield and selectivity (Scheme 8). The amino group activates the nucleophile via (partial) deprotonation, while the thiourea group coordinates to the nitro function of the α, β -unsaturated olefin via hydrogen bonding.



Scheme 8: Michael addition of diethyl malonate to trans- β -nitrostyrene.

Since then, bifunctional organocatalysts have been successfully applied to a wide range of reactions like the Henry-^[24], and Strecker reactions.^[25] Another reaction employing multifunctional/bifunctional chiral catalysis is the Morita-Baylis-Hillman reaction and its aza-counterpart, which will be discussed in detail in section 1.2.

1.2. Morita-Baylis-Hillman Reaction

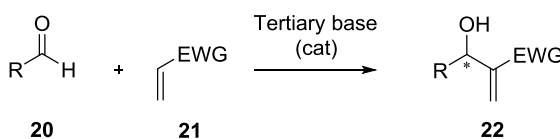
1.2.1. General Aspects

Carbon-carbon bond formation and functional group transformations are two of the most fundamental reactions in present day synthetic organic chemistry. In the last number of years, much effort has gone into not only the development of new methodologies for these transformations but also in the development of new catalysts, reagents, and strategies for these reactions, often involving the concepts of atom economy and selectivity. With the importance of generating chiral centres throughout bioactive compounds for the pharmaceutical industry, atom economy and selectivity (chemo-, regio-, stereo-) are of a premium requirement in any efficient reaction.

Due to the MBH reactions atom economy and ability to produce highly functionalised compounds with a newly created chiral centre, it has become increasingly important as a method for carbon-carbon bond formation.

1.2.2. Origin and Development

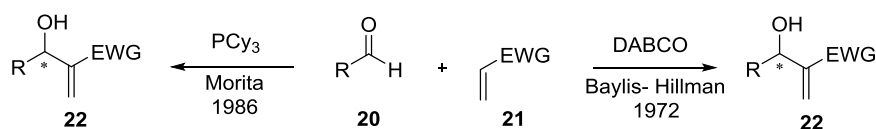
The Morita-Baylis-Hillman (MBH) reaction is one of most synthetically versatile carbon-carbon bond-forming reactions. It has been used to generate building blocks for the synthesis of many heterocycles, drug molecules and natural products. ^[26] Typically it takes place between an aldehyde and an activated alkene, in the presence of a tertiary base/ nucleophile (Scheme 9). (If the aldehyde is replaced by an imine the reaction is called aza-Morita-Baylis-Hillman (aza-MBH) (see section 1.3) reaction, which leads to very useful α -methylene- β -amino products. Each MBH adduct contains several functional groups with the potential to undergo a variety of organic transformations involving regio- and stereochemical control.



Scheme 9: General MBH Reaction.

The origin of the reaction dates back to 1968, when Morita et al., who originally worked with phosphine catalysts, demonstrated that the reaction of acrylonitrile or methyl acrylate with various aldehydes under the catalytic influence of PCy_3 led to densely functionalized products (Scheme 10).^[27a] However the reaction was not immediately utilised due to low conversion rates.

The reaction also takes its name from A.B. Baylis and M.E.D. Hillman, Baylis, who in 1972, reported a similar reaction between acetaldehyde and ethyl acrylate or acrylonitrile in the presence of catalytic amounts of Lewis bases such as DABCO to obtain similar products to those which Morita had obtained earlier.^[27b] The main difference in their report was that the use of DABCO instead of the phosphine derivative now meant that the adduct could be obtained in a much higher yield (Scheme 10).

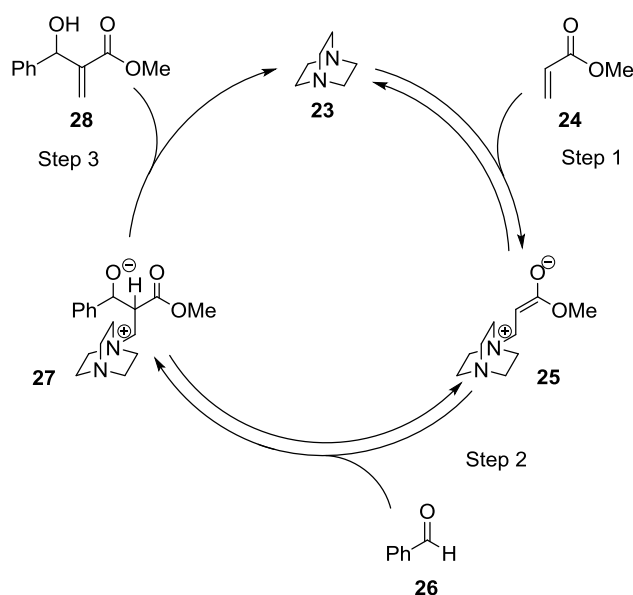


Scheme 10: Original patents of the MBH Reaction.

It was not however until the 1980s, that organic chemists fully explored the reactions utility after Drewes and Emslie, in 1982 applied an MBH adduct in the synthesis of integerrineic acid,^[28] and then in 1983 Hoffman and Rabe reported another MBH adduct in the synthesis of mikanecic acid.^[29] This led to the publication of the first review in 1988 by Drewes and Roos.^[30]

1.2.3. Mechanism

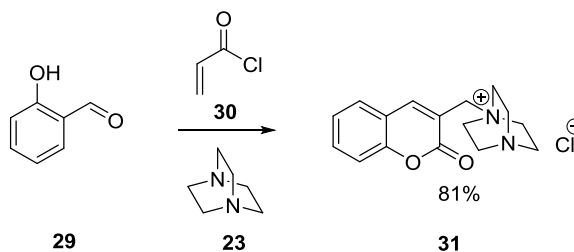
Based on pressure dependence, rate, and kinetic isotope effect data, the first mechanism was proposed by Hill and Isaacs showing a reversible Michael addition of a nucleophilic catalyst to an activated alkene to generate a zwitterionic 3- ammonium enolate. Nucleophilic addition of this enolate onto an aldehyde in aldol- type coupling gives a second zwitterionic intermediate, which undergoes an intramolecular proton transfer with elimination yielding the product and liberating the catalyst (Scheme 11). Initially Step 2 was suggested as the MBH rate-determining step RDS, due to a low kinetic isotopic effect ($\text{KIE} = 1.03 \pm 0.1$).^[31]



Scheme 11: Simplified mechanism for the MBH reaction.

This mechanism was supported by Bode and Kaye through kinetic data and was initially the most commonly accepted mechanism. Kaye et al. reacted pyridine carboxaldehydes with acrylate esters in the presence of DABCO in CDCl_3 . They monitored the reaction via NMR spectroscopy and observed a first-order dependence in catalyst, aldehyde, and acrylate, thus proposing a mechanism that contained the intermediates shown in Scheme 11 with the aldol-coupling as the RDS.^[32]

Further experimental evidence was provided by Drewes et al. They reacted methyl acrylate with 2-hydroxybenzaldehyde in DCM at 0° C in the presence of DABCO and isolated the second intermediate, coumarin salt, which was confirmed by X-ray crystallography (Scheme 12).^[33]



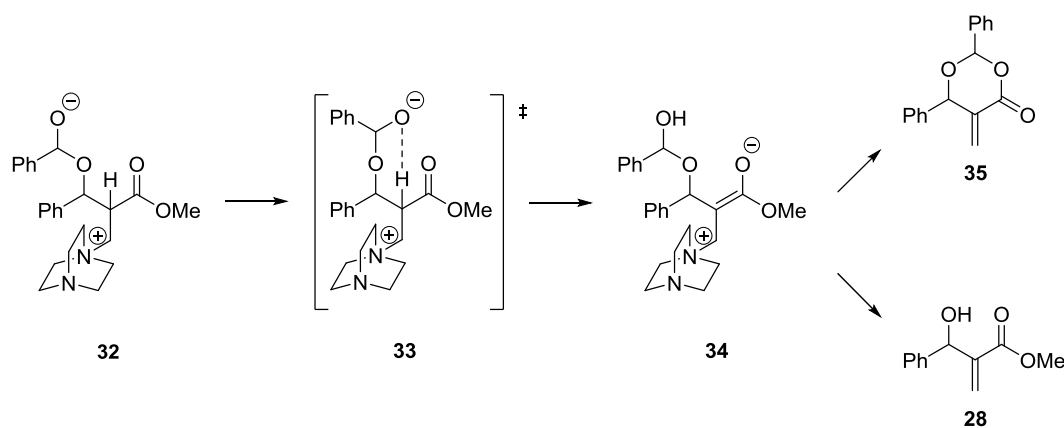
Scheme 12: Coumarin salt isolated by Drewes et al.

Eberlin et al. also intercepted all of the key intermediates in the mechanism (Scheme 11) using ESI-MS/MS.^[34] They examined reactions of two aldehydes, thiazole-2-carbaldehyde and 4-nitrobenzaldehyde with methyl acrylate and DABCO in MeOH at room temperature.

McQuade et al. re-evaluated the mechanism on the basis of rate and isotope data, due to unanswered questions in previous literature. They found that the reaction was first order in acrylate and DABCO, but second order in aldehyde in the reactions of various aromatic aldehydes with methyl acrylate, catalysed by DABCO, in polar, non-polar, and even protic solvents.^[35, 36] A large kinetic isotope effect was observed when α -deuterioacrylate was used in the DABCO catalysed reaction of methyl acrylate and 4-nitrobenzaldehyde (KIE, KH/KD= 2.2–5.2 depending on the solvent used), with a large inverse isotope effect (KH/KD=0.72–0.80) when α -deuterio-4-nitrobenzaldehyde was employed. Observation of a KIE greater than 2 indicates a deprotonation in the RDS. These results strongly suggested that deprotonation of α -H (D) atom of **27** (step 3) was rate-limiting (Scheme 11).

Based on this new data, McQuade et al. proposed a new mechanism, for the proton-transfer step. They suggested addition of the second zwitterionic intermediate onto a second molecule of aldehyde forms a hemiacetal intermediate/alkoxide, which undergoes proton transfer via a six membered transition state. The mechanism features

all of the intermediates previously proposed but now includes the formation of a hemiacetal that subsequently goes on to eliminate DABCO after proton transfer. The new mechanism also provides an explanation for the formation of dioxanone products. The proposed hemiacetal intermediate, **33**, can cyclize to yield a dioxanone product **35** (Scheme 13).

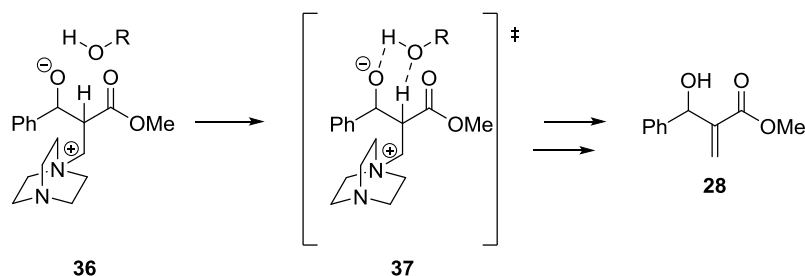


Scheme 13: Formation of the dioxanone by-product proposed by McQuade et al.

Aggarwal, Fulford and Lloyd-jones also proposed that the proton transfer step was the RDS based on their kinetic studies.^[37] They investigated the reaction of ethyl acrylate with benzaldehyde catalysed by quinuclidine without solvent.

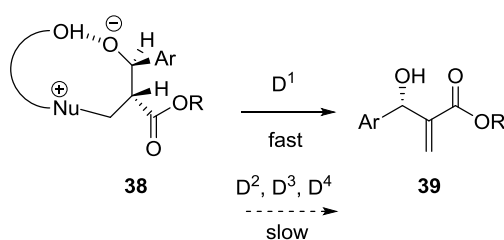
They observed at the start of the reaction, proton transfer was the RDS, when conducted in aprotic media as noted by McQuade. Below 20 % conversion, the non-deuterioacrylate was consumed more, but as the reaction proceeded however, the ratio of non-deuterated to α -deuterated ethyl acrylate remained constant. The proton migration becomes increasingly efficient which results in a shift of the RDS from the proton transfer to the aldol-type coupling in step 2 (Scheme 11).

It was proposed that the product serves as a hydrogen-donating co-catalyst to assist the proton transfer from the α -keto methine to the alkoxide via a six-membered transition state **37** (Scheme 14) thus making the reaction autocatalytic. This transition state also explains the large rate enhancements in the MBH reaction caused by water and other protic solvents or additives.



Scheme 14: Proton-transfer mechanism proposed by Aggarwal et al.

At the end of the report, the authors proposed a model for enantioselective MBH reactions with bifunctional chiral catalysts containing a Lewis basic and a Brønsted acidic moiety. Since the second intermediate of the MBH reaction, **38** contained two centres of chirality; four diastereoisomers could be formed with an enantiopure catalyst. They suggested that all four diastereomers are formed in the reaction, but only one has the hydrogen-bond donor suitably positioned to allow fast proton transfer, while the other diastereomers revert back to starting materials. This implied that the proton migration step determined the enantioselectivity of the reaction (Scheme 15).



D¹⁻⁴ are diastereomers of the alkoxide adduct.

Scheme 15: Model for enantioselective MBH reactions proposed by Aggarwal and Lloyd-Jones ($\text{Nu}^+ \cap \text{OH} =$ chiral bifunctional catalyst).

Sunoj and Roy reported the first ab initio and DFT investigations on the mechanism of the MBH reaction.^[39] Initially acrolein was reacted with formaldehyde in the presence of trimethylamine (NMe_3) in order to establish the reaction profile (model system). Once established, the reaction profile was then applied to a real system in which MVK was reacted with benzaldehyde catalysed by DABCO. They showed that the rate-

limiting step was the intramolecular proton transfer in the second zwitterionic intermediate **27** (Scheme 11). The intramolecular proton transfer was found to be the highest point on the reaction profile, with the activation barrier for C-C bond formation in the reaction between the initial zwitterion and benzaldehyde to be 20.2 kcal mol⁻¹ lower. The CBS-4M, MP2/6-31+G* and mPW1K/6-31+G* levels of theories were used in the calculations and solvation effects were accounted for by use of the continuum dielectric method included in the polarisable continuum model (IEF-PCM).

Subsequently, Aggarwal, Robiette and Harvey carried out an extensive computational investigation which supported their own kinetic observations and those of McQuade in regard to the proton transfer step.^[40] Their study focused on the reaction between methyl acrylate and benzaldehyde catalysed by a tertiary amine in both the presence and absence of alcohol.

In the presence of methanol it acts as a hydrogen-bond donor to activate the reaction by allowing the proton-transfer step to occur via a concerted lower-energy mechanism in which one molecule of alcohol (or water) can act as a shuttle to transfer the proton from the α -position of **27** to the alkoxide of the second zwitterionic intermediate.

Based on the proposals by McQuade and Aggarwal that the proton-transfer step is the RDS, Eberlin et al. performed complementary investigations on the MBH reaction using ESI-MS/MS techniques with the aim of intercepting and characterising the intermediates demonstrated in the key rate-determining proton-transfer step.^[41]

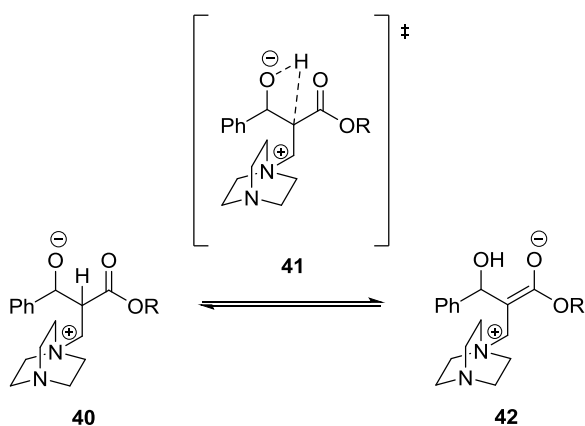
They monitored the DABCO-catalysed reaction of methyl acrylate with excess benzaldehyde without solvent and were able to intercept the intermediate of type **33** proposed by McQuade (Scheme 13). When the MBH reaction was studied using the same experimental protocol, but adding β -naphthol (external proton source), they intercepted an intermediate of type **37** (Scheme 14), supporting Aggarwal's proposal.

Eberlin et al. also investigated the MBH reaction of formaldehyde and acrolein in the presence of NMe₃ as catalyst and MeOH as solvent.^[42] Their results clearly showed that the proton transfer step is the RDS and that MeOH is important as it acts as a proton shuttle between the carbon and oxygen centres, as Aggarwal et al. had proposed earlier. The group also confirmed in non-protic solvents the reaction appeared to follow a different pathway involving a hemiacetal species as proposed by McQuade et al.

More recently, Cantillo and Kappe presented a detailed computational and experimental reinvestigation on the amine catalysed MBH reaction of benzaldehyde with methyl acrylate.^[43] Initially, they evaluated the proposed reversible character of the MBH reaction, and pointed to a strong temperature dependence of the equilibrium constant. The production of the adduct is favoured at low temperatures, while the reactants are favoured at elevated temperatures. The reaction shifts from exergonic to endergonic when heated at temperatures above 330 K (57° C) in the case of the benzaldehyde/methyl acrylate system, and 380K (107° C) for 4-nitrobenzaldehyde (due to the higher reaction exothermicity), showing a need for the reaction to be performed at moderate temperatures.

Due to a proposed limitation of the B3LYP hybrid density functional, used in of the computational mechanistic work as already described, Cantillo and Kappe revisited the MBH reaction mechanism using the M06-2X computational method. The results provided by this theoretical approach however are still in agreement with all the previous experimental/kinetic evidence such as reaction order, acceleration by protic species, and autocatalysis.

From this re-evaluation, the authors show the direct proton transfer from **40** to form **42** through a four membered ring transition structure **41** calculated at the M06-2X level has an energy barrier of 41.8 kcal mol⁻¹ (Scheme 16). This relatively high energy barrier explains the observed KIE when using isotopically labelled methyl acrylate.^[32]



Scheme 16: Direct proton transfer through a 4-membered transition structure.

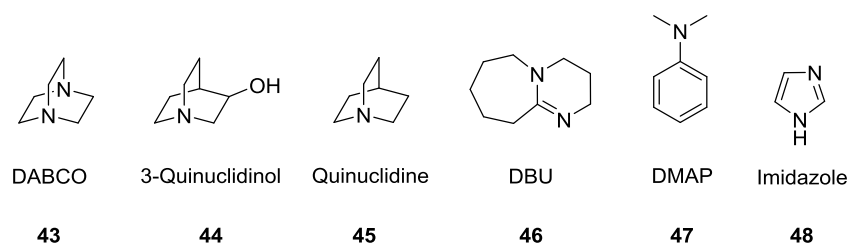
McQuade's intermediate **33** for the proton transfer which takes place through a six-membered-ring transition structure has a free energy of activation of 22.4 kcal mol⁻¹. Since this energy barrier is still higher than the carbon-carbon bond formation, this mechanistic proposal explains both the KIE effect and the second-order kinetics for the aldehyde component.

Aggarwal's methanol-catalysed proton transfer (Scheme 14) has an energy barrier of 22.6 kcal mol⁻¹, suggesting these similar energetics can result in competitive reactions. Therefore depending on the amount of protic species and the reaction progress both pathways can take place.

1.2.4. Catalysis of the Morita-Baylis-Hillman Reaction

Various nucleophilic Lewis bases can be employed to initiate the MBH reaction. This includes amine, phosphine, selenide or sulphide.^[45] However, presence of a Lewis acidic co-catalyst is necessary to obtain an efficient catalytic activity for selenide or sulphide.^[44]

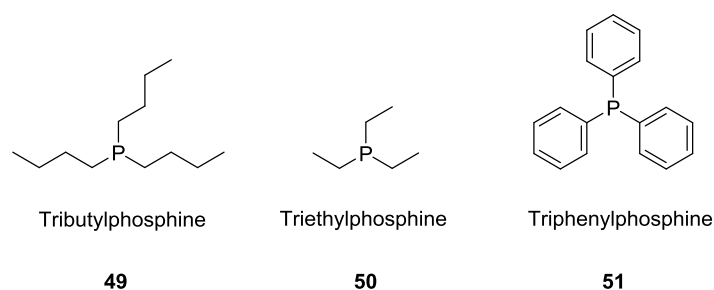
Baylis and Hillman reported DABCO as their catalyst of choice and, subsequently, most researchers initially used DABCO as the catalyst for MBH reactions. However, because of the slow reaction rates with some substrates, researchers began to explore alternative nucleophilic catalysts which might give better yields and increased reaction rates. Other N-Lewis base catalysts for the MBH reaction are 3-quinuclidinol,^[45] quinuclidine,^[45] DBU,^[46] DMAP,^[47] and imidazole.^[48] (Scheme 17).



Scheme 17: Typical N-Lewis base catalysts used in the MBH reaction.

Aggarwal et al. examined the reactivity of the series of quinuclidine -based catalysts such as **43**, **44** and **45** in the MBH reaction. They established a correlation between the basicity of the catalysts and reactivity, according to which more basic catalysts in this series are more reactive.

Compared to their nitrogen analogues, P-centered Lewis bases have higher nucleophilicity and weaker proton-basicity.^[49] They also adopt a similar trend in which more strongly basic alkyl phosphines, such as tributylphosphine (pK_a (8.43) and diphenylmethylphosphine (pK_a (6.50)), are typically more effective than aryl phosphines, such as triphenylphosphine (pK_a (2.73)).^[50] Because of reduced nucleophilicity, triarylphosphines like triphenylphosphine (PPh_3) can only initiate the reaction in the presence of a suitable co-catalyst like phenol.^[51] On the other hand, due to their high air-sensitivity, the potential efficiency of trialkylphosphines in MBH reactions is somewhat reduced. Typical P-containing Lewis bases for the MBH reaction are tributylphosphine, triethylphosphine, and triphenylphosphine (Scheme 18).

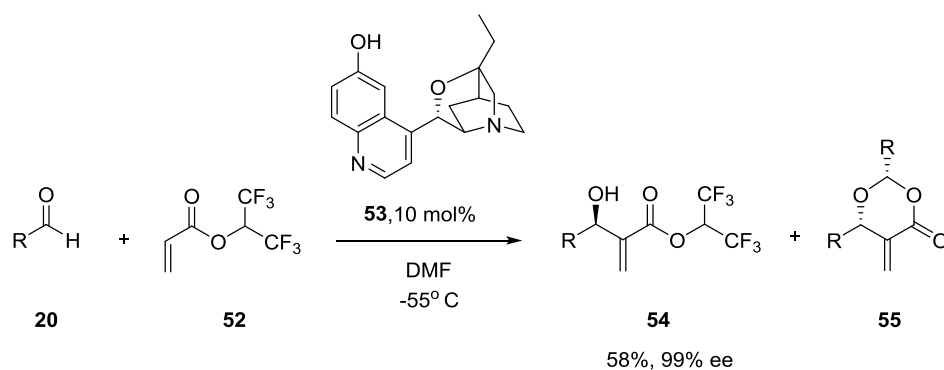


Scheme 18: Typical P-Lewis base catalysts used in the MBH reaction.

Recently, considerable efforts have been devoted to development of asymmetric MBH reactions. The formation of a new chiral centre in the MBH product allows asymmetric transformations. Incorporation of a chiral source into any of the three components involved in the MBH reaction (catalyst, activated alkene, or carbon electrophile), asymmetric transformations of the MBH product can be realised. Unfortunately, the scope and applications of chiral activated alkenes and electrophiles are limited. Therefore the real attraction lies in the development of chiral catalysts. Recently, strategy around employing bifunctional catalysts in MBH reactions has proven to be very successful in asymmetric catalytic variants.

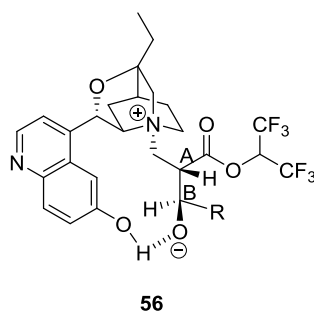
As already mentioned, Brønsted acids are efficient co-catalysts for the MBH reaction and lead to significant rate enhancements. A Brønsted acid and a Lewis base can be positioned onto a chiral backbone to activate the MBH reaction cycle and enhance selectivity.

The first practical chiral catalyst was developed in 1999 by Hatakeyama et al. who applied a cinchona alkaloid derivative, β -isocupreidine **53** as catalyst for the MBH reaction of various aldehydes with **52**. The reaction was performed at -55°C in DMF obtaining the corresponding product, **54** in enantioselectivities up to 99% ee (Scheme 19).^[52]



Scheme 19: β -ICD-Catalysed MBH reaction.

The explanation for the enhanced enantioselectivity and rate acceleration was based on some unique features of the catalyst: 1) its increased nucleophilicity via reduced steric hindrance and 2) the presence of the free phenolic hydroxyl group on the quinoline ring. The nucleophilic nitrogen atom in the quinuclidine moiety of **53** acts as a Lewis base to initiate the MBH reaction, whereas the phenolic OH group acts as a Lewis acid to stabilise and organise the enolate intermediate and also to promote the subsequent aldol addition (Scheme 20).

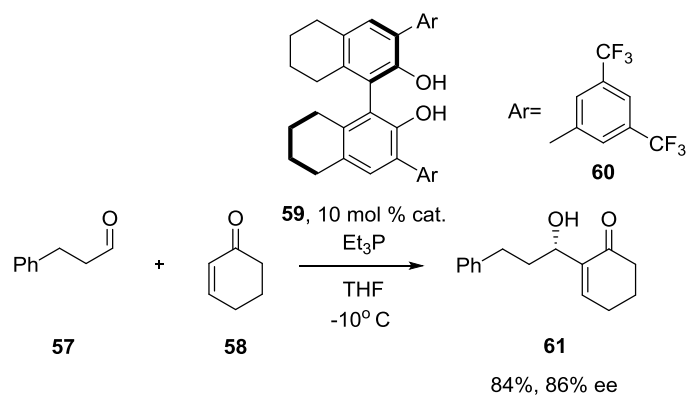


Scheme 20: Hatekeyama's rationalizations for the formation of adduct **54**.

Since the chirality of the catalyst is fixed, and intermediate **56** contains two chiral centres, (A and B), four diastereoisomers can be formed. The authors postulated that diastereoisomer **56** is the most stable and has a nearly ideal conformation for the subsequent elimination reaction. Elimination of the catalyst in intermediate **56** leads to the MBH product with the same stereoconfiguration of the ester **54**.

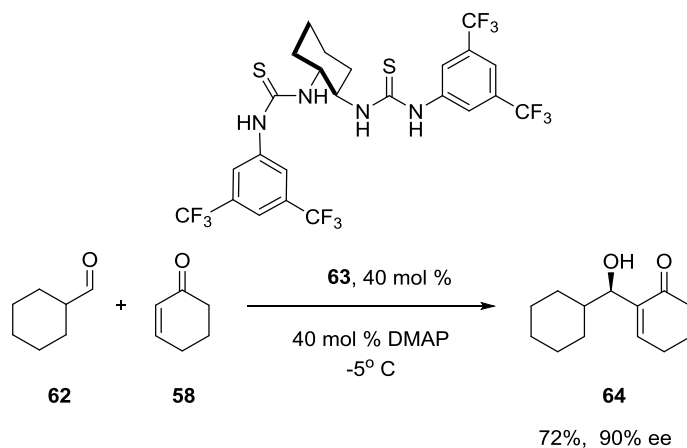
Unfortunately, there is a disadvantage of Hatakeyama's catalytic system, with the formation of a dioxanone by-product, as explained by McQuade with the opposite absolute stereoconfigurations and worse enantioselectivity.

In 2003, Schaus et al. reported the MBH reaction of cyclohexenone with aldehydes using a chiral BINOL-derived Brønsted acid as the catalyst and triethylphosphine (PEt₃) as the nucleophilic promoter.^[53] Good to excellent enantioselectivities were achieved with aliphatic aldehydes, while conjugated aldehydes such as benzaldehyde and cinnamaldehyde led to products in low yields and enantioselectivities. It was suggested that the Brønsted acid promotes the conjugate addition step of the reaction, and then remains hydrogen-bonded to the resulting enolate in the enantioselectivity-determining aldehyde addition step. Substitution of one Brønsted acid equivalent from the BINOL-derived catalyst resulted in reduced catalytic activity and no enantioselectivity. The highest levels of enantioselectivity were achieved with presence of bulky substituents at the 3, 3'-positions (Scheme 21).



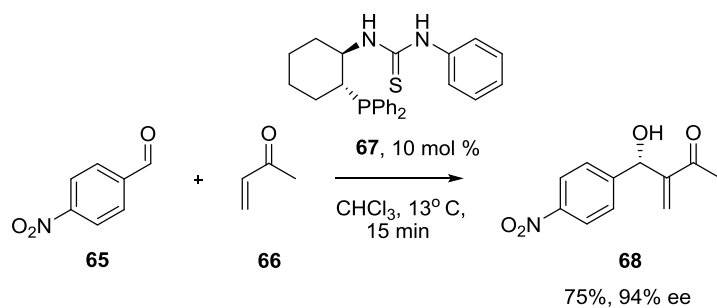
Scheme 21: BINOL derivative **59** and PEt_3 co-catalysed MBH reaction.

Nagasawa et al. developed a new bis-thiourea type catalyst **63** which could promote the MBH reaction of cyclohexanecarboxaldehyde with cyclohexenone in the presence of DMAP to give the desired product with good yield and high enantioselectivity (Scheme 22). They proposed that the aldehyde and the enone become activated via coordination to the thiourea units of the catalyst, through hydrogen bonding interactions.^[54]



Scheme 22: DMAP and bis-thiourea co-catalysed MBH reaction.

An example of a chiral phosphine-catalysed MBH reaction was reported by Wu et al.^[55] They employed a series of chiral phosphine thioureas derived from trans-2-amino-1-(diphenylphosphino) cyclohexane to promote the MBH reaction of various aromatic aldehydes with MVK. The MBH adducts were obtained under mild conditions in short reaction times with excellent enantiomeric excesses (Scheme 23).



Scheme 23: MBH reaction of aldehyde and MVK catalysed by **67**.

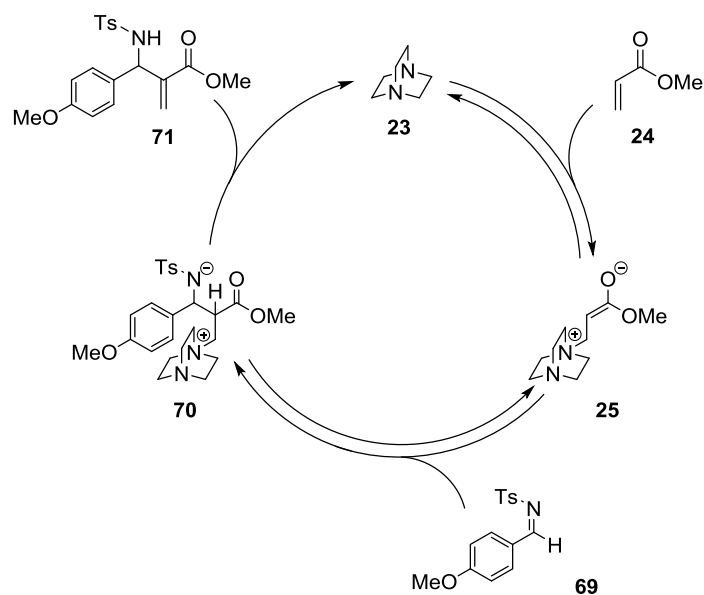
1.1.3. Aza-Morita-Baylis-Hillman Reaction

1.3.1. General Aspects

The first example of the aza-Morita Baylis– Hillman (aza-MBH) reaction came in 1984 when Perlmutter and Teo reported that *N*-tosyl imines reacted with ethyl acrylate in the presence of DABCO to give adducts in moderate to good yields.^[56]

In a standard aza-MBH reaction, activated alkenes are coupled with imines, catalysed by Lewis bases such as amines or phosphines, resulting in highly functionalised allylic amines. However it can also be performed as a three component reaction in which aldehyde, activated alkene and tosylamide or diphenylphosphinamide are coupled in one pot.^[57]

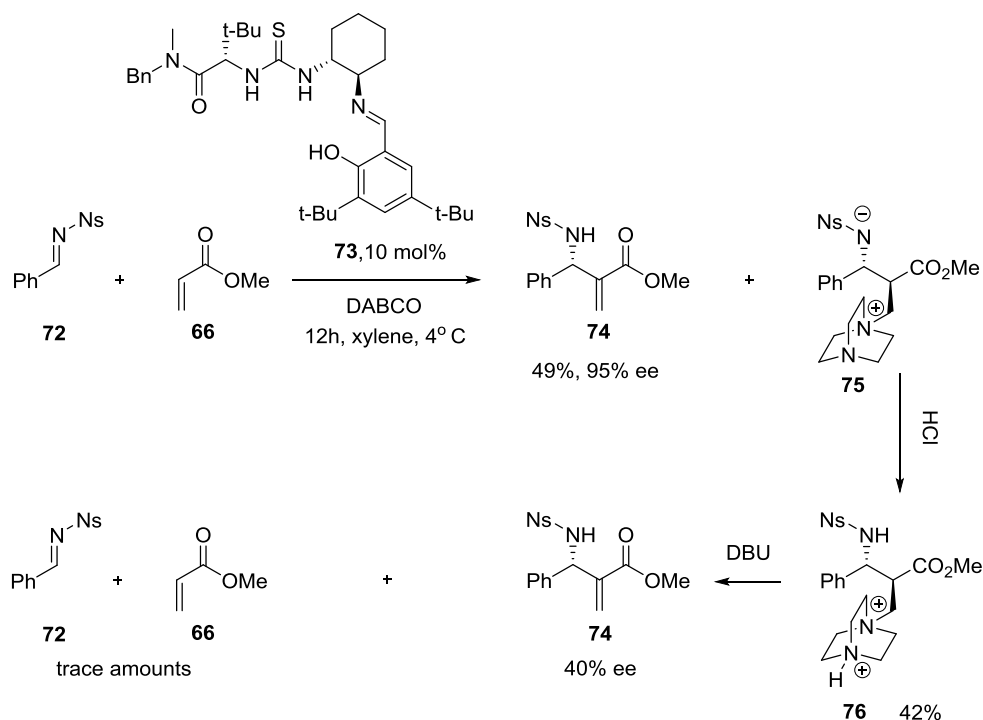
The catalytic cycle is initiated by the reversible conjugate addition of a Lewis base to the activated alkene **24** to generate the corresponding enolate, which performs a Mannich-type addition on the imine forming the zwitterion **70**. Finally, a proton transfer followed by an elimination of the catalyst furnishes the aza-MBH adduct **71**. (Scheme 24). The proton transfer constitutes the RDS.



Scheme 24: Simplified mechanism for the aza-MBH reaction.

1.3.2. Mechanism

In 2005, Jacobsen et al. investigated the asymmetric aza-MBH reactions of N-p-nitrobenzenesulfonylimines with methyl acrylate catalysed by chiral thiourea derivatives.^[58] Under the optimized reaction conditions, electron-donating, withdrawing, and heteroaromatic substrates were successfully employed with high enantioselectivities albeit with modest isolated yields (Scheme 25).



Scheme 25: The aza-MBH reaction catalysed by a chiral thiourea, with isolation and characterisation of the dihydrochloride salt **76**.

During the study, the authors isolated and characterised the second zwitterionic intermediate of the catalytic cycle **75** as a yellow precipitate. Upon treatment with excess hydrochloric acid, they obtained the dihydrochloride salt **76** as a glassy solid. The salt **76** was highly diastereomerically pure with the relative stereochemistry of the major isomer assigned as anti. However when zwitterionic compound **75** was regenerated in DMSO-d₆/ CDCl₃ through deprotonation by DBU, methyl acrylate **66** and imine **72** were also detected, indicating that **75** undergoes reversion to its precursors (Scheme 25).

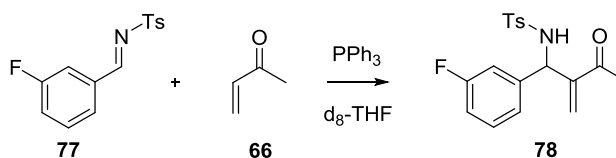
When generated in this manner, **75** underwent further proton transfer to provide the product, confirming its presence as an intermediate in the catalytic cycle.

Because the reaction mixture disclosed in (Scheme 25) was not homogeneous, the authors studied the uncatalysed reaction of methyl acrylate and imine promoted by DABCO in CHCl₃ which provided a homogeneous mixture. Monitoring the reaction by gas chromatography analysis, the reaction showed a first order kinetic dependence on both DABCO **23** and methyl acrylate **24**, with an observed rate saturation for the imine as electrophile. When α -deuterioacrylate was used, a prominent primary kinetic isotope effect was also observed ($k_H/k_D = 3.8$), strongly suggesting that the proton transfer step is rate-limiting.

Subsequently the authors attempted to detect the influence of the electrophile on the elimination reaction. They investigated the DBU mediated elimination of **76** in methanol via IR spectroscopy and found a first-order reaction rate profile for more than 4 half-lives. This is consistent with the rapid and irreversible deprotonation of **76** to **75**, and intramolecular proton transfer of **75** to the corresponding enolate **76**. Since the imine **72** had no effect on the rate of elimination, they concluded that the electrophile did not play a role in mediating the elimination step.

As a result, it was also proposed that the zwitterionic species **75** exists as both syn and anti diastereomers but that **75**_{syn} is generated in high ee and decomposes relatively rapidly by intramolecular proton transfer/ elimination to generate **74** in high ee. In contrast, **75**_{anti} may undergo a relatively slow elimination to **74** due to less favourable steric interactions and therefore its concentration builds up during the course of the reaction leading to precipitation. This also explains why solvent systems that effectively solubilise both diastereomers of **75** lead to formation of **74** in reduced ee.

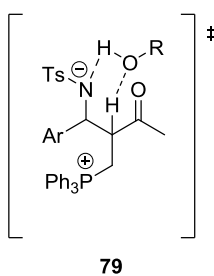
Leitner et al. initially performed kinetic studies on the aza-MBH reaction of methyl vinyl ketone **66** with *N*-(3- fluorobenzylidene)-4-methylbenzenesulfonamide **77** in the presence of PPh₃ in THF at room temperature, monitored by ¹⁹F NMR spectroscopy (Scheme 26).^[59] No evidence for autocatalysis was observed, and the broken order of 0.5 in imine **77** indicated that the RDS is partly influenced by proton transfer.



Scheme 26: Kinetic study performed by Leitner et al.

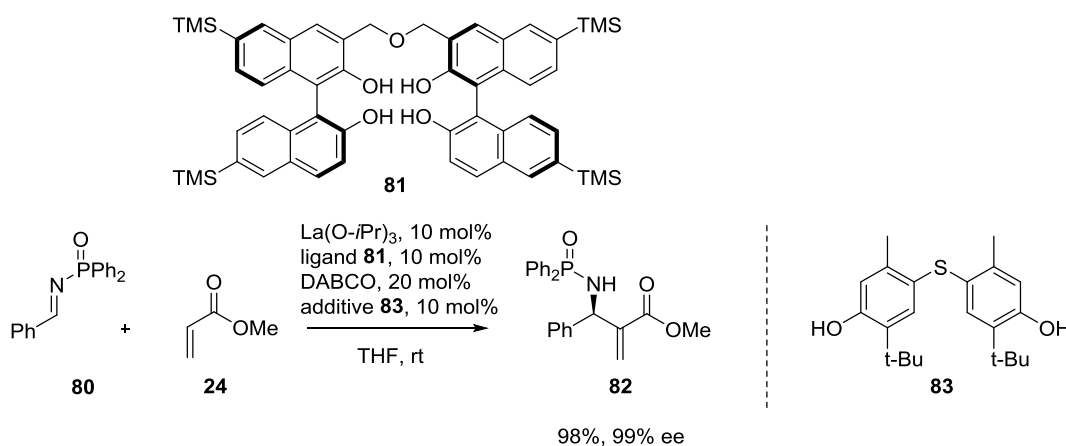
The group then conducted experiments to assess the influence of Brønsted acidic additives with different pK_a values ranging from 3-16. 3, 5-bis (trifluoromethyl) phenol ($\text{pK}_a \sim 8$) was the best, displaying a 14-fold rate enhancement relative to the reaction without additive. Water also gave a significant rate enhancement, but if more acidic additives are used, the enhancement is reduced, postulated to be because of formation of the protonated enolate.

Further examination of the kinetics revealed a change in the rate law of the reaction in the presence of Brønsted acid (PhOH), showing first-order dependence on imine **77**. This demonstrated that the elimination step is not involved in the RDS, and that the proton transfer is accelerated by these additives. This was rationalised by transition state **79** involving a Brønsted acid assisted proton transfer step, which is somewhat similar to autocatalysis (Scheme 27).



Scheme 27: Transition state proposed for the Brønsted Acid-Assisted Proton transfer by Leitner et al.

Recently, Shibasaki et al. investigated the aza-MBH reaction of various N-diphenylphosphinoyl imines with methyl acrylate in the presence of Lewis base DABCO, Lewis acid $\text{La}(\text{O}-i\text{Pr})_3$, ligand **81**, and a phenol-type additive **83**. Aryl, heteroaryl, alkenyl, and alkyl imines were all suitable for this reaction at ambient temperature, giving products in 67-99% yield and 81-98% ee.^[60]



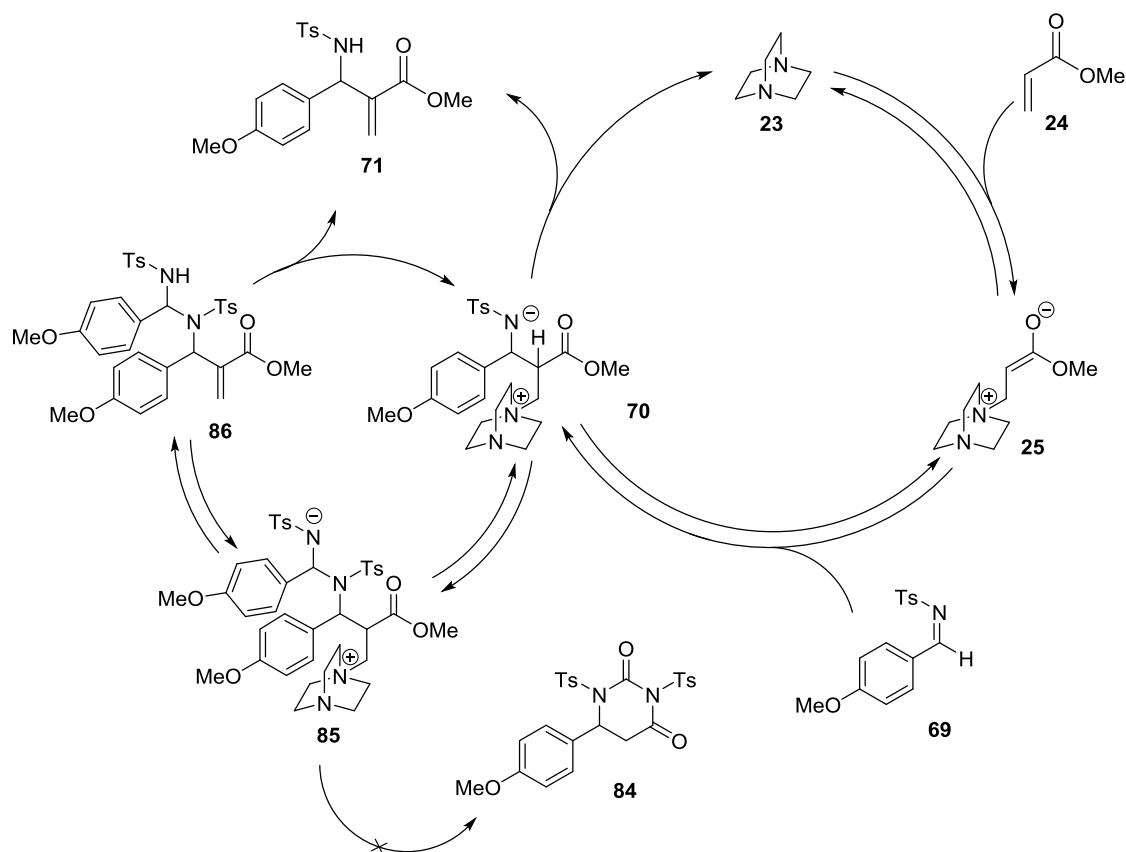
Scheme 28: $\text{La}(\text{O}-i\text{Pr})_3$ and DABCO cocatalysed aza-MBH reaction.

Kinetic studies pointed to the importance of the nucleophilicity of an intermediate La-enolate species as well as the Brønsted basicity of the catalyst, rather than its Lewis acidity, for accelerating the enantioselective aza-MBH reaction. No kinetic isotope effect was observed ($k_{\text{H}}/k_{\text{D}} = 1$), when α -deuterioacrylate was used, indicating that the proton transfer step is not the RDS in this system. On the other hand in the absence of phenol-additive **83**, a kinetic isotope effect ($k_{\text{H}}/k_{\text{D}} = 2.5$) was observed, suggesting the importance of a proton source in the proton transfer step. Based on the kinetic data of a first-order dependence on acrylate, a zeroth-order dependence on $\text{La}(\text{O}-i\text{Pr})_3$ -ligand complex and imine, and a 1.4th-order dependence on DABCO. It was proposed that the RDS was Michael addition of DABCO to methyl acrylate, and that the chiral $\text{La}(\text{O}-i\text{Pr})_3$ -ligand complex was involved in the enantioselectivity-determining step via the interaction with the zwitterionic enolate and the activation of the imine component (Scheme 28).

Very recently, Eberlin et al. investigated the DABCO-catalysed aza-MBH reaction of methyl acrylate with imine in ACN by ESI-MS/MS spectrometry, intercepting the key intermediates **70**, and **71**. However they also identified a unique bis-sulfonamide intermediate **85**.^[61] This intermediate, resulting from the nucleophilic attack of the N-tosyl anion on the electrophilic carbon of **69**, facilitates the rate determining intramolecular proton transfer via a stable six-membered intermediate, justifying increased rate in the aza-MBH reactions (Scheme 29). Subsequently there is no need for a resolution step to increase the enantiomeric excess.

This mechanism also shows great similarity to other successful asymmetric MBH variants, although the aza-intermediate **85** does not cyclise to a pyrimidinone derivative **84** as observed in analogous reactions displaying a dioxanone cyclisation intermediate. Intrigued by this observation, the group employed a hexafluoroisopropyl acrylate, instead of the methyl acrylate, in an attempt to facilitate the formation of a cyclisation intermediate due to the efficiency of hexafluoroisopropanoxide as a leaving group. Surprisingly no product was formed, which lead the group to suggest that the basicity of the sulfonylated nitrogen ion may be sufficiently high to promote intermolecular proton transfer via **85** through a six membered transition state, but low enough to prevent the intramolecular nucleophilic attack on the carbonyl of the hexafluoroisopropyl acrylate that would afford the pyrimidinone intermediate.

The group also confirmed that the second intermediate on the catalytic cycle **70** undergoes a retro-aza-MBH reaction forming the aza-enolate **25**, accompanied by acrylate and imine resonances in different concentrations. This supports the observation of Jacobsen et al. of a similar molecule displaying a retro-aza-MBH reaction.



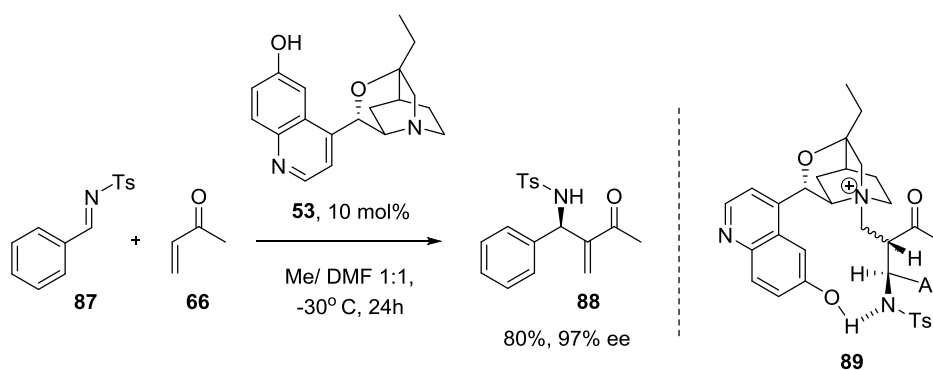
Scheme 29: Mechanistic cycle proposed for the aza-MBH reaction of methyl acrylate with imine, with the inception of the bis-sulfonamide intermediate **85**.

1.3.3. Catalysis of the aza- Morita-Baylis-Hillman Reaction

In general, the nucleophilic N- and P-containing Lewis bases, already discussed as catalysts for the MBH reaction, can also be applied to mediate the aza-MBH reaction. However for the asymmetric aza-MBH reaction, different catalytic systems are incorporated.

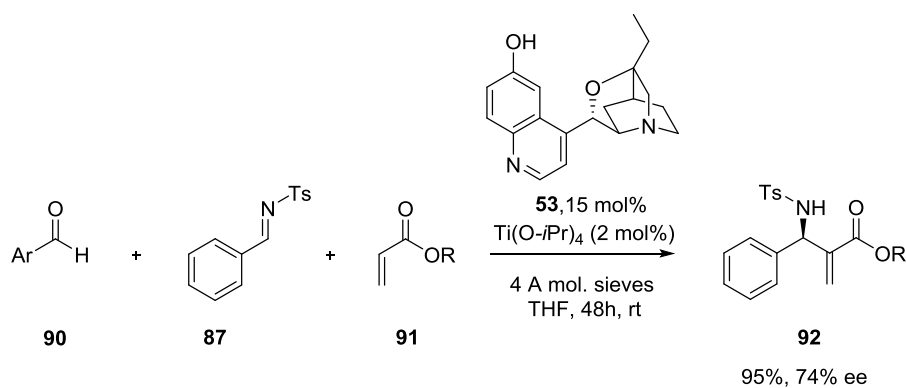
Following on from the pioneering work of Hatekeyama with cinchona alkaloid derivative β -ICD, Shi et al. reported the same catalyst in the asymmetric aza-MBH reaction of tosylimine with MVK or methyl acrylate obtaining high yield and enantioselectivity. As with Hatekeyama, They also rationalised that the key factor for high enantioselectivity is the intramolecular hydrogen bond between the phenolic

hydroxyl group and the nitrogen-centered anion, stabilised by a sulfonyl group to give a relatively rigid transition state **89** (Scheme 30).^[62]



Scheme 30: β -ICD-Catalysed aza-MBH reaction.

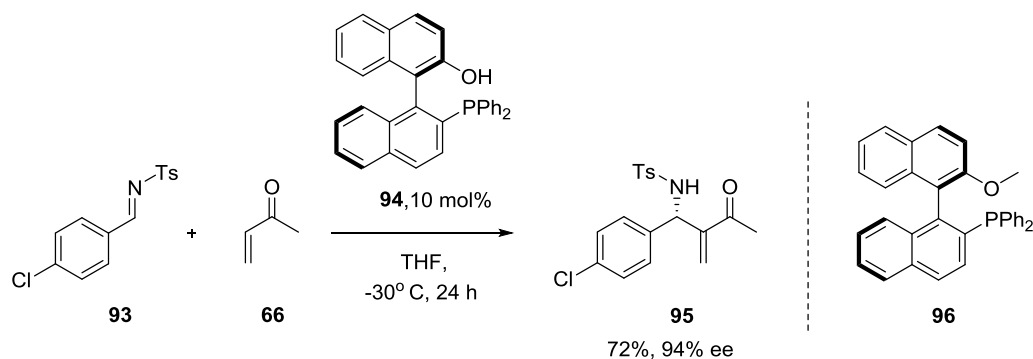
In 2003 Adolfsson et al. also utilised β -ICD and a catalytic amount of $\text{Ti}(\text{O-}i\text{Pr})$ in a three component aza-MBH reaction of aldehyde, tosylamide and activated alkene, with enantioselectivities up to 99% ee (Scheme 31).^[57]



Scheme 31: β -ICD-Catalysed three component aza-MBH reaction.

In 2003 Shi et al. developed one of the most successful chiral bifunctional phosphine-based catalytic systems for the aza-BH reaction.^[63] The binol derivative **94** containing a phosphorus-centered Lewis base and a Brønsted acid moiety was initially tested in the coupling of aromatic tosylaldimines like **93** with simple Michael acceptors like MVK

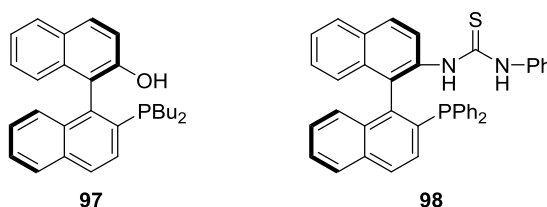
66 and phenyl acrylate to give the corresponding adducts in good yields and high enantioselectivity (Scheme 32).



Scheme 32: aza-MBH reaction catalysed by phosphine BINOL derived catalyst **94**.

They proposed that the Lewis base phosphine initiates the reaction sequence, while the phenolic OH group serves as a Lewis acid to activate the electrophile and to stabilize the phosphonium enolate intermediate through hydrogen bonding. When the hydroxyl group was replaced by a methoxy group, (as in catalyst **96**) significantly reduced catalytic reactivity and enantioselectivity was observed.

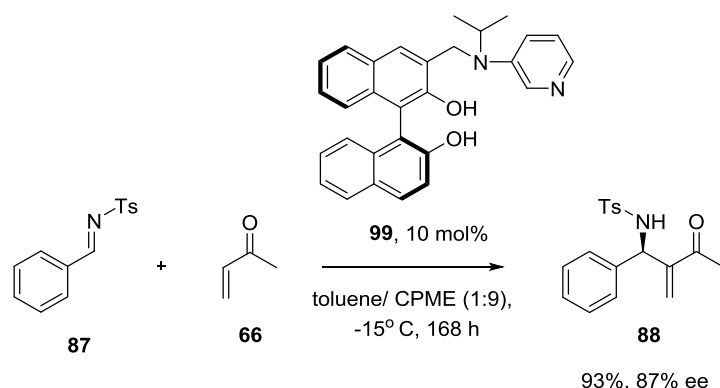
Based on the same 1, 1'-binaphthalene framework, a series of multi/bifunctional catalysts were also developed (Scheme 33). Shi et al. reported BINOL-type bifunctional chiral catalysts which have been incorporated as enantioselective catalysts in the aza-MBH reactions.^[64-65]



Scheme 33: Other BINOL-derived bifunctional catalysts.

Along the same lines, Sasai et al. investigated the reaction of aromatic tosylaldimines like **87** with MVK **66** catalysed by a BINOL-based bifunctional organocatalyst **99** (Scheme 34).^[66] In a mixed solvent system of toluene and CPME, enantioselectivities were obtained in up to 95% ee.

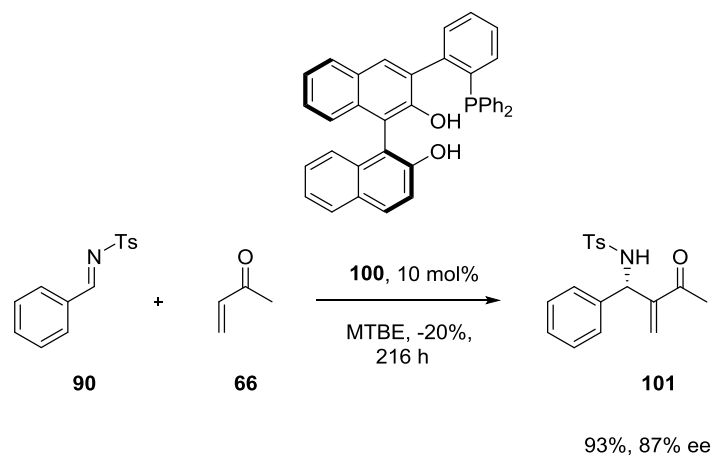
The authors proposed that the reaction is strongly influenced by the exact position of the active units within the catalyst. One pair of the acid-base unit fixes the conformation of the organocatalyst, while the other pair activate the alkyl vinyl ketone in a synergistic interaction promoting the reaction with high enantiocontrol. This theory was supported by molecular orbital calculation of **99**. They also showed that similar catalysts with varying chain length of spacers between the catalytic moieties, and other catalysts with different positions of the pyridine nitrogen relative to the Brønsted acidic group were often inactive or non-selective.



Scheme 34: BINOL-based bifunctional organocatalyst for the aza-MBH reaction.

In 2006 Sasai et al. developed another BINOL-based chiral phosphine catalyst. They attached a phosphine unit through an aromatic ring as a chiral Brønsted acid and tested it in the aza-MBH reaction of imine **90** with MVK **66** affording the corresponding *S*-allylamine **101** in high yield and with excellent enantioselectivity, albeit with a very slow reaction rate (Scheme 35).

When both catalytic moieties of this bifunctional catalyst were positioned where no synergistic interaction between the Lewis base and the Brønsted acid was possible in an intramolecular fashion, the selectivity decreased dramatically.



Scheme 35: The aza-MBH reaction catalysed by **100**.

1.4. Self-assembling catalysts

There are many examples of self-assembled systems where hydrogen-bonding plays a key role, as in enzymes and DNA.^[67] Often, these systems do not contain any metal centres and thus form the basis for organocatalysis. An ambition of this area is to be able to mimic enzymatic processes while simultaneously achieving the same high selectivity and turn-over with a synthetic organocatalytic system. Significant advances have been made in this area in recent years with considerably increased activity in this field due to the many opportunities organocatalytic systems may offer in terms of catalyst design. However control of self-assembly of small molecules and subsequent use in catalysis is a relatively unexplored area.

A modular system for organocatalysis, rather than a single molecule containing both catalytic and asymmetry inducing regions, offers several improvements. Large molecule synthesis usually requires a long multi-step synthesis, thus resulting in low yields. In a binary system, it is possible to construct the two components individually, generating both modules in a relatively low number of steps and in high yields. Modification of the catalyst structure only needs simple replacement of the modules, with the potential to build a library of diverse organocatalysts.

A literature search revealed that there are few examples of self-assembly of small molecules. However in 1990 Kelly et al. reported a host-guest system, in which substrates are bound through hydrogen-bonding interactions that align the components for reaction (Figure 1).^[68] These systems provided an excellent starting point for the design of a self-assembling system, through a hydrogen-bonding array.

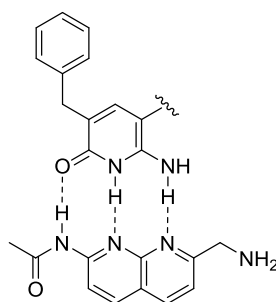


Figure 1: Guest-host interaction investigated by Kelly et al.

Another piece of inspiration came from Clarke et al. who in 2007; reported the first example of the self-assembly of prolinamide-based organocatalysts for the Michael addition of ketones to nitroalkenes, wherein the addition of achiral pyridinone derivatives to a chiral organocatalyst host can transform an unselective chiral prolinamide catalyst into a highly effective one through hydrogen-bonding interactions. [69]

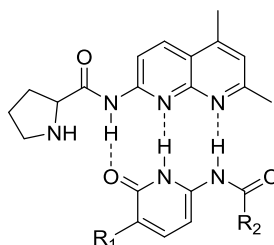


Figure 2: Clarke's self-assembled modules with catalyst and co-catalyst

One drawback however, in this system is that the catalytic centre is proximal to the assembly array and this may result in interference with either the catalytic or assembly event. Our approach, will differ from Clark and aim to bring together two molecules with unique roles, harnessing hydrogen-bonding as an assembly mechanism (Figure 3). To achieve this goal, following optimisation of the hydrogen-bonding array, we can then investigate catalytic applications through simple changes on the catalytic site or the selectivity induction point, rather than changing elements contributing to the hydrogen-bonded scaffold.

1.5. Research Objectives

Recently, considerable efforts have been dedicated to the development of asymmetric MBH/aza-MBH reactions. Significant progress has been made in the design and synthesis of new chiral catalysts based on the concept of bi/multifunctionality achieving high enantioselectivity.

However, as of yet there is no single catalyst which is capable of tolerating a broad range of substrates. Thus, the development of effective catalysts for the asymmetric MBH/aza-MBH reactions that are applicable to all or at least to most of the commonly used activated alkenes and electrophiles is of the utmost importance. These new advances in an asymmetric version can make this reaction a valuable chiral source for asymmetric synthesis of various enantiomerically pure molecules of biological importance.

All successful chiral catalysts to date contain at least two groups with distinct functionalities within the same molecule, generally a Brønsted acid and a Lewis basic centre. In this bifunctional strategy, these units can be situated onto a chiral backbone to facilitate a synergistic interaction between the functional groups in the MBH reaction cycle. The Lewis base functionality serves to initiate the Michael addition step of the reaction, while the Brønsted acidity stabilizes the zwitterionic intermediates, promoting the subsequent aldol and proton transfer-elimination step. Positioning of both catalytically active sites in close proximity with favourable geometry facilitates asymmetric addition, analogous to enzyme catalysis. Just as enzymes control incoming reagents and catalytic residues in ideal geometries, the combination of basic and acidic sites within a small molecule could provide a similar scenario. These bifunctional catalysts may represent a solution for synthetic chemists in the development of chemical catalysts with enzyme-like reactivity and selectivity.

The primary objective of this project is to realise the development of an effective stereoselective MBH catalyst. In our system, a Catalytic Module, CM (with both a catalytic centre and a component at which hydrogen-bonding can occur), and a Selectivity Inducing Module, SIM (consisting of both hydrogen-bonding scaffold and a site through which selectivity, such as enantioselectivity, may be induced), are bound through hydrogen-bonding interactions to give a modular catalyst (Figure 3).

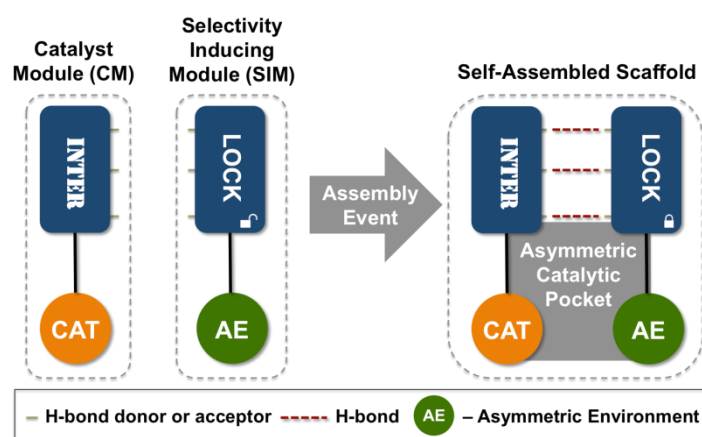


Figure 3. Modular representation of the self-assembling catalyst.

The focus of this research will be on design and preparation of this system. Computational modelling will be used in the design of the module predicting its interaction. Following design of the modules, they will be synthesised using robust organic syntheses to produce multigram quantities of both modules. Following synthesis, the catalyst will be applied in test MBH reactions for initial catalysis screening.

References (i)

- [1] P. I. Dalko, L. Moisan *Angewandte Chemie-International Edition* **2001**, *40*, 3726-3748.
- [2] P. I. Dalko, L. Moisan *Angewandte Chemie-International Edition* **2004**, *43*, 5138-5175.
- [3] K. A. Ahrendt, C. J. Borths, D. W. C. MacMillan *J. Am. Chem. Soc.* **2000**, *122*, 4243-4244.
- [4] S. Pizzarello, A. L. Weber *Science* **2004**, *303*, 1151-1151.
- [5] U. Eder, G. Sauer, R. Weichert *Angewandte Chemie-International Edition* **1971**, *10*, 496.
- [6] Z. G. Hajos, D. R. Parrish *J. Org. Chem.* **1974**, *39*, 1615-1621.
- [7] B. List, R. A. Lerner, C. F. Barbas *J. Am. Chem. Soc.* **2000**, *122*, 2395-2396.
- [8] J. Seayad, B. List *Organic & Biomolecular Chemistry* **2005**, *3*, 719-724.
- [9] M. S. Taylor, N. Tokunaga, E. N. Jacobsen *Angewandte Chemie-International Edition* **2005**, *44*, 6700-6704.
- [10] W. S. Jen, J. J. M. Wiener, D. W. C. MacMillan, *J. Am. Chem. Soc.* **2000**, *122*, 9874-9875.
- [11] S. P. Brown, N. C. Goodwin, D. W. C. MacMillan *J. Am. Chem. Soc.* **2003**, *125*, 1192-1194.
- [12] W. Notz, F. Tanaka, S. Watanabe, N. S. Chowdari, J. M. Turner, R. Thayumanavan, C. F. Barbas *J. Org. Chem.* **2003**, *68*, 9624-9634.
- [13] B. List, P. Pojarliev, H. J. Martin *Org. Lett.* **2001**, *3*, 2423-2425.
- [14] J. C. Ruble, J. Tweddell, G. C. Fu *J. Org. Chem.* **1998**, *63*, 2794-2795.
- [15] M. A. Calter, R. K. Orr, W. Song *Org. Lett.* **2003**, *5*, 4745-4748.
- [16] A. G. Wenzel, E. N. Jacobsen *J. Am. Chem. Soc.* **2002**, *124*, 12964-12965.
- [17] P. Vachal, E. N. Jacobsen *Org. Lett.* **2000**, *2*, 867-870.
- [18] Y. Huang, K. A. Unni, A. N. Thadani, V. H. Rawal, *Nature (London)*, **2003**, *424*, 146.
- [19] T. Akiyama, Y. Tamura, J. Itoh, H. Morita, K. Fuchibe *Synlett* **2006**, 141-143.

- [20] J. Seayad, A. M. Seayad, B. List, *J. Am. Chem. Soc.* **2006**, *128*, 1086-1087.
- [21] T. Akiyama, Y. Tamura, J. Itoh, H. Morita, K. Fuchibe, *Synlett* **2006**, 141-143.
- [22] M. Shibasaki, H. Sasai, T. Arai, *Angew. Chem. Int. Ed.* **1997**, *36*, 1236-1256.
- [23] T. Okino, Y. Hoashi, Y. Takemoto *J. Am. Chem. Soc.* **2003**, *125*, 12672-12673.
- [24] T. Marcelli, R. N. S. van der Haas, J. H. van Maarseveen, H. Hiemstra, *Synlett* **2005**, 2817-2819.
- [25] S. B. Tsogoeva, D. A. Yalalov, M. J. Hateley, C. Weckbecker, K. Huthmacher *European Journal of Organic Chemistry* **2005**, 4995-5000.
- [26] C. G. Lima-Junior, M. L. A. A. Vasconcellos *Bioorg. Med. Chem.* **2012**, *20*, 3954-3971.
- [27] (a) K. Morita, Z. Suzuki, H. Hirose *Bull. Chem. Soc. Jpn.* **1968**, *41*, 2815. (b) A. B. Baylis, M. E. D. Hillman, *German Chem. Abstr.* **1972**, 77.
- [28] S. E. Drewes, N. D. J. Emslie *Chem. Soc., Perkin Trans.* **1982**, 2079.
- [29] Hoffman and Rabe *Helv. Chim. Acta* **1983**, *67*, 413.
- [30] S. E. Drewes, G. H. P. Roos *Tetrahedron* **1988**, *44*, 4653-4670.
- [31] (a) J. S. Hill, N. S. Isaacs *Tetrahedron Lett.* **1986**, *27*, 5007-5010. (b) J. S. Hill, N. S. Isaacs *Journal of Physical Organic Chemistry* **1990**, *3*, 285-288.
- [32] M. L. Bode Kaye *Tetrahedron Lett.* **1991**, *32*, 5611.
- [33] S. E. Drewes, O. L. Njamela, N. D. Emslie, N. Ramesar, J. S. Field *Synthetic Communications* **1993**, *23*, 2807-2815.
- [34] L. S. Santos, C. H. Pavam, W. P. Almeida, F. Coelho, M. N. Eberlin *Angewandte Chemie-International Edition* **2004**, *43*, 4330-4333.
- [35] K. E. Price, S. J. Broadwater, B. J. Walker, D. T. McQuade *J. Org. Chem.* **2005**, *70*, 3980-3987.
- [36] K. E. Price, S. J. Broadwater, H. M. Jung, D. T. McQuade *Org. Lett.* **2005**, *7*, 147-150.
- [37] V. K. Aggarwal, S. Y. Fulford, G. C. Lloyd-Jones *Angewandte Chemie-International Edition* **2005**, *44*, 1706-1708.
- [38] V. K. Aggarwal, D. K. Dean, A. Mereu, R. Williams *J. Org. Chem.* **2002**, *67*, 510-514.
- [39] D. Roy, R. B. Sunoj *Org. Lett.* **2007**, *9*, 4873-4876.

- [40] R. Robiette, V. K. Aggarwal, J. N. Harvey *J. Am. Chem. Soc.* **2007**, *129*, 15513-15525.
- [41] G. W. Amarante, H. M. S. Milagre, B. G. Vaz, B. R. V. Ferreira, M. N. Eberlin, F. Coelho *J. Org. Chem.* **2009**, *74*, 3031-3037.
- [42] G. W. Amarante, M. Benassi, H. M. S. Milagre, A. A. C. Braga, F. Maseras, M. N. Eberlin, F. Coelho *Chemistry-a European Journal* **2009**, *15*, 12460-12469.
- [43] D. Cantillo, C. O. Kappe *J. Org. Chem.* **2010**, *75*, 8615-8626.
- [44] T. Kataoka, T. Iwama, S. Tsujiyama, T. Iwamura, S. Watanabe *Tetrahedron* **1998**, *54*, 11813-11824.
- [45] V. K. Aggarwal, I. Emme, S. Y. Fulford *J. Org. Chem.* **2003**, *68*, 692-700.
- [46] D. Basavaiah, D. S. Sharada, N. Kumaragurubaran, R. M. Reddy *J. Org. Chem.* **2002**, *67*, 7135-7137.
- [47] K. Y. Lee, J. H. Gong, J. N. Kim *Bulletin of the Korean Chemical Society* **2002**, *23*, 659-660.
- [48] S. Z. Luo, B. L. Zhang, J. Q. He, A. Janczuk, P. G. Wang, J. P. Cheng *Tetrahedron Lett.* **2002**, *43*, 7369-7371.
- [49] J. L. Methot, W. R. Roush *Advanced Synthesis & Catalysis* **2004**, *346*, 1035-1050.
- [50] Y. L. Shi, M. Shi *Tetrahedron* **2006**, *62*, 461-475.
- [51] M. Shi, Y. H. Liu *Organic & Biomolecular Chemistry* **2006**, *4*, 1468-1470.
- [52] Y. Iwabuchi, M. Nakatani, N. Yokoyama, S. Hatakeyama, *J. Am. Chem. Soc.* **1999**, *121*, 10219-10220.
- [53] N. T. McDougal, S. E. Schaus *J. Am. Chem. Soc.* **2003**, *125*, 12094-12095.
- [54] Y. Sohtome, A. Tanatani, Y. Hashimoto, K. Nagasawa *Tetrahedron Lett.* **2004**, *45*, 5589-5592.
- [55] K. Yuan, L. Zhang, H. Song, Y. Hu, X. Wu *Tetrahedron Lett.* **2008**, *49*, 6262-6264.
- [56] P. Perlmutter, C. C. Teo *Tetrahedron Lett.* **1984**, *25*, 5951-5952.
- [57] D. Balan, H. Adolfsson *Tetrahedron Lett.* **2003**, *44*, 2521-2524.
- [58] I. T. Raheem, E. N. Jacobsen *Advanced Synthesis & Catalysis* **2005**, *347*, 1701-1708.
- [59] P. Buskens, J. Klankermayer, W. Leitner *J. Am. Chem. Soc.* **2005**, *127*, 16762-16763.

- [60] T. Yukawa, B. Seelig, Y. Xu, H. Morimoto, S. Matsunaga, A. Berkessel, M. Shibasaki *J. Am. Chem. Soc.* **2010**, *132*, 11988-11992.
- [61] T. Regiani, V. G. Santos, M. N. Godoi, B. G. Vaz, M. N. Eberlin, F. Coelho *Chemical Communications* **2011**, *47*, 6593-6595.
- [62] Y. X. M. Shi *Angew. Chem. Int. Ed.* **2002**, *41*, 4507.
- [63] M. Shi, L. H. Chen *Chemical Communications* **2003**, 1310-1311.
- [64] Z. Lei, X. Liu, M. Shi, M. Zhao *Tetrahedron-Asymmetry* **2008**, *19*, 2058-2062.
- [65] Y. Shi, M. Shi *Advanced Synthesis & Catalysis* **2007**, *349*, 2129-2135.
- [66] K. Matsui, S. Takizawa, H. Sasai *J. Am. Chem. Soc.* **2005**, *127*, 3680-3681.
- [67] D. Philp, J. F. Stoddart *Angew. Chem., Int. Ed. Engl.* **1996**, *35*, 1155.
- [68] T. R. Kelly, G. J. Bridger, C. Zhao *J. Am. Chem. Soc.* **1990**, *112*, 8024-8034.
- [69] M. L. Clarke, J. A. Fuentes *Angew. Chem. Int. Ed.* **2007**, *46*, 930.

2. Results and Discussion

2.1. General considerations

The synthetic plan was devised with three key aspects to consider: a) the hydrogen-bonding array, b) incorporation of a suitable catalyst and c) inclusion of a component to induce selectivity. The modular catalysts can thus be prepared with a common hydrogen array, but simple substitution of catalyst or symmetry-inducing functionality can produce modular catalysts for a broad range of reaction types. The hydrogen-bonding system chosen for this investigation is based around the amidonaphthyridine/pyridinone hydrogen bonding scaffolds proposed by Kelly et al. and utilised by Clarke et al. (Figure 1 & 2). However, while Clarke has demonstrated the incorporation of a proline catalyst in a bimolecular system, location of the chiral centre directly adjacent to the hydrogen-bonding array may account for the selectivity observed. To ensure that this is not the case in the designed catalyst, it was planned to ensure that there was a suitable linker separating the catalyst moiety from the hydrogen-bonding scaffold.

The MBH reaction was chosen as a model reaction to demonstrate proof-of-concept for the modular catalyst system, and thus the CM and SIM were chosen to best suit this chemistry. For the catalyst, a quinuclidine moiety was chosen, as quinuclidine (and quinuclidinol) have been shown to greatly enhance the MBH reaction due to their increased nucleophilicity with respect to other amine bases.^[1] Such cyclic tertiary amines are substantially more nucleophilic than the corresponding open structures, with decreased steric hindrance ensured by the locked structure around the nitrogen atom.

Previous studies have demonstrated that hydroxyl groups are effective co-catalysts in the MBH reaction, especially phenolic hydroxyl groups.^[2] They enhance the rate through stabilisation of the zwitterionic intermediates and have been extensively utilised in BINOL-derived asymmetric catalysts for the MBH/ aza-MBH reactions.

2.2. Computational studies

Following identification of suitable components, CM and SIM structures were proposed that should come in close proximity to facilitate asymmetric addition following a self-assembly event (Figure 4). Computational investigations looking at structure optimisations and frequency calculations at DFT//B3LYP/6-31+G(d,p) were used to predict likely interactions. The SIM and CM were initially optimised individually, scanning through possible conformations at five degree intervals to find the lowest energy conformation. The CM was optimised with and without the quinuclidine component, as the catalytic centre should be sufficiently distant that it will not affect the interaction between the two modules.

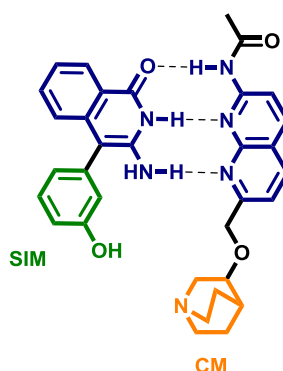


Figure 4: Our proposed self-assembled catalyst.

Following individual geometry optimisations, the modules were placed together and optimised. When placed in close proximity to mimic binding, the modules pushed apart, though they remained close enough together to indicate atomic interactions. Additionally, when the modules were placed far beyond interacting distances, they came together and achieved a similar geometry.

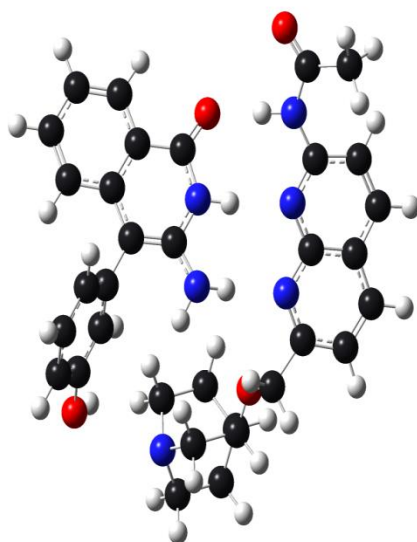


Figure 5: Structures of the proposed CM and SIM

Frequency calculations were run on this optimised structure to verify that it was a transition state. The frequency calculation yielded one negative eigenvalue (one imaginary frequency), verifying the transitional nature of the complex. The resulting transition state displayed one eigenvalue at -42.08cm^{-1} , corresponding to a true transition state.

An intrinsic reaction coordinate (IRC) calculation then verified that the transition state emerged from the two modules converging from a distance greater than interaction distance. The distance between the SIM oxygen and the CM hydrogen was found to be 1.79 \AA , while the hydrogen attached to the SIM heterocyclic nitrogen was separated from the CM heterocyclic nitrogen by 2.02 \AA and, finally, the hydrogen attached to the SIM amine functionality was 2.09 \AA from the second CM heterocyclic nitrogen (Figure 6). While these distances do not indicate that the two modules are bound, they are well within atomic distances known to interact.

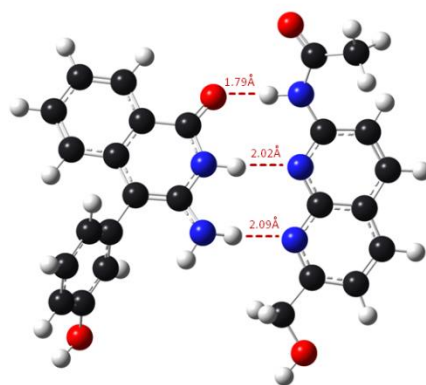


Figure 6: Self-assembly with bond distances

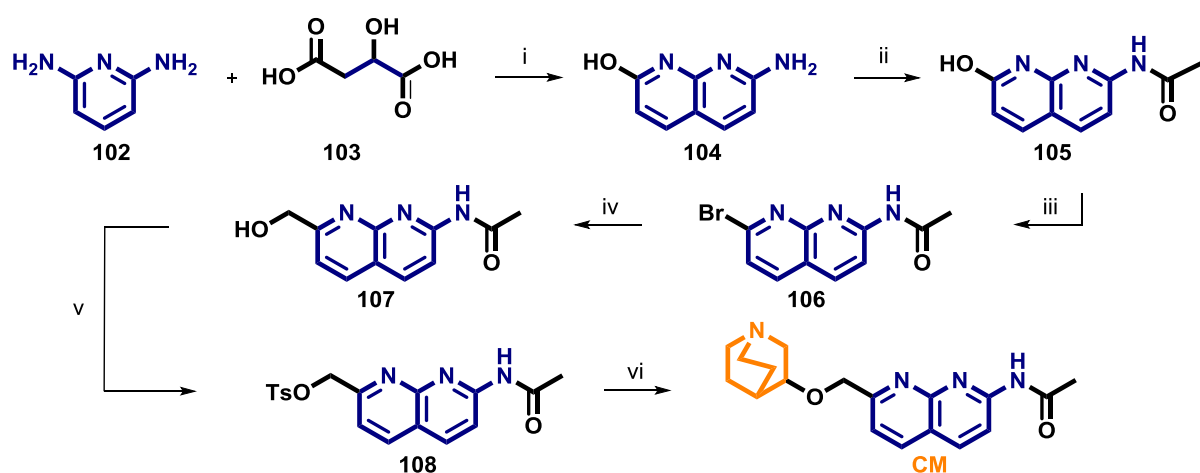
From these preliminary calculations, the system shown in Figures 5 and 6 above should engage in suitable hydrogen-bond interactions. We anticipate that the module could bring a substrate in close proximity to the phenolic proton shuttle while still allowing the structural freedom necessary to tune enantiomeric selectivity. Importantly, computational investigations showed that optimum interaction in the MBH transition state would be achieved using (R)-(-)-quinuclidinol in the CM.

2.3. Synthetic strategy

Following identification of the proposed CM and SIM structures, synthetic routes were devised based on literature procedures. Only steps which had a minimum published yield of 60% or above with commercially available starting materials were considered. Each step of the synthesis was initially performed on ~ 1 mmol scale, and subsequently scaled up if successful.

2.3.1. Synthesis of the CM

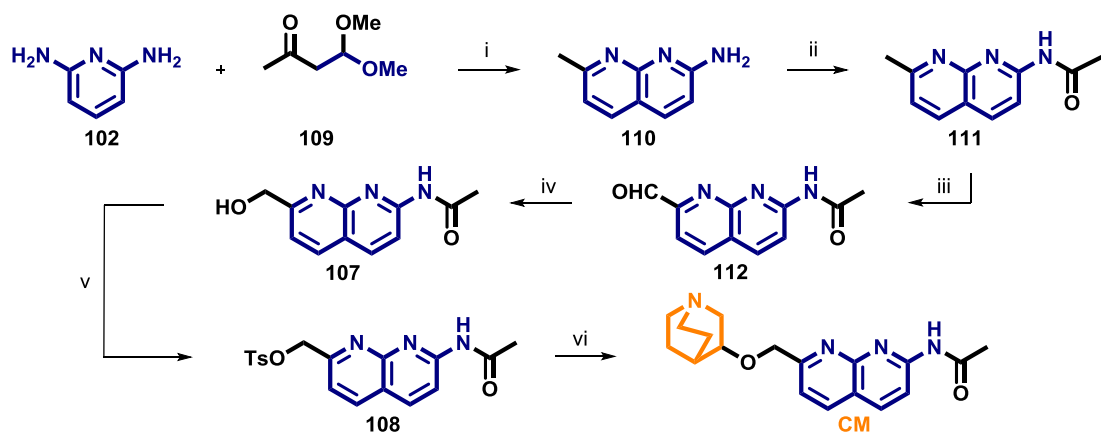
As shown in Scheme 36, the original synthetic route devised was a 6-step synthesis, utilising a ring-forming reaction from the literature to construct the amidonaphthyridine structure in the first step (i). Following acetylation (ii), it was proposed to convert the hydroxyl group to a bromide using phosphorus oxybromide (iii) and to extend the side chain to a hydroxymethyl using DMF and a reduction step (iv). This would then be converted to a tosyl leaving group (v) to then undergo a substitution reaction using quinuclidinol producing the desired CM (vi).



Scheme 36: Proposed synthesis of catalytic module, CM.

(i) H_2SO_4 , 110 °C, 2-3 h; (ii) Ac_2O , 140 °C; (iii) POBr_3 , 95 °C, 1-2 h; (iv) BuLi , toluene, -78 °C, 2 h then DMF/NaBH_4 ; (v) TsCl , pyridine; (vi) 3-quinuclidinol then NaH .

Unfortunately, early into the synthesis it was found that step iii did not proceed as proposed. Subsequently a paper describing the same reaction was found, also detailing that the reaction was unreactive at room and elevated temperature.^[3] As a consequence the synthesis was revised and an alternative route proposed, wherein the bromide was replaced by an aldehyde **112** (Scheme 37). This could then be easily reduced to the desired alcohol **107**. Construction of the methyl-amidonaphthyridine **110** could be achieved using a similar literature procedure as used in Scheme 36, and the acetylated product **111** could be converted to an aldehyde using selenium dioxide. Reduction to the alcohol (iv) should proceed readily and following tosylation (v) the quinuclidinol catalyst could be incorporated as initially planned.

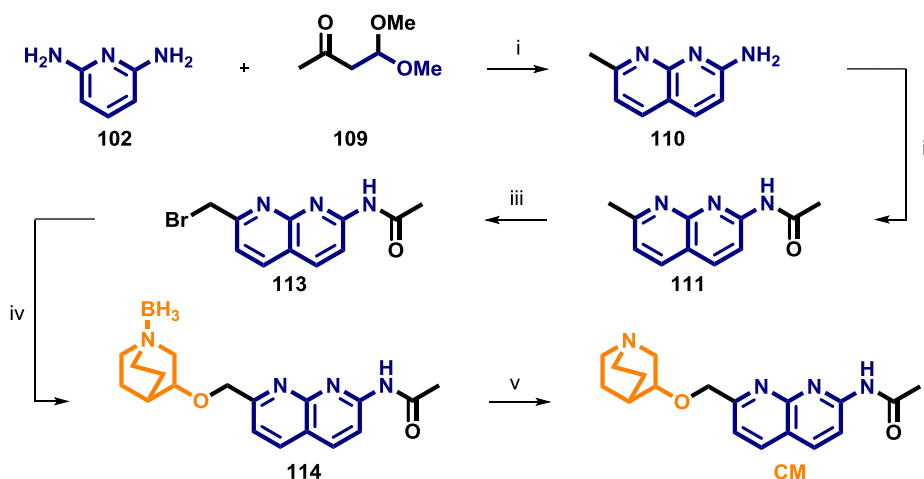


Scheme 37: Revised synthesis of the CM via aldehyde **112**.

(i) H_3PO_4 , 90-115 °C, 3 h; (ii) Ac_2O , 80 °C, 12 h; (iii) SeO_2 , Dioxane, 50-55 °C, 4 h; 70% (iv) NaBH_4 , EtOH, 0 °C, 3-4 h; (v) NaH , -20 °C, 16 h., then TsCl , rt, 1 h; (vi) 3-quinuclidinol then NaH .

However, further difficulties were encountered at step v of this synthesis. While ^1H NMR spectroscopic analysis of the crude product showed that the desired tosylated product had formed, it appeared that the product was completely unstable and decomposed to a black solid over time, which could not be characterised.

Following this, it was decided that a different leaving group would need to be employed. After a literature search, bromine was chosen as replacement (Scheme 38). Again, the core methyl-amidonaphthyridine structure could be constructed as per Scheme 37, but the acetylated product **111** could be brominated using *N*-Bromosuccinimide. Although a reduced yield was anticipated, direct addition of bromine to **111** would reduce the synthesis by two synthetic steps.



Scheme 38: Final synthetic route to the CM.

(i) H_3PO_4 , 90-115 °C, 3 h; 96% (ii) Ac_2O , 80 °C, 12 h; 87% (iii) NBS, $[\text{C}_6\text{H}_5\text{C}(\text{O})]_2\text{O}_2$, DMC, 110 °C, 0.25 h; 28% (iv) (R)-N-Boranyl-1-aza bicyclo [2.2.2] octan-3-ol, NaH, DMF, rt, 1h; 34% (v) 1.25M HCl-MeOH 0 °C, 0.5h, rt, 0.5 h, 37%.

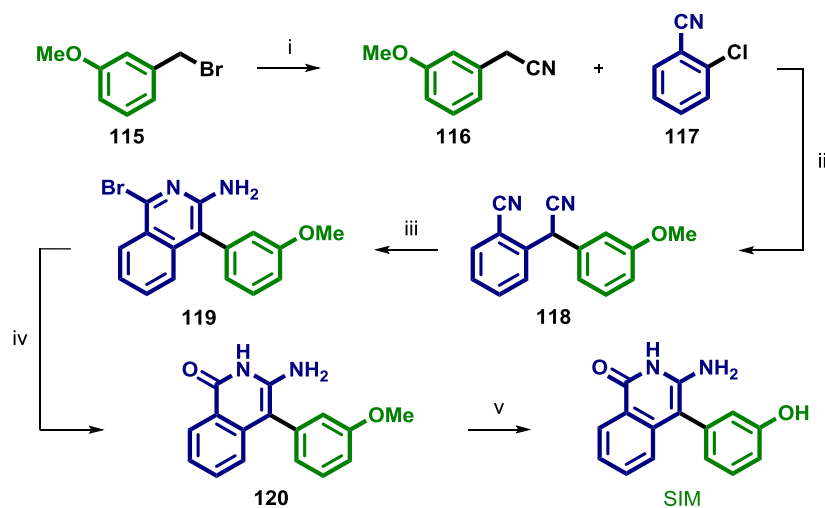
Gratifying, using this route the CM was prepared, albeit in a low yield. The initial design criteria had intended for the synthesis to be high-yielding and readily scalable at each step and this was not the case for the final synthesis. As anticipated, the free radical bromination step (iii) presented some difficulties but optimisation of the reaction time ensured the best possible yields (up to 30%). A reaction time of no more than 15 mins was found to be optimum, as prolonged reaction times resulted in a dibromination of **111**. However, purification of the compound presented a challenge as the crude product contained starting material, the desired monobromination product **113** and the dibromination product. Initial purification was employed with a mobile phase of 2% MeOH/ DCM on silica as this gave the best separation of the components on TLC. However, using these conditions in flash column chromatography showed that the bromination products eluted quickly and did not separate well (although the starting material was removed). Due to the rapid nature in which the dibromination was collected, a re-evaluation of solvents was performed on a small scale and EtOAc/DCM was found to be the best mobile phase to elute the dibromination product at a rate which kept **113** on the column. Following removal of the dibromination by-product, **113** was collected in 2-4% MeOH/DCM.

Furthermore, initially step iv was performed overnight, but analysis by ^1H NMR spectroscopy showed that deacetylation of the amide had occurred. Reducing the time scale of the reaction increased the yield of **114**, however there was always presence of the unacetylated product also. Due to the use of sodium hydride in step v in Scheme 36 over a period of hours, where no deacetylation was observed, it was assumed that it was the alkoxide of 3-quinuclidinol that was causing the observed deacetylation. Optimisation of purification allowed separation of the desired product from the deacetylated by-product, which could then be reacylated using acetyl chloride (although full conversion to **114** was never achieved, even at reduced temperature).

In the final synthesis, it was necessary to protect the quinuclidinol nitrogen using borane prior to introduction of the catalyst (iv). In the last step of the synthesis (v), a solution of hydrogen chloride in methanol was employed to remove the BH_3 protecting group. Again, optimisation of reaction time was crucial, 30 mins was found to be the optimum time scale for the reaction as prolonged time resulted in deacetylation of the amide again. To ensure the free nitrogen was deprotonated, a basic work up was performed after the reaction. Initially sodium hydroxide was applied, however ~20% yields were obtained, with any by-products formed being uncharacterisable. When a weaker base for work up was employed, yields increased on small scale up to 58% however. Potassium phosphate tribasic was chosen as the weaker base as its $\text{p}K_{\text{a}}$ of 12 was a perfect choice to deprotonate the quinuclidine derivative with a $\text{p}K_{\text{a}}$ of 11. ^[4] Due to the nucleophilic nature of the CM, extra care was taken to prevent any alkylation on the nitrogen in any alkyl solvents. Pleasingly none has been observed while working with the compound.

2.3.3. Synthesis of SIM

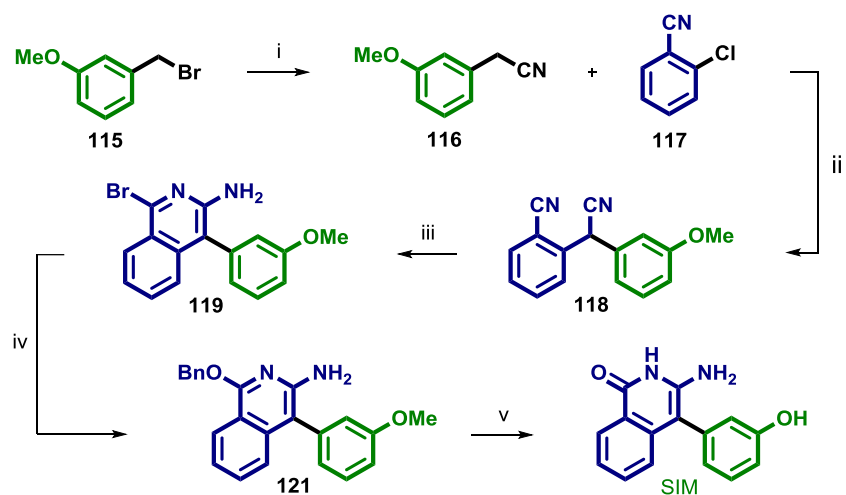
As shown in Scheme 39, the original synthetic route devised was a 5-step synthesis, in which the desired symmetry-inducing functionality was incorporated early in the synthesis (steps i-ii), followed by formation of the 3-aminoquinoline scaffold using a literature procedure. This would then be converted to the desired pyridinone using CuI/DMEDA in microwave conditions and finally deprotection of the phenolic hydroxyl group would give the desired SIM.



Scheme 39: Proposed synthesis of asymmetrical environment module SIM.

(i) NaCN; (ii) KO^tBu, DMF, rt, 1 h; (iii) HBr/HOAc; (iv) CuI/DMEDA, K₃PO₄, H₂O, 180 °C, 30 min; (v) 1-decanethiol, KO^tBu, DMF, 110 °C, 3-4h.

However, due to the unavailability of a microwave for Scheme 39 (iv), this step was revised. A search of the literature showed that a benzyloxy group could be introduced instead of the bromide. This was a favourable functional group for the next step as now both the benzyl and methyl could be removed from the aryl ethers in the last step, simply by increasing the equivalents of boron tribromide employed (Scheme 40).



Scheme 40: Final synthesis of the SIM.

(i) NaCN, EtOH, 80 °C, 2 h; 98% (ii) KO^tBu, DMF, rt, 1 h; 95% (iii) HBr/HOAc, rt, 2 h; 62% (iv) BnOH, NaH, DMF, 0° C; 73% (v) BBr₃, DCM, 24 h, rt; 62%.

2.4. Assessment of assembly event

Following preparation of the CM and SIM components, the next step in development of a self-assembling catalyst was to investigate the hydrogen bonding of the modules. To do this, several NMR spectroscopic tests were carried out.

2.4.1. Dosy Test

Due to the formation of hydrogen bonding (which is considerably larger than Van de Waals forces) between CM and SIM, the translational diffusion movements of these two compounds would be hindered,^[5] and possibly merge into a single diffusion movement of the new-formed dimer. Hence, by measuring the variation of diffusion coefficients of the two components, the possible formation of the hydrogen bonding could be directly detected.

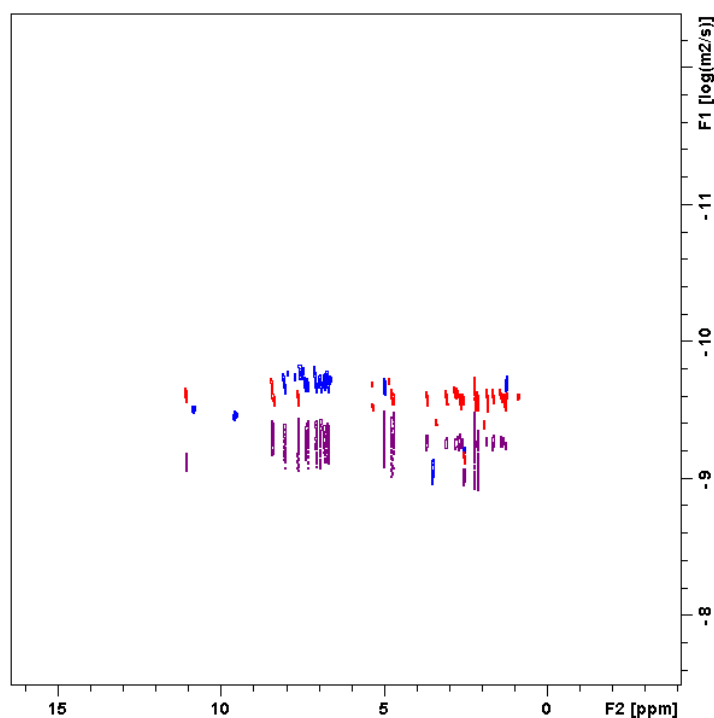


Figure 7: Dosy spectrum of CM and SIM in DMSO-d₆

Experimental setup: BPGPDSTE with LED and Presaturation;

Diffusion time: 49.5 ms; Gradient Length: 4.4 ms.

As shown in Figure 7, the diffusion coefficients of SIM (blue) and CM (red) are 1.982×10^{-10} and 2.506×10^{-10} respectively. However, the diffusion coefficient of the mixture (purple) solution has a single value around 5.470×10^{-10} , this is the direct evidence of the formation of dimer in the sample.

2.4.2. TV NMR Test

Due to the Born-Oppenheimer approximation's breakdown in the case of internal energy's influence over hydrogen bonding,^[6] a temperature variation NMR test of the compound would be a good indication of the existence of hydrogen bonding in the sample.

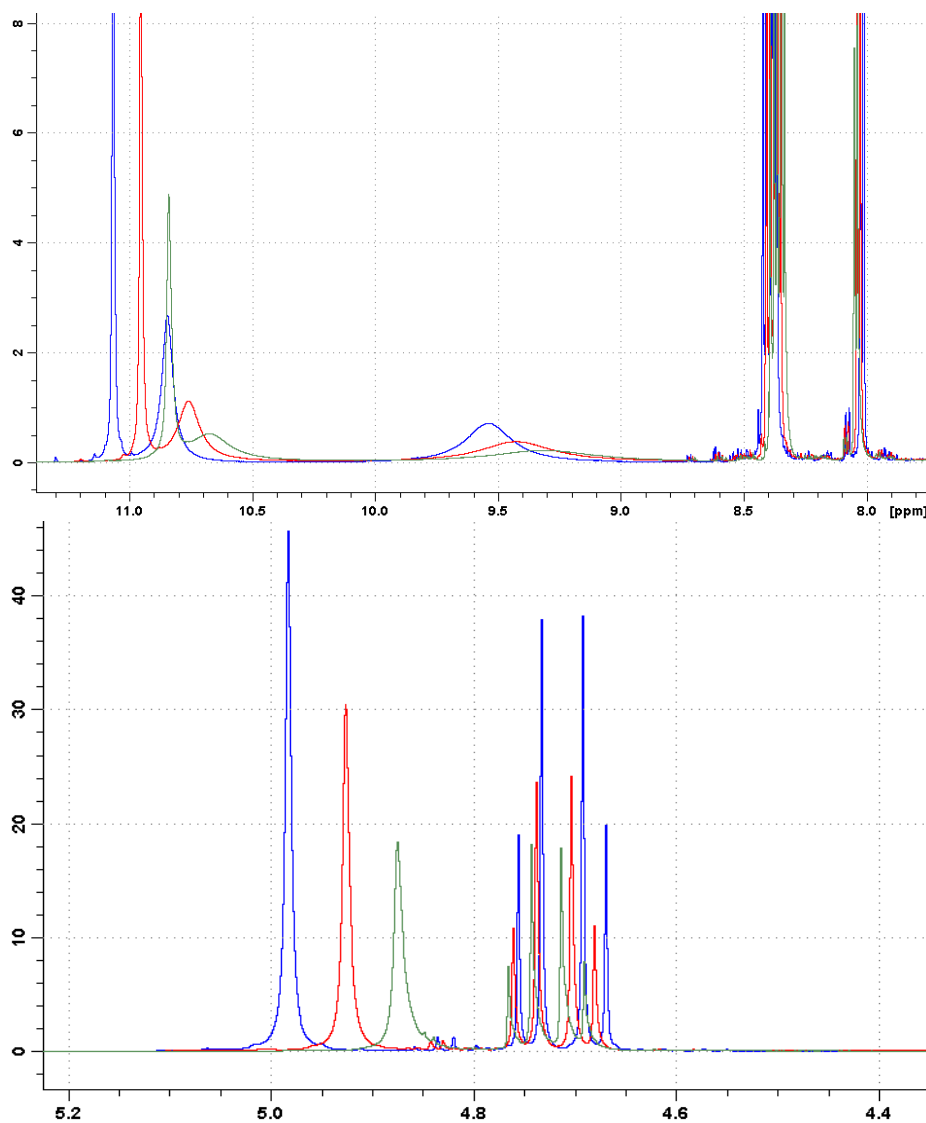


Figure 8: TV NMR Test of CM and SIM in DMSO-d₆

Experimental detail: 293 K (blue), 313 K (red), 333 K (green)

As demonstrated in Figure 8, the large change (around 0.1 ppm) in the chemical shifts of these protons at assumed hydrogen bonding positions, in comparison to the small shifts (around 0.01 ppm) for other protons in the compound (caused by the thermal induced increment of the vibrational energy), is a strong proof of the presence of hydrogen bonding at these positions. However, the major drawback of this method is the inability to correlate the hydrogen bonding with the formation of dimer.

2.4.3. Simple Chemical Shift Demonstration Test

As discussed by many previous studies,^[7] chemical shift could be largely affected by the presence of hydrogen bonding, and due to the de-shielding effect other bonding nucleus casted on the proton, normally the formation of hydrogen bonding would shift $\delta(H)$ to low field.

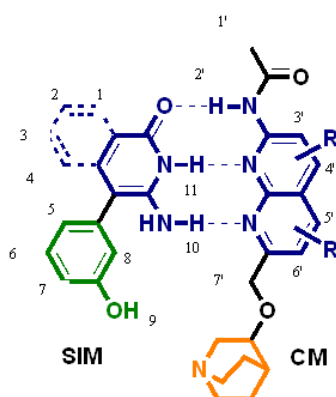


Figure 9: Relevant interactions between CM and SIM

As demonstrated in Figure 10, the $\delta(H)$ of 2', 10 and 11 undertake a shift of 0.02 ppm, 0.03 ppm, 0.03 ppm toward the low field, respectively, this is consistent with observation from other studies in regard to hydrogen bonding effect on the chemical shift of the bonding protons.^[8, 9]

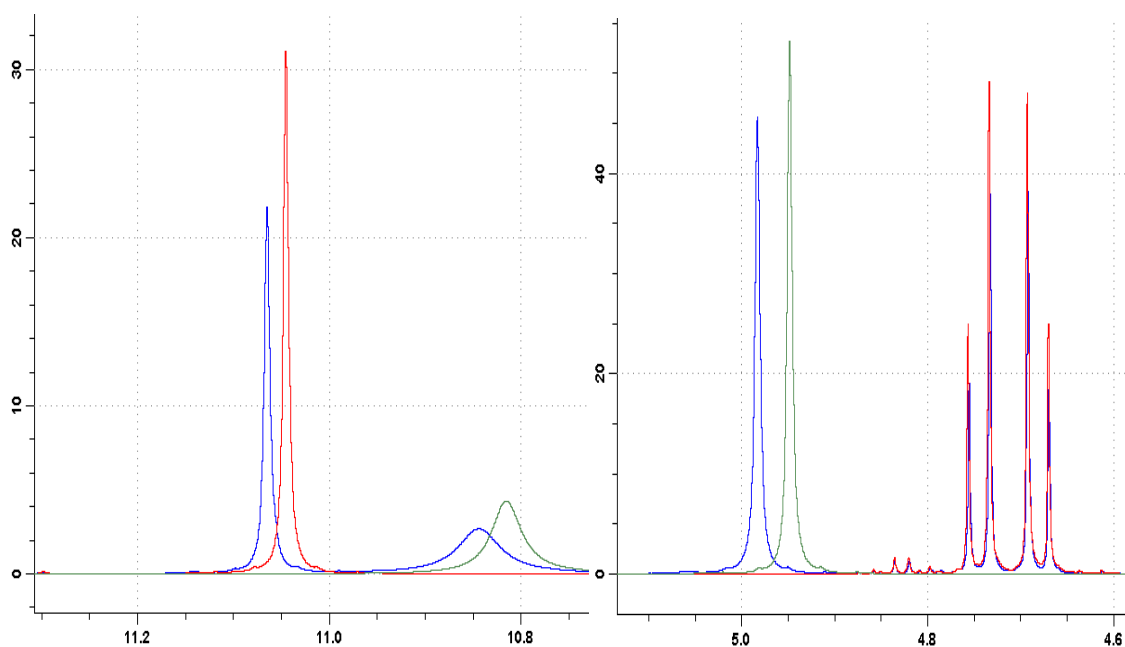


Figure 10: Change in chemical shift during the simple chemical shift demonstration test in DMSO-d₆

Experimental Detail: CM (red), SIM (green), Mixture (blue).

2.4.4. Hydrogen bonding equilibrium disturbing test by NMR

As several other papers^[10, 11] have indicated, the formation of hydrogen bonding could cause a change in chemical shift of the interested protons, due to the de-shielding effect the bonding nuclei has on the target proton. Hence, a disruption of hydrogen bonding equilibrium would have an effect on the observed chemical shift of proton assumed to be undergoing hydrogen bonding.

Generally, two sets of experiments could be carried out in this respect. One is by varying the substrate's concentration, the template's hydrogen-bonding proton would have a different chemical shift in regard to this concentration differences. The second approach is by varying the concentration of the whole mixture (namely both compounds), a new equilibrium of hydrogen bonding would be formed, which would further vary the degree of change in the chemical shift of proton caused by the formation of hydrogen bonding. As shown in Figure 11, dilution of the sample leads to a shift in the $\delta(\text{H})$ of 2', 10 and 11 toward the low field, once again. This suggests that hydrogen bonding has occurred.

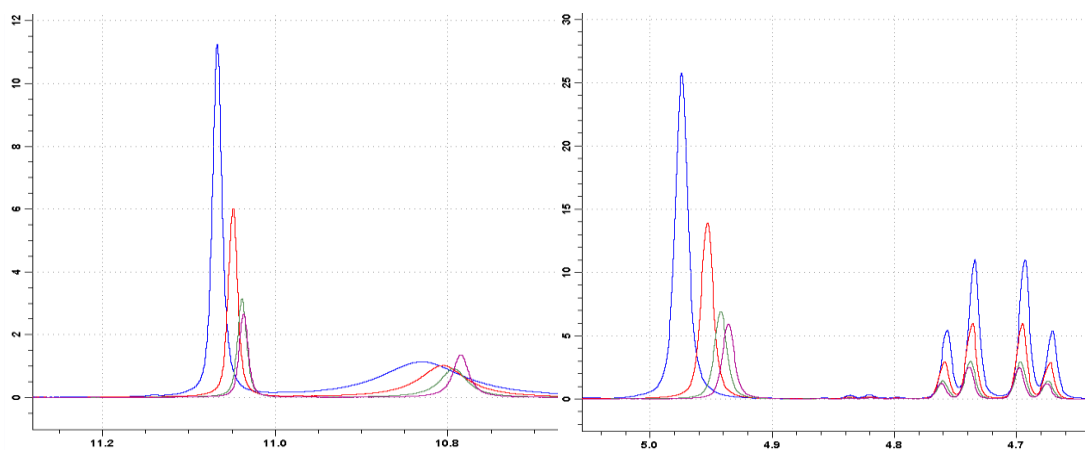
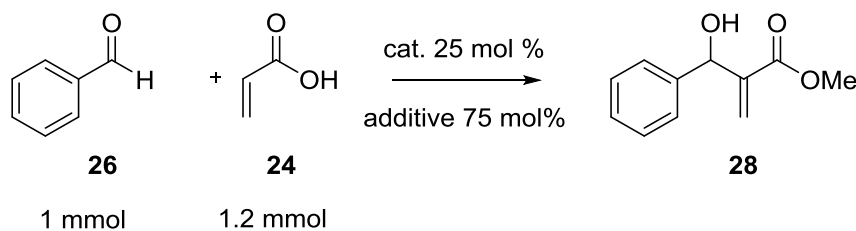


Figure 11: Dilution test in DMSO-d₆

Experimental Detail: 0.05M (blue), 0.025M (light red), 0.0125M (green), 0.00625M (dark red)

2.5. Catalytic rate studies

Following NMR spectroscopic investigations of the CM and SIM to investigate that the desired hydrogen bonding occurred, the final consideration was effectiveness as a catalyst. The reaction of benzaldehyde with methyl acrylate was chosen as a model reaction for rate studies (Scheme 41).



Scheme 41: Model reaction for investigation of MBH reaction.

Initial investigations looked at unbound quinuclidine catalysts, quinuclidinol (3-QD) and DABCO using methanol or phenol as hydrogen bond donors. Conditions were based on studies conducted by Aggarwal et al.^[1] and proposals from Cantilo et al,^[12] in which they suggest that the MBH reaction should be performed at moderate temperature, due to the reactions endergonic nature. We choose to perform the study in triplicate at rt and 0 °C to identify the best thermal window for our catalyst.

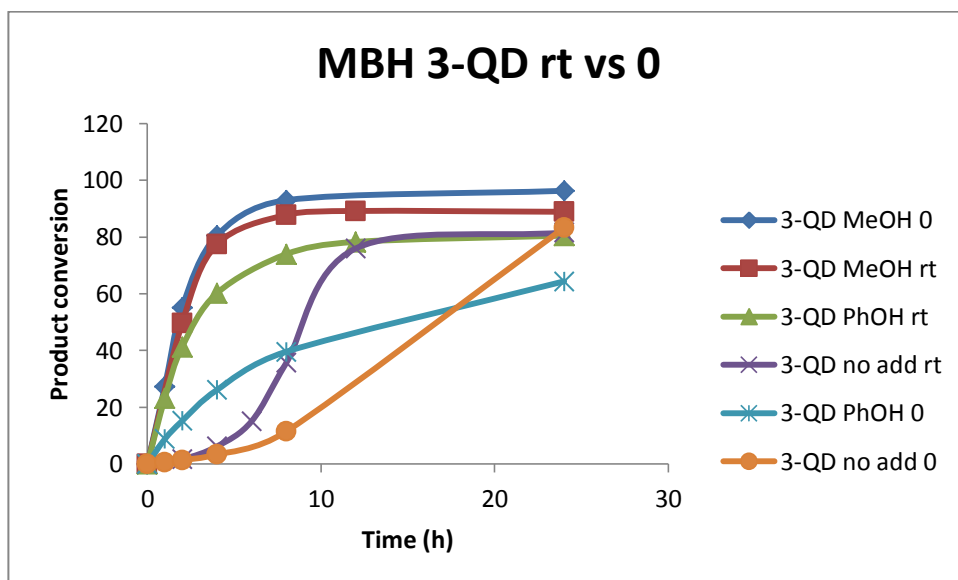


Figure 12: Rate of MBH reaction using unbound 3- quinuclidol (3-QD), with and without proton donor additive at room temperature and 0°C

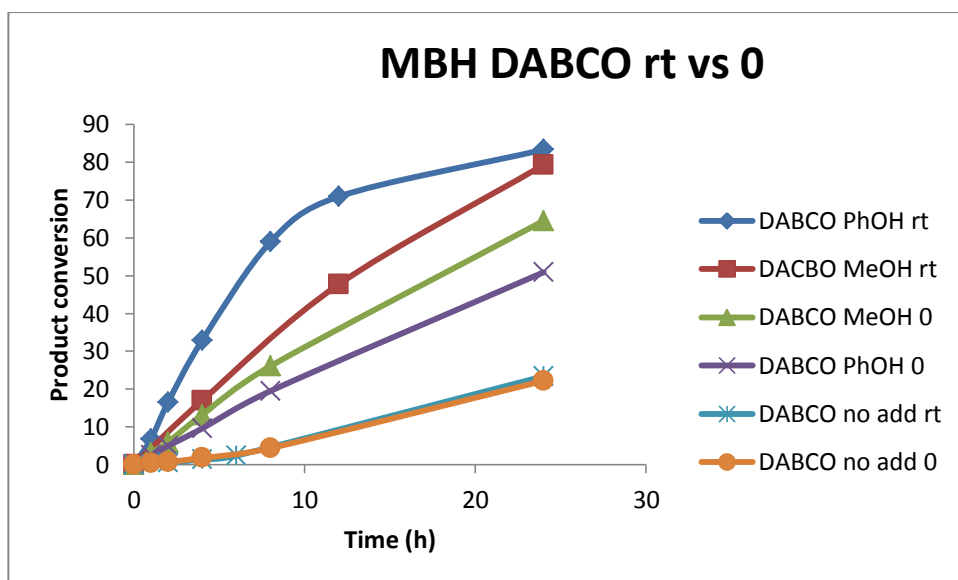


Figure 13: Rate of MBH reaction using unbound 3- quinuclidol (3-QD), with and without proton donor additive at room temperature and 0°C

These results show that while 3-quinuclidinol and DABCO were both effective catalysts, presence of a proton donor additive (3:1 proton donor/catalyst ratio) gave a pronounced rate enhancement (Figure 12 & 13). To investigate use of the CM-SIM modular catalyst, the studies were conducted using (R)-3-QD and PhOH as this system should mimic our modular catalyst. The test was performed at rt due the large rate decrease of the 3-QD/ PhOH system at 0 °C (Figure 12).

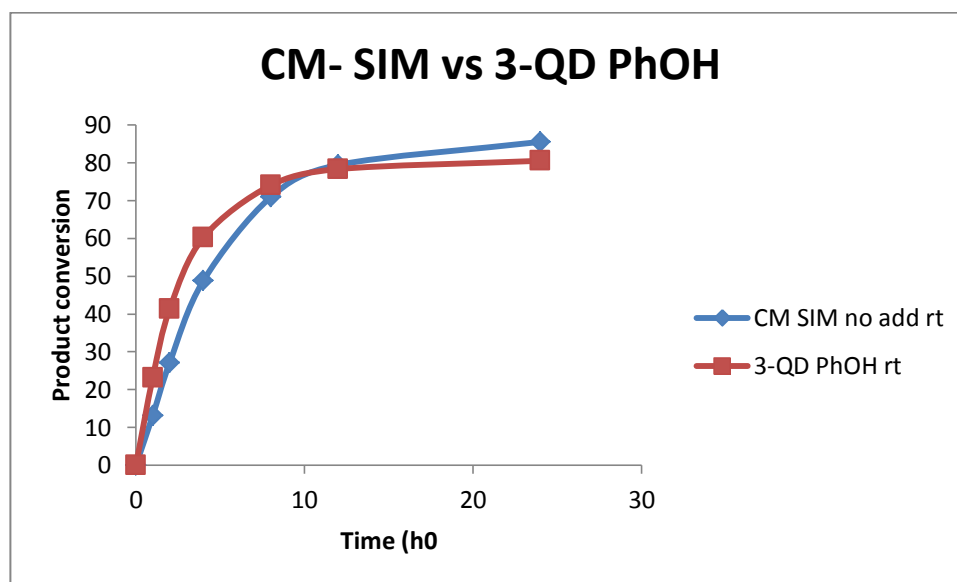


Figure 14: Rate study using CM-SIM in comparison to 3-QD/ PhOH

After confirming the rate enhancement of the MBH reaction with our catalyst without additive, the final factor to consider was induction of selectivity. It was envisaged that the use of the self-assembled modular catalyst would induce selectivity. Therefore the product of the reaction using the CM-SIM and the product from the (R)-3-QD/PhOH reactions were isolated by column chromatography and the optical rotation of each was obtained. Gratifying a modest enhancement of selectivity was observed using the CM-SIM ($[\alpha]_{24} = -4.99^\circ$), while use of (R)-(-)-3- quinuclidinol gave a racemic mixture ($[\alpha]_{24} = 0.48^\circ$). Although the former value is a long way off the literature value of -94.3° for (R)-Methyl 2-(hydroxy(phenyl)methyl)acrylate **28**,^[13] it does demonstrate that the selectivity induced is not due to the presence of a chiral centre in the catalyst moiety alone and must instead be the result of the SIM interaction.

2.6. Conclusion

In this thesis, the rational development of a new enantioselective catalytic system for the MBH reaction was described. After initial shortcomings, the CM and SIM module were synthesised in <6 steps. NMR spectroscopic tests show presence of assembly through hydrogen bonding. Preliminary catalytic tests demonstrate rate enhancement in the MBH test with no additional additive. Due to the racemic product produced by (R)-(-)-3-Quinuclidinol, some asymmetric induction has been induced by the catalyst produced.

2.6.1. Outlook

With the low yields in the final steps of the CM synthesis (Scheme 38), and subsequent small amount of product produced for testing, there are still tests that need to be completed. Re-optimization of these steps will be required to increase the overall yield. More analysis on the assembly event is also necessary, which can pinpoint the interactions occurring. This should heighten our understanding of what is happening in the reaction and hopefully help to increase the induced selectivity.

On a broader scale, results herein only signify the starting point of a new type of catalysis for a much wider range of substrates and reactions.

References (ii)

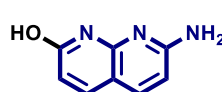
- [1] V. K. Aggarwal, I. Emme, S. Y. Fulford *J. Org. Chem.* **2003**, *68*, 692-700.
- [2] Y. Wei, M. Shi *Acc. Chem. Res.* **2010**, *43*, 1005-1018.
- [3] C. A. Anderson, P. G. Taylor, M. A. Zeller, S. C. Zimmerman *J. Org. Chem.* **2010**, *75*, 4848-4851.
- [4] V. K. Aggarwal, S. Y. Fulford, G. C. Lloyd-Jones *Angewandte Chemie-International Edition* **2005**, *44*, 1706-1708.
- [5] A. Berkessel, S. S. Vormittag, N. E. Schloerer, J. Neudoerfl *J. Org. Chem.* **2012**, *77*, 10145-10157.
- [6] R. C. Dougherty *J. Chem. Phys.* **1998**, *109*, 7372-7378.
- [7] Grant, D.M. and R.K. Harris, *Encyclopedia of nuclear magnetic resonance*, New York: John Wiley, **1996**.
- [8] W. D. Arnold, E. Oldfield *J. Am. Chem. Soc.* **2000**, *122*, 12835-12841.
- [9] P. Borowski, T. Janowski, K. Wolinski *Mol. Phys.* **2000**, *98*, 1331-1341.
- [10] T. R. Kelly, G. J. Bridger, C. Zhao *J. Am. Chem. Soc.* **1990**, *112*, 8024-8034.
- [11] J. A. Fuentes, T. Lebl, A. M. Z. Slawin, M. L. Clarke *Chemical Science* **2011**, *2*, 1997-2005.
- [12] D. Cantillo, C. O. Kappe *J. Org. Chem.* **2010**, *75*, 8615-8626.
- [13] H. Xiaoyu; *Organic & Biomolecular Chemistry*. **2011**, *9*, 6734-6740.

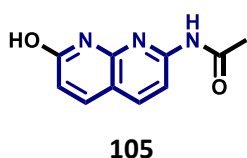
Experimental

General

All reagents were purchased from commercial sources and were used without further purification, unless otherwise stated. Dry solvents were purchased from Sigma Aldrich or Fisher (Acros Chemicals) and handled under an inert atmosphere. Dichloromethane was freshly distilled from calcium hydride and handled under argon. Tetrahydrofuran was freshly distilled from sodium/benzophenone and handled under argon. Acetone was freshly distilled from calcium sulphate and handled under argon. Deuterated solvents were purchased from Fluorochem. Thin layer chromatography (TLC) was performed on Machery-Nagel ALUGRAM® Xtra SILG/UV₂₅₄ aluminium-backed plates and spots were visualised using UV light (254 nm). Column chromatography purifications were carried out using the flash technique on DAVISIL LC60A (35-70 µm) silica gel. NMR spectra were recorded on Bruker Avance 400 and Bruker Avance Ultrashield 600 spectrometers. The chemical shifts (δ) for ¹H and ¹³C are given in parts per million (ppm) referenced to the residual proton signal of the deuterated solvent (CHCl₃ at δ 7.26 ppm, 77.16 ppm, respectively); coupling constants are expressed in hertz (Hz). All experiments were conducted under an atmosphere of dry argon unless otherwise noted, using Schlenk technique.^[1]

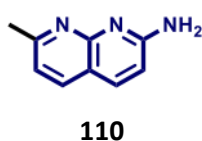
Preparation of the CM and SIM modules

 **7-Amino-1,8-naphthyridin-2-ol 104:**^[2] DL-Malic acid (7.5 g, 55.0 mmol) and 2,6-diaminopyridine (5.5 g, 50.0 mmol) were ground into a powder in a pestle and mortar, and transferred to a round bottom flask. The flask was immersed in an ice bath, and conc. H₂SO₄ (25 mL) was added dropwise. The solution was heated to 110 °C in an oil bath for 3 h and then made alkaline with conc. NH₄OH. Vacuum filtration gave **104** as a brown solid (7.5 g, 46.5 mmol, 93%) which was used in subsequent reaction without further purification. ¹H NMR (400 MHz, DMSO-d₆) δ : 6.11 (dd, *J* = 9.1, 1.5 Hz, 1H), 6.34 (d, *J* = 8.6 Hz, 1H), 6.97 (br. s, 2H), 7.64 (d, *J* = 8.6 Hz, 1H), 7.65 (d, *J* = 9.1 Hz, 1H), 11.83 (br. s, 1H).



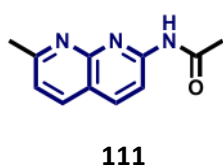
***N*-(7-Hydroxy-1,8-naphthyridin-2-yl)acetamide 105:**^[2] A suspension of 7-amino-1,8-naphthyridin-2-ol **104** (7.4 g, 46.4 mmol) in 140 mL of acetic anhydride was heated at reflux for 3 h.

The resulting mixture was cooled to room temperature, and the precipitate was collected by vacuum filtration, washed with Et₂O, and air-dried to give **105** as a yellow solid (8.4 g, 41.8 mmol, 90%). The product was used in subsequent reactions without further purification. ¹H NMR (400 MHz, DMSO-d₆) δ: 2.14 (s, 3H), 6.42 (dd, *J* = 9.6, 1.5 Hz, 1H), 7.84 (d, *J* = 9.6 Hz, 1H), 7.92 (d, *J* = 8.3 Hz, 1H), 8.05 (d, *J* = 8.3 Hz, 1H), 10.58 (br. s, 1H), 11.92 (br. s, 1H).



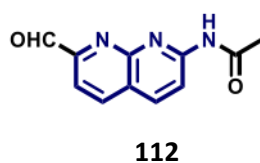
7-Methyl-1,8-naphthyridin-2-amine 110:^[3] 2,6-Diaminopyridine (5.5 g, 50.0 mmol) and H₃PO₄ (40 mL) were heated to 90 °C until melted. 4,4-Dimethoxy-2-butanone (6.6 mL, 50.0 mmol) was then added dropwise over 0.5 h and the reaction mixture was heated

under reflux at 115 °C for 3 h. After cooling to room temperature, NH₄OH was added dropwise in an ice bath until pH > 10. The resultant mixture was extracted numerous times with chloroform and then a 2:1 mixture of chloroform/ethanol. The combined organics were washed with brine, dried (Na₂SO₄) and concentrated in vacuo to give **110** as a brown solid (7.6 g, 48.0 mmol, 96%), which was used in subsequent reaction without further purification. ¹H NMR (400 MHz, CDCl₃) δ: 2.68 (s, 3H), 5.03 (br. s, 2H), 6.71 (d, *J* = 8.6 Hz, 1H), 7.07 (d, *J* = 8.1 Hz, 1H), 7.81 (d, *J* = 8.6 Hz, 1H), 7.82 (d, *J* = 8.1 Hz, 1H).

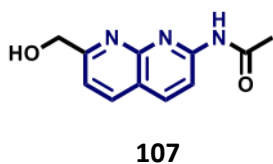


***N*-(7-Methyl-1,8-naphthyridin-2-yl)acetamide 111:**^[3] Acetic anhydride (25 mL) was added to 7-methyl-1,8-naphthyridin-2-amine **110** (7.5 g, 47.0 mmol) and the reaction mixture was stirred overnight at 80 °C. After, the excess acetic anhydride was removed

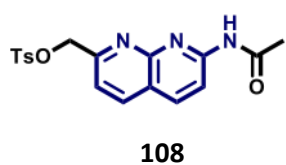
in vacuo. To this, Et₂O was added and the solid separated was collected by vacuum filtration, and air-dried to afford **111** as a brown solid (8.2 g, 40.9 mmol, 87%). ¹H NMR (400 MHz, CDCl₃) δ: 2.29 (s, 3H), 2.75 (s, 3H), 7.29 (d, *J* = 8.1 Hz, 1H), 8.02 (d, *J* = 8.3 Hz, 1H), 8.15 (d, *J* = 8.8 Hz, 1H), 8.47 (d, *J* = 8.8 Hz, 1H), 8.98 (br. s, 1H).



***N*-(7-Formyl-1,8-naphthyridin-2-yl)acetamide 112** :^[3] To a stirred solution of selenium dioxide (4.4 g, 39.7 mmol) in dioxane (400 mL) containing 5 mL of H₂O, **111** (8.0 g, 40 mmol) was added and heated for 4 h at 50-55 °C. The hot solution was filtered through a plug of Celite and the solvent was removed under vacuum. The residue was extracted numerous times with CHCl₃ and washed well with H₂O, dried (Na₂SO₄) and concentrated in vacuo. Purification by flash column chromatography (6% MeOH/DCM with 1% TEA) gave **112** as a red/ brown solid (6.0 g, 27.8 mmol, 70%). ¹H NMR (400 MHz, CDCl₃) δ: 2.32 (s, 3H), 8.05 (d, *J* = 8.1 Hz, 1H), 8.28 (d, *J* = 8.8 Hz, 1H), 8.33 (dd, *J* = 8.3, 0.7 Hz, 1H), 8.46 (br. s, 1H), 8.67 (d, *J* = 8.8 Hz, 1H), 10.24 (d, *J* = 0.8 Hz, 1H).

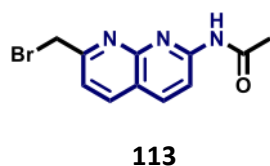


***N*-[7-(Hydroxymethyl)-1,8-naphthyridin-2-yl]acetamide 107**:^[3] To an ice-cold solution of **112** (5.8 g, 27.0 mmol) in EtOH (135 mL) was added NaBH₄ (2.0 g, 54.0 mmol) in portions. After observing disappearance of the starting material by TLC, the reaction mixture was quenched by dropwise addition of sat. aq. NH₄Cl. The reaction was then allowed to warm to rt and the EtOH was removed. The resulting aqueous solution was extracted with CHCl₃ and the combined organics were washed with brine, dried (Na₂SO₄), filtered and concentrated in vacuo. Purification by flash column chromatography (6% MeOH/DCM with 1% TEA) gave **107** as an orange oil (3.8 g, 17.5 mmol, 64%). ¹H NMR (400 MHz, CDCl₃) δ: 2.28 (s, 3H), 4.18 (br. s, 1H), 4.96 (s, 2H), 7.32 (d, *J* = 8.1 Hz, 1H), 8.14 (d, *J* = 8.1 Hz, 1H), 8.21 (d, *J* = 8.8 Hz, 1H), 8.53 (d, *J* = 8.8 Hz, 1H), 8.54 (br. s, 1H).



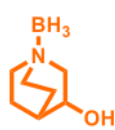
[7-(Acetylamino)-1,8-naphthyridin-2-yl]methyl 4-methylbenzenesulfonate 108:^[3] NaH (60% dispersion in oil, 0.7 g, 17.9 mmol) was added in portions to a solution of *N*-[7-(hydroxymethyl)-1,8-naphthyridin-2-yl]acetamide **107** (3.7 g, 17.0 mmol) in DCM (20 mL) and stirred at reflux overnight. After, it was cooled to -20 °C; and a solution of TsCl (3.3 g, 17.0 mmol) in DCM (20 mL) was added dropwise.

This mixture was allowed to warm to rt and stirred for a further 1 h. The reaction was quenched with dropwise addition of sat. aq. NH₄Cl, and extracted with CHCl₃. The crude was concentrated in vacuo to give **108** as a brown solid which subsequently decomposed (6.3 g, 17.0 mmol, quantitative yield). ¹H NMR (400 MHz, CDCl₃) δ: 2.21 (s, 3H), 2.37 (s, 3H), 5.25 (s, 2H), 7.28 (d, *J* = 8.1 Hz, 1H), 7.51 (d, *J* = 8.1 Hz, 1H), 7.80 (d, *J* = 8.4 Hz, 2H), 8.11 (d, *J* = 8.4 Hz, 1H), 8.15 (d, *J* = 8.8 Hz, 1H), 8.51 (d, *J* = 8.8 Hz, 1H), 9.89 (br. s, 1H).



***N*-[7-(Bromomethyl)-1,8-naphthyridin-2-yl]acetamide 113 :** **111** (13.3 g, 66.1 mmol), NBS (11.7 g, 65.7 mmol), and benzoyl peroxide (75% remainder H₂O, 10.7 g, 33.1 mmol) in dimethyl carbonate (200 mL) were refluxed in a preheated oil bath at 110 °C for 0.25 h. After cooling to room temperature, the reaction mixture was dissolved in CHCl₃ washed with H₂O, dried (Na₂SO₄), filtered and concentrated in vacuo.

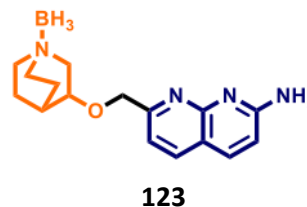
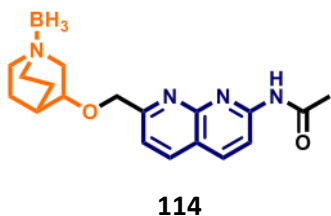
Purification by flash column chromatography (50/50 DCM/ethyl acetate and then 2-2.5% MeOH/DCM) gave **113** as a white solid (5.2 g, 18.6 mmol, 28%). ¹H NMR (400 MHz, CDCl₃) δ: 2.29 (s, 3H), 4.69 (s, 2H), 7.58 (d, *J* = 8.1 Hz, 1H), 8.16 (d, *J* = 8.1 Hz, 1H), 8.19 (d, *J* = 8.8 Hz, 1H), 8.55 (d, *J* = 8.8 Hz, 1H), 8.96 (br. s, 1H).



(R)-N-Boranyl-1-aza-bicyclo[2.2.2]octan-3-ol 122:^[5] A solution of borane-THF complex solution (1.0 M in THF, 50 mL, 50.0 mmol) was added dropwise to a solution of (*R*)-(-)-3-quinuclidinol (6 g, 47.2 mmol) in THF (40 mL) in an ice bath at 0 °C. The reaction mixture was allowed to

warm to room temperature, stirred for 24 h, and then evaporated in vacuo. The resulting residue was dissolved with CHCl₃, washed with water, then brine, dried (Na₂SO₄), and

then filtered and concentrated in vacuo. The resulting residue was dissolved in Et₂O and treated with hexane. The resulting fine white precipitate was collected by vacuum filtration to afford (R)-*N*-boranyl-1-aza-bicyclo[2.2.2]octan-3-ol **122** as a white solid (5.5 g, 39.0 mmol, 83%). ¹H NMR (400 MHz, CDCl₃) δ: 1.54-1.70 (m, 3H), 1.80-1.88 (m, 2H), 2.02- 2.06 (m, 1H), 2.10-2.19 (m, 1H), 2.81- 3.11 (m, 5H), 3.21-3.27 (m, 1H), 4.06-4.10 (m, 1H).



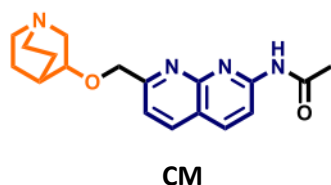
***N*-(7-[[*N*-Boranyl-1-azabicyclo[2.2.2]oct-3-yloxy]methyl]-1,8-naphthyridin-2-yl)acetamide **114**:**^[5] A solution of (R)-*N*-boranyl-1-aza-bicyclo[2.2.2]octan-3-ol **122** (5.1 g, 36.2 mmol) in DMF was treated with NaH (60% dispersion in oil, 1.4 g, 35.0 mmol), stirred for 5 min then treated with **111** (5.0 g, 17.8 mmol). The reaction was monitored by TLC and stopped after disappearance of the starting material. The mixture was quenched with water, filtered through a plug of celite, and then extracted numerous times with chloroform. It was then dried (Na₂SO₄), filtered and evaporated in vacuo. Purification by flash column chromatography (ethyl acetate and then 2% MeOH/DCM) gave **114** as a yellow solid (2.1 g, 6.2 mmol, 34%). ¹H NMR (400 MHz, CDCl₃) δ: 1.45-1.54 (m, 2H), 1.71-1.79 (m, 1H), 1.94-2.01 (m, 1H), 2.18 (s, 3H), 2.21-2.23 (m, 1H), 2.73- 3.01 (m, 5H), 3.13-3.19 (m, 1H), 3.71-3.75 (m, 1H), 4.62 (d, *J* = 13.6 Hz, 1H), 4.71 (d, *J* = 13.6 Hz, 1H), 7.48 (d, *J* = 8.4 Hz, 1H), 8.07 (d, *J* = 8.4 Hz, 1H), 8.10 (d, *J* = 8.8 Hz, 1H), 8.43 (d, *J* = 8.8 Hz, 1H), 10.37 (br. s, 1H).

Depending on the length of time of the reaction, varying amounts of the unacetylated compound **123** were also formed. Isolation of **123** as a yellow solid could be achieved by flash column chromatography using 6% MeOH/DCM with 1% TEA. ¹H NMR (400 MHz, DMSO-*d*₆) δ: 1.52-1.62 (m, 2H), 1.73-1.81 (m, 1H), 1.88-2.00 (m, 1H), 2.24-2.28 (m, 1H), 2.70-2.89 (m, 5H), 3.17-3.24 (m, 1H), 3.82-3.86 (m, 1H), 4.57 (d, *J* = 13.4 Hz, 1H), 4.64 (d, *J* = 13.4 Hz, 1H), 6.79 (d, *J* = 8.8 Hz, 1H), 6.81 (br. s, 2H), 7.25 (d, *J* = 8.1 Hz, 1H), 7.91 (d, *J* = 8.8 Hz, 1H), 8.04 (d, *J* = 8.1 Hz, 1H).

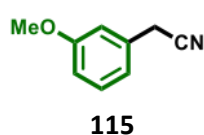
Reacylation of **123:** A solution of acetyl chloride (0.2 mL, 3.0 mmol) in DCM (3 mL) was added dropwise to a stirred solution of **123** (0.3 g, 1.0 mmol) and TEA (0.4 mL, 3.0

mmol) in DCM (6 mL) in an ice bath. The reaction mixture was allowed to warm to rt and stirred for an additional 2 h. The reaction mixture was then dissolved in CHCl₃ and washed with H₂O, dried (Na₂SO₄), filtered and concentrated in vacuo. Purification by flash column chromatography (6% MeOH/DCM with 1% TEA) gave **114** as yellow solid (0.16 g, 0.5 mmol, 48%).

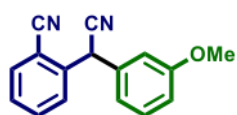
***N*-(7-[[1-Azabicyclo[2.2.2]oct-3-yloxy]methyl]-1,8-naphthyridin-2-yl)acetamide**



CM:^[5] A solution of **114** (2.1 g, 6.1 mmol) in acetone (35 mL) in an ice bath at 0 °C was treated with HCl solution (1.25 M in MeOH, 70 mL, 87.5 mmol), stirred at 0 °C for 0.5 h, and then stirred at room temperature for 0.5 h. The reaction mixture was neutralised with sat. aq. K₃PO₄, dried (Na₂SO₄), filtered and concentrated in vacuo. Purification by flash column chromatography (9% MeOH/DCM in 1% TEA) gave **CM** as a white solid (0.7 g, 2.2 mmol, 37%). ¹H NMR (400 MHz, CDCl₃) δ: 1.30-1.43 (m, 2H), 1.62-1.70 (m, 1H), 1.85-1.92 (m, 1H), 2.07-2.11 (m, 1H), 2.25 (s, 3H), 2.62-2.94 (m, 5H), 3.09-3.15 (m, 1H), 3.59-3.63 (m, 1H), 4.70 (d, *J* = 13.9 Hz, 1H), 4.79 (d, *J* = 13.9 Hz, 1H), 7.62 (d, *J* = 8.4 Hz, 1H), 8.11 (d, *J* = 8.3 Hz, 1H), 8.15 (d, *J* = 8.8 Hz, 1H), 8.49 (d, *J* = 8.8 Hz, 1H), 9.73 (br. s, 1H); ¹³C NMR (100 MHz, CDCl₃) δ: 19.3, 24.4, 24.5, 25.0, 46.8, 47.6, 56.0, 71.6, 76.2, 115.3, 118.9, 119.6, 137.1, 139.3, 154.1, 154.2, 163.7, 170.1. HRMS [M + H]⁺: m/z calcd 326.1743, found 327.1817.

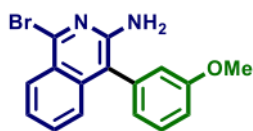


(3-Methoxyphenyl)acetonitrile 115^[6] 3-Methoxybenzyl bromide (10.1 g 50.2 mmol) was dissolved in a mixture of EtOH (6 mL) and H₂O (3 mL), and then NaCN (3.2 g, 65.3 mmol) was added. The mixture was heated to reflux and stirred for 3 h, and then the crude was concentrated in vacuo. The orange residue was dissolved with DCM and washed with H₂O. The organic layer was dried (Na₂SO₄), filtered and concentrated in vacuo giving **115** as a colourless oil (7.2 g, 48.9 mmol, 98%). The product was used in subsequent reactions without further purification. ¹H NMR (400 MHz, CDCl₃) δ: 3.71 (s, 2H), 3.81 (s, 3H), 6.91 (m, 3H), 7.31 (td, *J* = 7.6, 1.8 Hz, 1H)



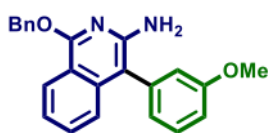
118

2-[Cyano(3-methoxyphenyl)methyl]benzonitrile 118:^[7] To a solution of potassium *tert*-butoxide (10.8 g, 96.2 mmol) in DMF (20 mL) in an ice bath, a mixture of 2-chlorobenzonitrile (8.6 g, 62.5 mmol) and (3-methoxyphenyl)acetonitrile **115** (7.1 g, 48.2 mmol) in DMF (12 mL) was added dropwise. The mixture was stirred at room temperature for 1 h, and then quenched with sat. aq. NH₄Cl. The solution was extracted with Et₂O, washed with H₂O, dried (Na₂SO₄), filtered and concentrated in vacuo. Purification by flash column chromatography (10-15% EtOAc/hexane) gave **118** an orange oil (11.3 g, 45.5 mmol, 94%). ¹H NMR (400 MHz, CDCl₃) δ: 3.80 (s, 3H), 5.53 (s, 1H), 6.87 (ddd, *J* = 8.3, 2.5, 0.8 Hz, 1H), 6.94 (t, *J* = 2.1 Hz, 1H), 6.99-7.01 (m, 1H), 7.30 (t, *J* = 7.9 Hz, 1H), 7.47 (td, *J* = 7.6, 1.5 Hz, 1H), 7.65-7.73 (m, 3H); ¹³C NMR (100 MHz, CDCl₃) δ: 41.0, 55.5, 112.0, 113.6, 114.3, 117.0, 118.4, 119.9, 128.9, 129.2, 130.7, 133.7, 134.0, 135.6, 139.5, 160.3



119

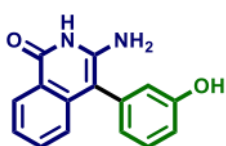
1-Bromo-4-(3-methoxyphenyl)isoquinolin-3-amine 119: A solution of HBr (30% in acetic acid, 73 mL, 378.9 mmol) was added to **118** (11.2 g, 45.1 mmol), and stirred for 2 h at rt. The crude was then neutralised by addition of aq. sat. NaHCO₃, extracted with ethyl acetate, washed with H₂O, dried (Na₂SO₄), filtered and concentrated in vacuo. Purification by flash column chromatography (1-5% EtOAc/benzene) gave **119** as a yellow oil (9.2 g, 27.9 mmol, 62%). ¹H NMR (400 MHz, CDCl₃) δ: 3.84 (s, 3H), 4.43 (br. s, 2H), 6.90 (dd, *J* = 2.5, 1.5 Hz, 1H), 6.94 (dt, *J* = 7.6, 1.3 Hz, 1H), 7.00 (ddd, 8.4, 2.8, 1.0 Hz, 1H), 7.27-7.33 (m, 2H), 7.41-7.45 (m, 1H), 7.47 (t, *J* = 7.8 Hz, 1H), 8.12 (d, *J* = 8.6 Hz, 1H), ¹³C NMR (100 MHz, CDCl₃) δ: 55.5, 111.6, 114.0, 115.9, 122.8, 123.5, 123.8, 124.1, 128.9, 130.8, 131.1, 136.4, 139.0, 143.4, 150.9, 160.6



121

1-(Benzyloxy)-4-(3-methoxyphenyl)isoquinolin-3-amine

121:^[8] A solution of benzyl alcohol (8.4 mL, 81.2 mmol) in DMF (30 mL) was cooled to 0 °C, treated with NaH (60% mineral oil dispersion; 3.2 g, 80.0 mmol) in portions and stirred at 0 °C for 0.5 h. Subsequently it was added to a solution of **119** (8.9 g, 27.0 mmol) in DMF (8 mL) at the same temperature. The mixture was warmed to rt and stirred for an additional 1.5 h. The reaction was quenched with the addition of sat. aq. NaHCO₃, and extracted with Et₂O, washed with H₂O, dried (Na₂SO₄), and concentrated in vacuo. Purification by flash column chromatography (1% EtOAc/benzene) gave **121** as a yellow solid (7.0 g, 19.5 mmol, 73%). ¹H NMR (400 MHz, CDCl₃) δ: 3.88 (s, 3H), 4.28 (br. s, 2H), 5.65 (s, 2H), 7.01-7.05 (m, 3H), 7.21-7.25 (m, 1H), 7.33 (d, *J* = 8.3 Hz, 1H), 7.38-7.51 (m, 5H), 7.61 (d, *J* = 7.1 Hz, 2H), 8.27 (d, *J* = 7.8 Hz, 1H); ¹³C NMR (100 MHz, CDCl₃) δ: 55.4, 67.8, 104.8, 113.3, 114.3, 116.5, 122.0, 122.8, 123.5, 124.3, 127.9, 128.0, 128.6, 130.5, 130.6, 137.7, 137.9, 139.7, 149.0, 159.6, 160.4.

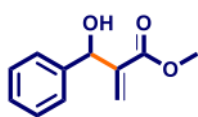


SIM

3-Amino-4-(3-hydroxyphenyl)isoquinolin-1(2H)-one SIM:^[9]

A solution of **121** (6.8 g, 19.1 mmol) in DCM (300 mL) was chilled to 0 °C. To this solution was added a solution of BBr₃ (5.5 mL, 57.1 mmol) in DCM (250 mL) at the same temperature. After, the reaction was allowed to warm to rt and stirred for 24 h. The mixture was quenched with H₂O, extracted with CHCl₃, to remove soluble impurities and then extracted with EtOAc. The organic layer was washed with H₂O, dried (Na₂SO₄), and concentrated in vacuo. Purification by flash column chromatography (6% MeOH/DCM) gave **SIM** as a yellow solid (3.0 g, 11.8 mmol, 62%). ¹H NMR (400 MHz, DMSO-d₆) δ: 4.93 (br. s, 2H), 6.65-6.69 (m, 2H), 6.78 (ddd, *J* = 8.1, 2.5, 1.0 Hz, 1H), 6.70 (d, *J* = 8.1 Hz, 1H), 7.04 (ddd, *J* = 8.1, 7.1, 1.0 Hz, 1H), 7.29 (t, *J* = 7.8 Hz, 1H), 7.37 (ddd, *J* = 8.3, 6.8, 1.5 Hz, 1H), 8.00 (dd, *J* = 8.1, 1.5 Hz, 1H), 9.50 (s, 1H), 10.78 (s, 1H). ¹³C NMR (100 MHz, DMSO-d₆) δ: 93.3, 114.3, 118.3, 119.3, 120.9, 121.7, 122.1, 126.8, 130.3, 132.2, 136.1, 140.4, 142.1, 158.0, 161.4. HRMS [M + H]⁺: m/z calcd 252.0899, found 253.0972.

Catalytic studies



28

(R)-Methyl 2-(hydroxy(phenyl)methyl)acrylate **124:**^[10]

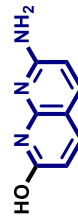
To a stirred mixture of the benzaldehyde (0.1 mL, 1.0 mmol) and methyl acrylate (0.11 mL, 1.2 mmol) were added the catalyst (0.25 mmol) and, where required, hydrogen bond donor (0.25-0.75 mmol).

The reaction mixture was stirred at rt, and upon completion, the reaction mixture was purified by flash column chromatography (20% EtOAc/hexane) to give **124** as a colourless oil (0.14 g, 0.7 mmol, 71%). ¹H NMR (400 MHz, CDCl₃) δ: 3.39 (br. s, 1H), 3.72 (s, 3H), 5.57 (br. s, 1H), 5.89 (s, 1H), 6.36 (s, 1H), 7.29-7.41 (m, 5H).

File Name S3Br(f)
Acquisition Time (sec) 3.9584
Date Stamp 10 Oct 2012 17:17
Frequency (MHz) 400.13

Owner Administrator
Solvent DMSO-d6
Temperature (degree C) 19.160
Nucleus 1H
Points Count 32768
Number of Transients 16
Pulse Sequence zg30
Spectrum Offset (Hz) 2467.9729
Origin spect

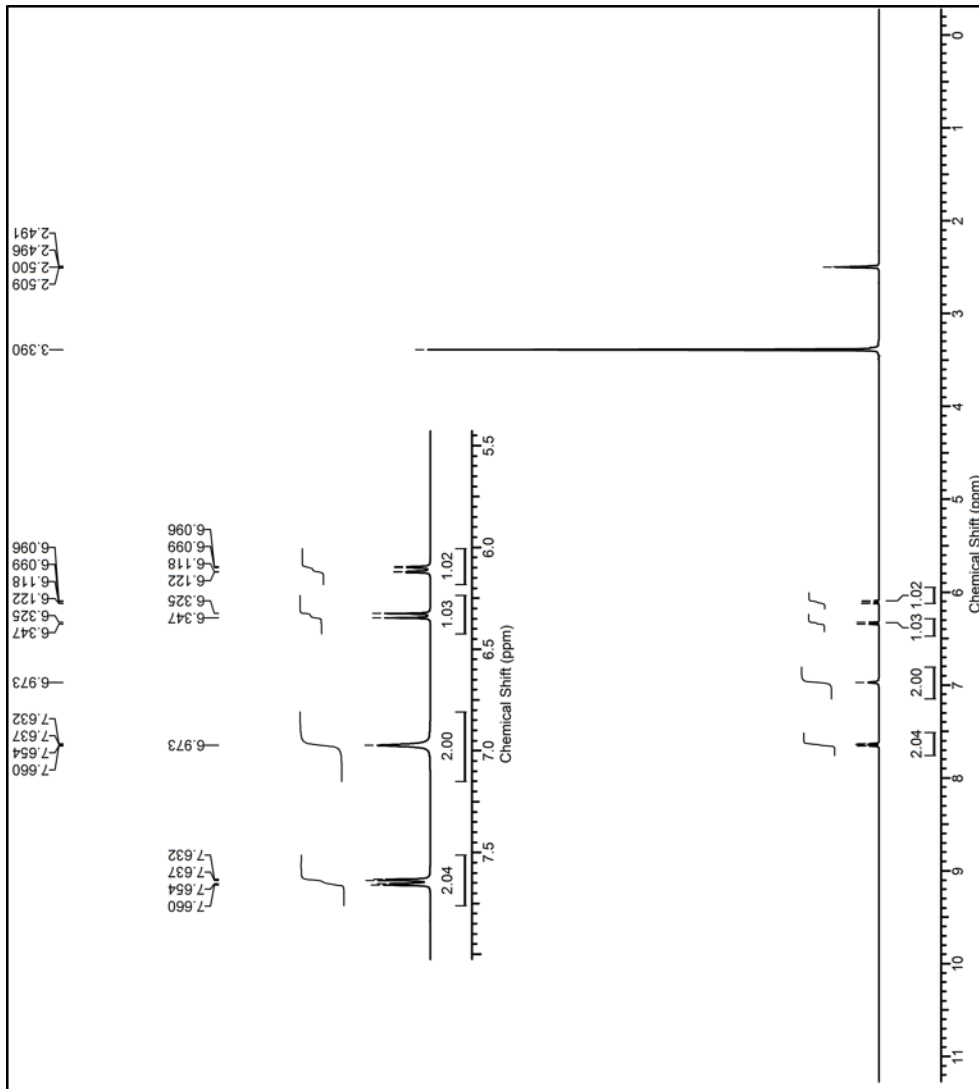
Receiver Gain 161.30
Spectrum Type STANDARD
Original Points Count 32768
SW(cyclical) (Hz) 8278.15
Sweep Width (Hz) 8277.89

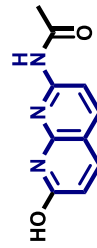
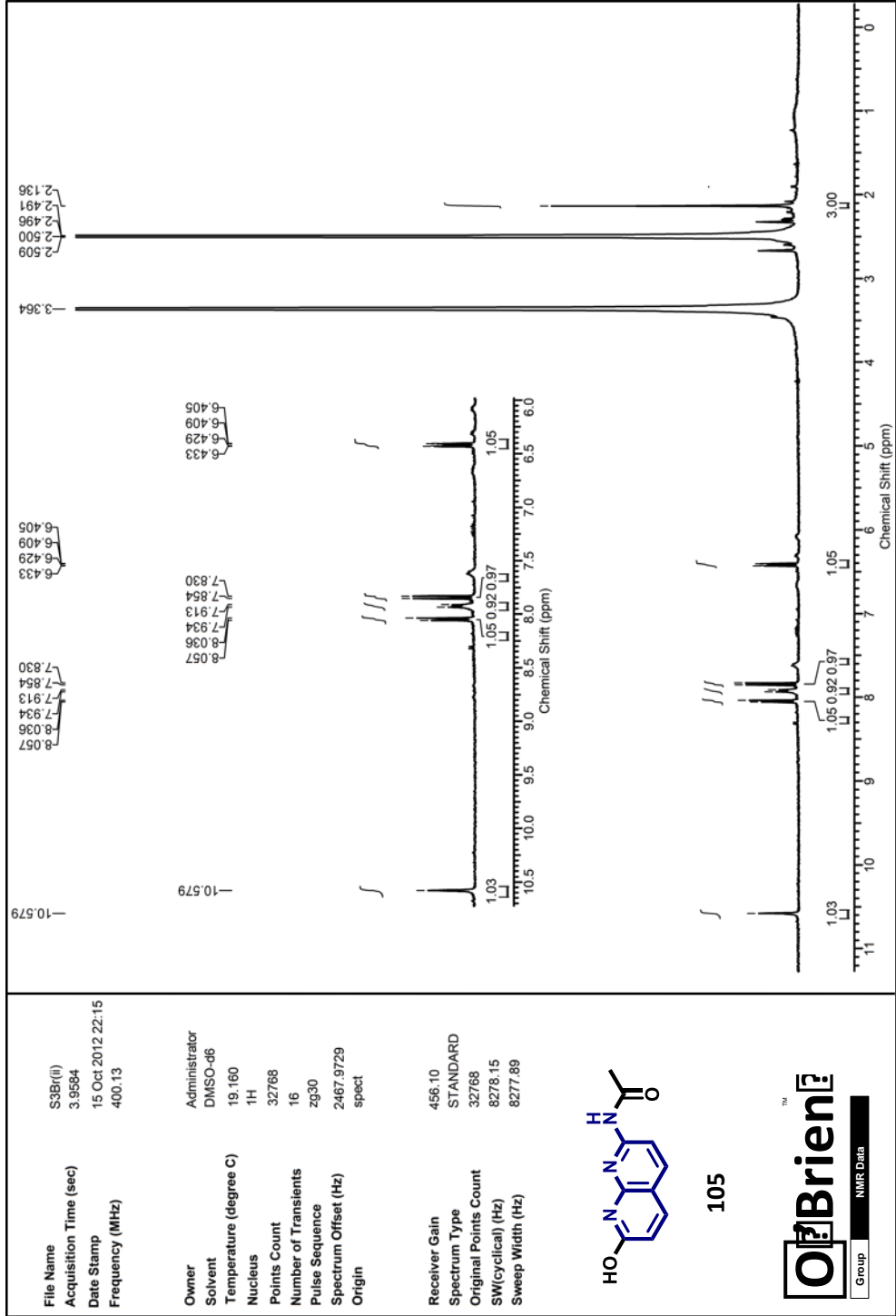


104

O'Brien

Group NMR Data

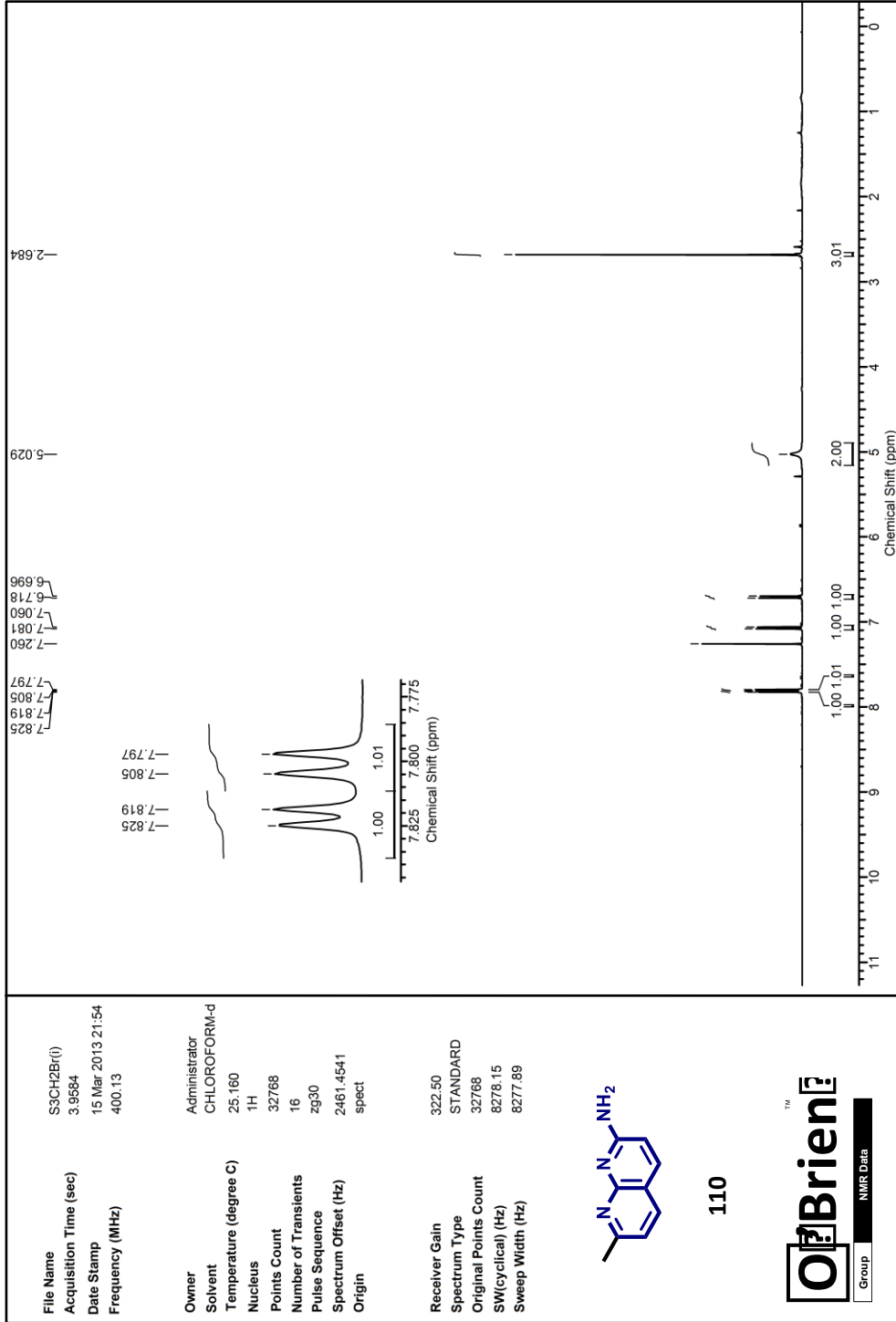




105



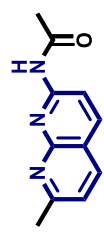
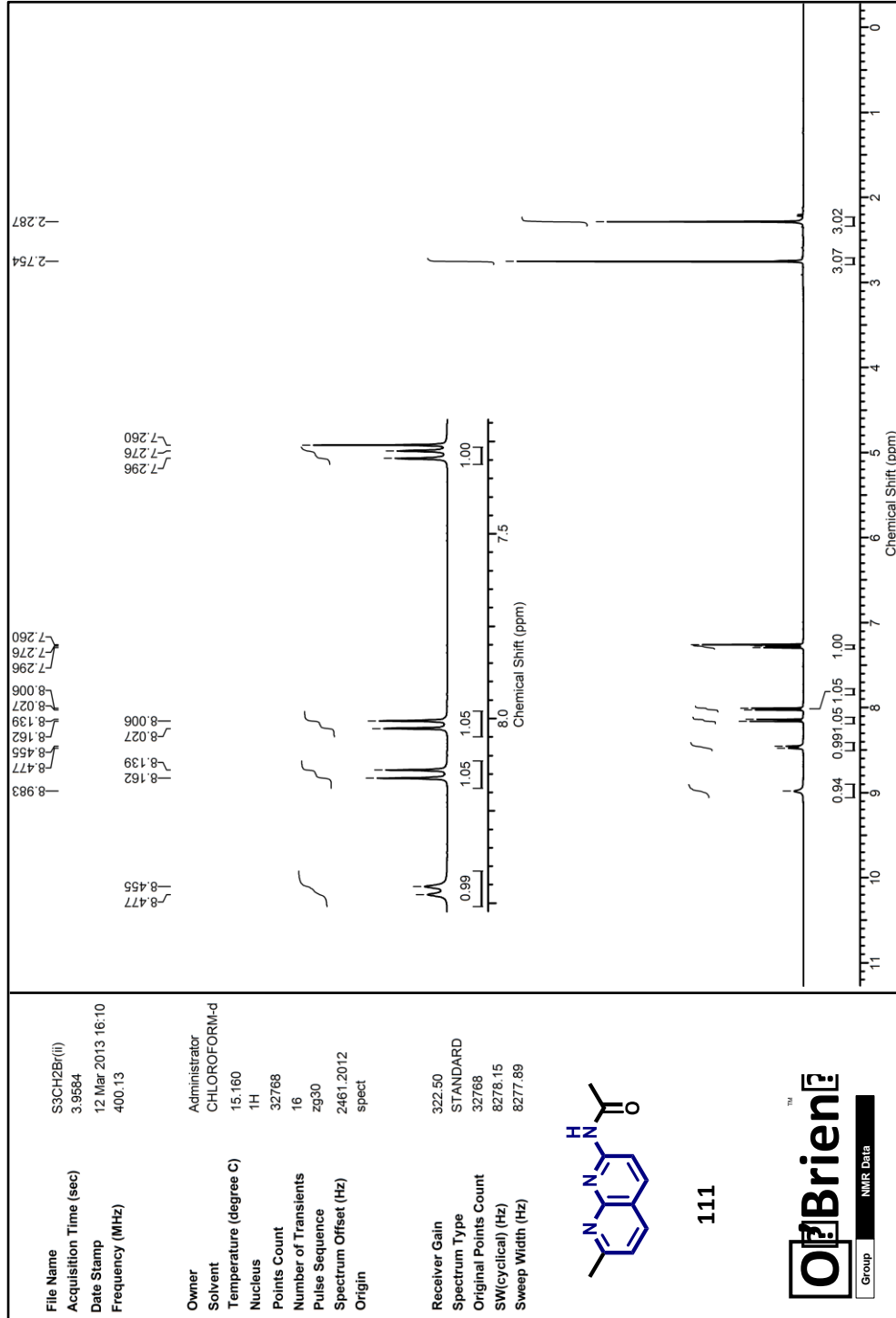
Group NMR Data



110

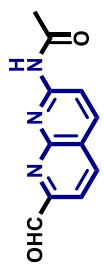
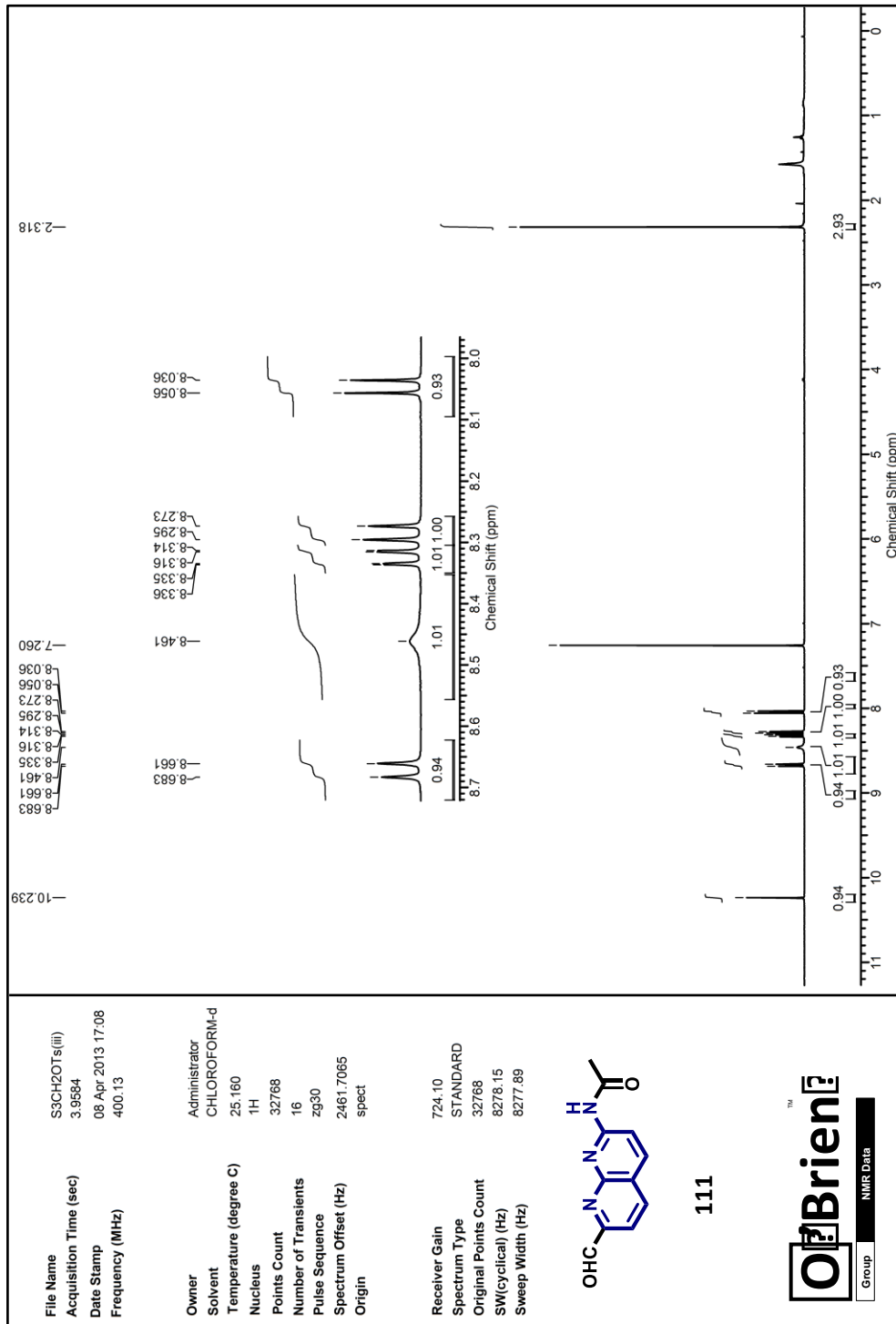


Group NMR Data



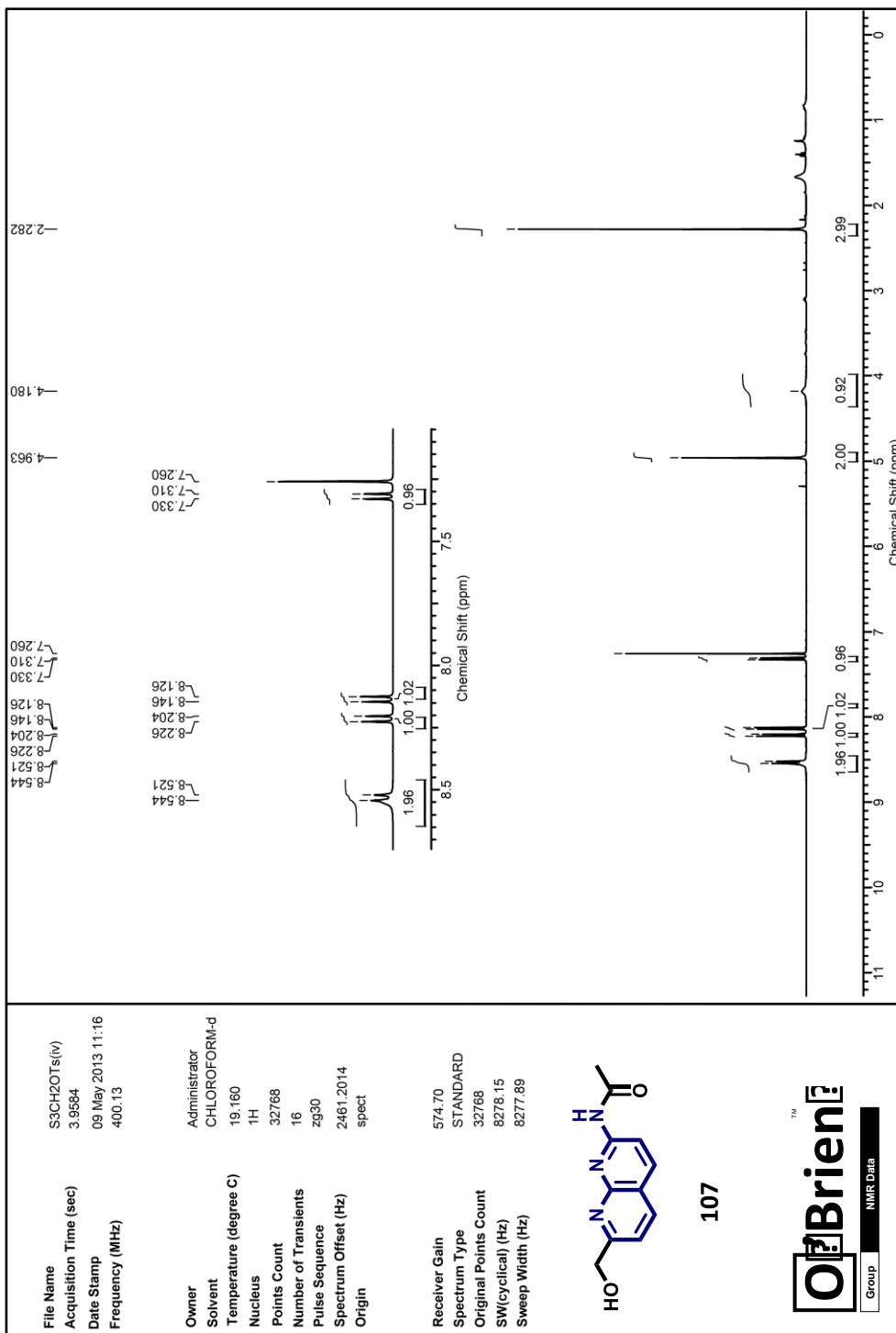
111

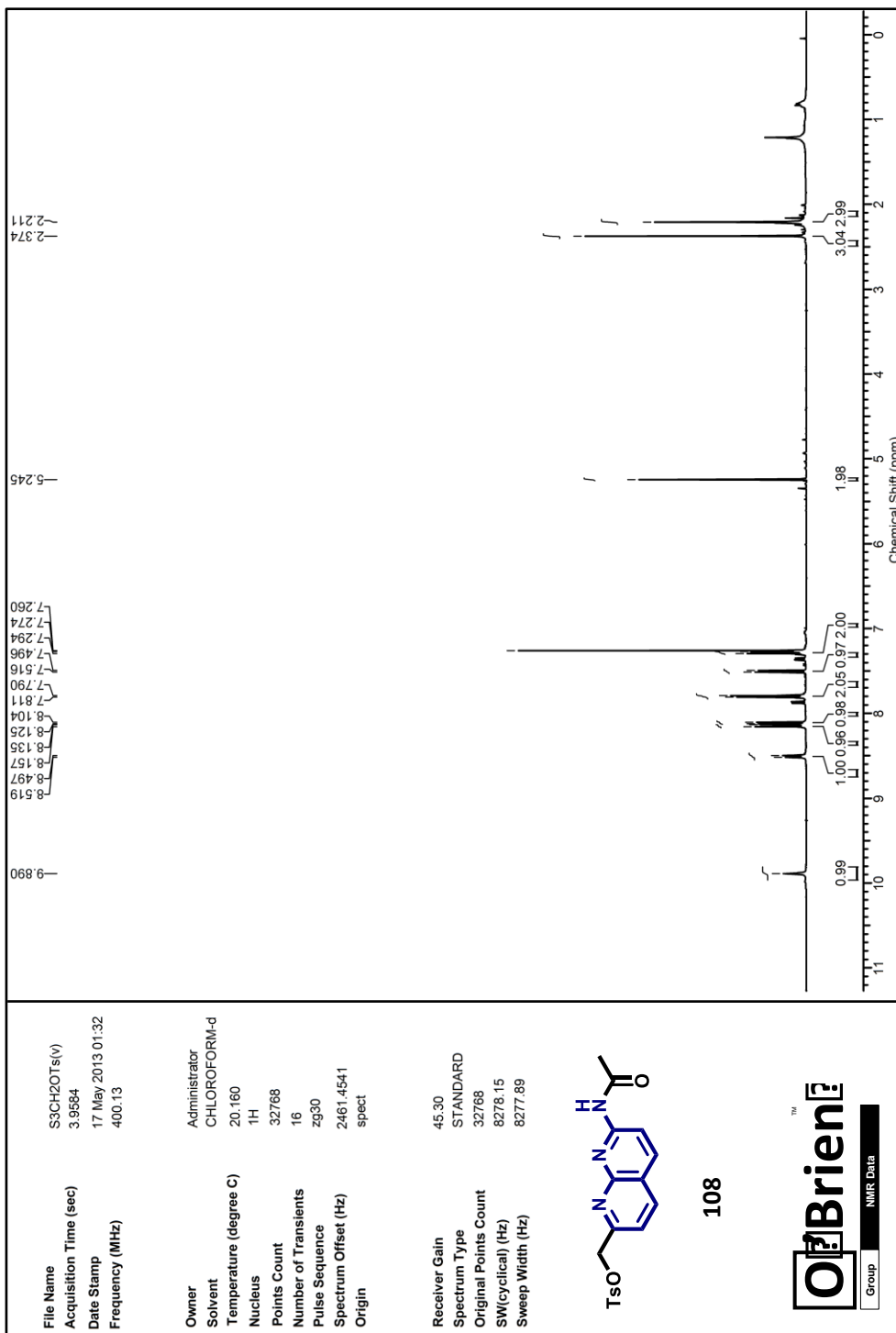


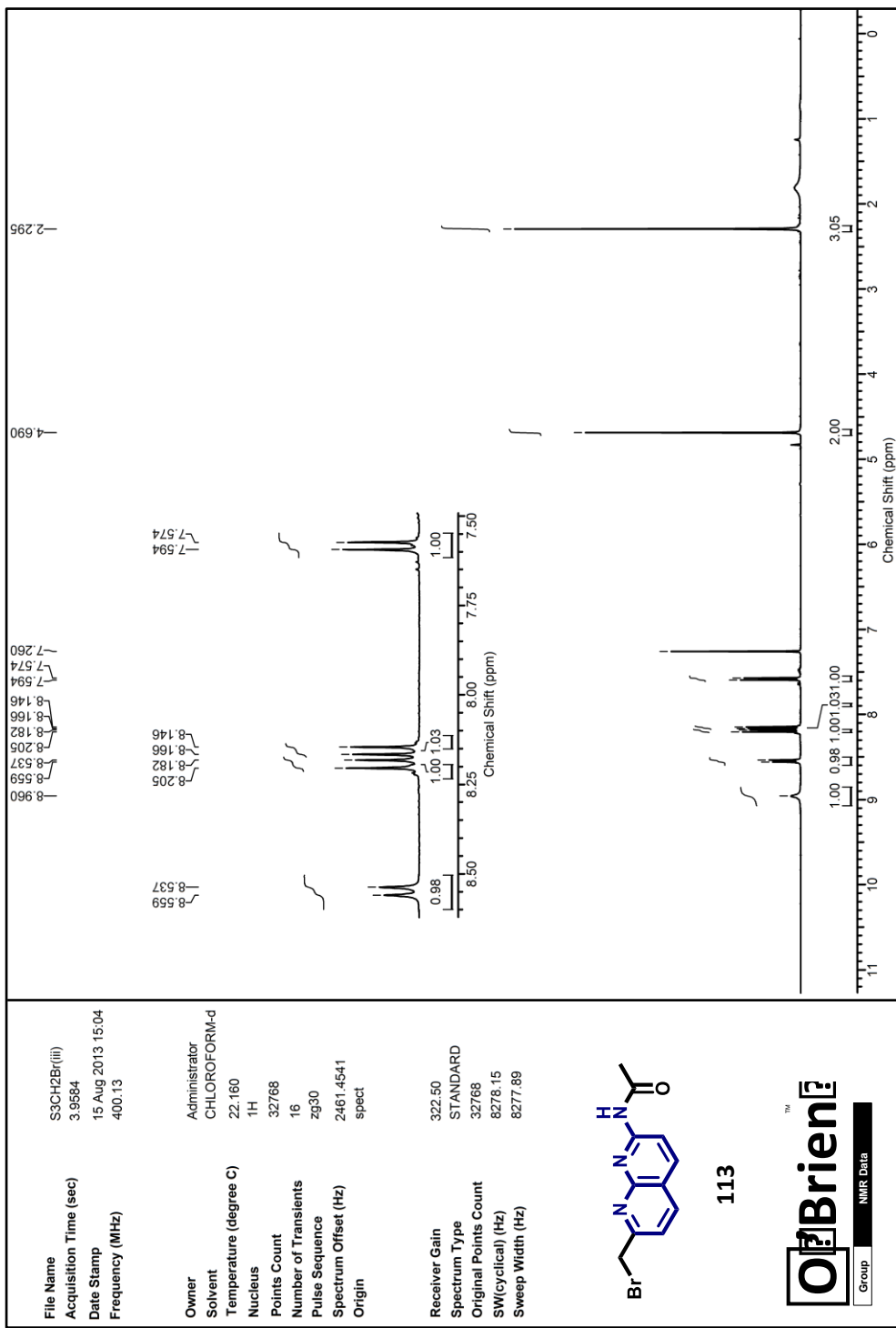


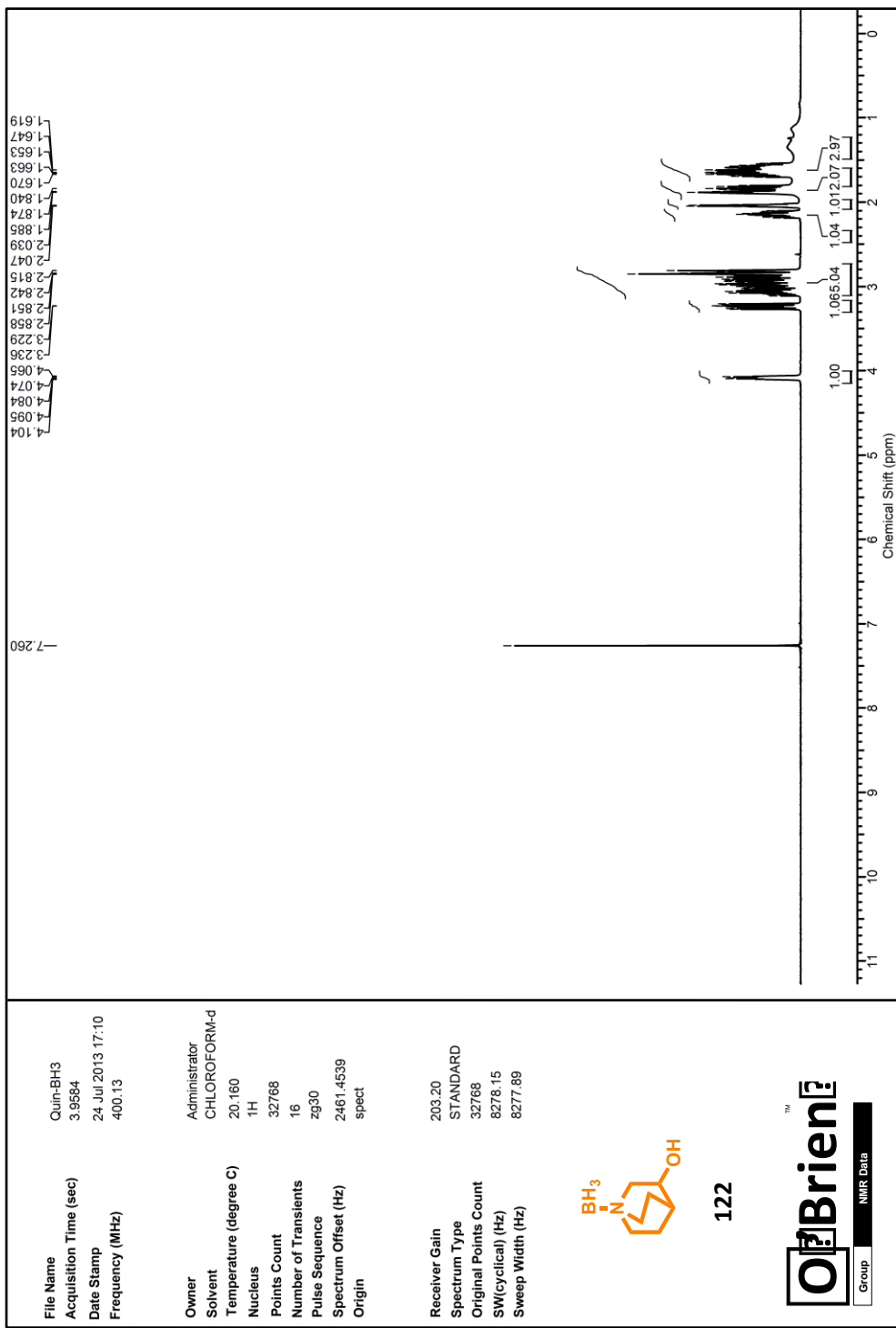
111

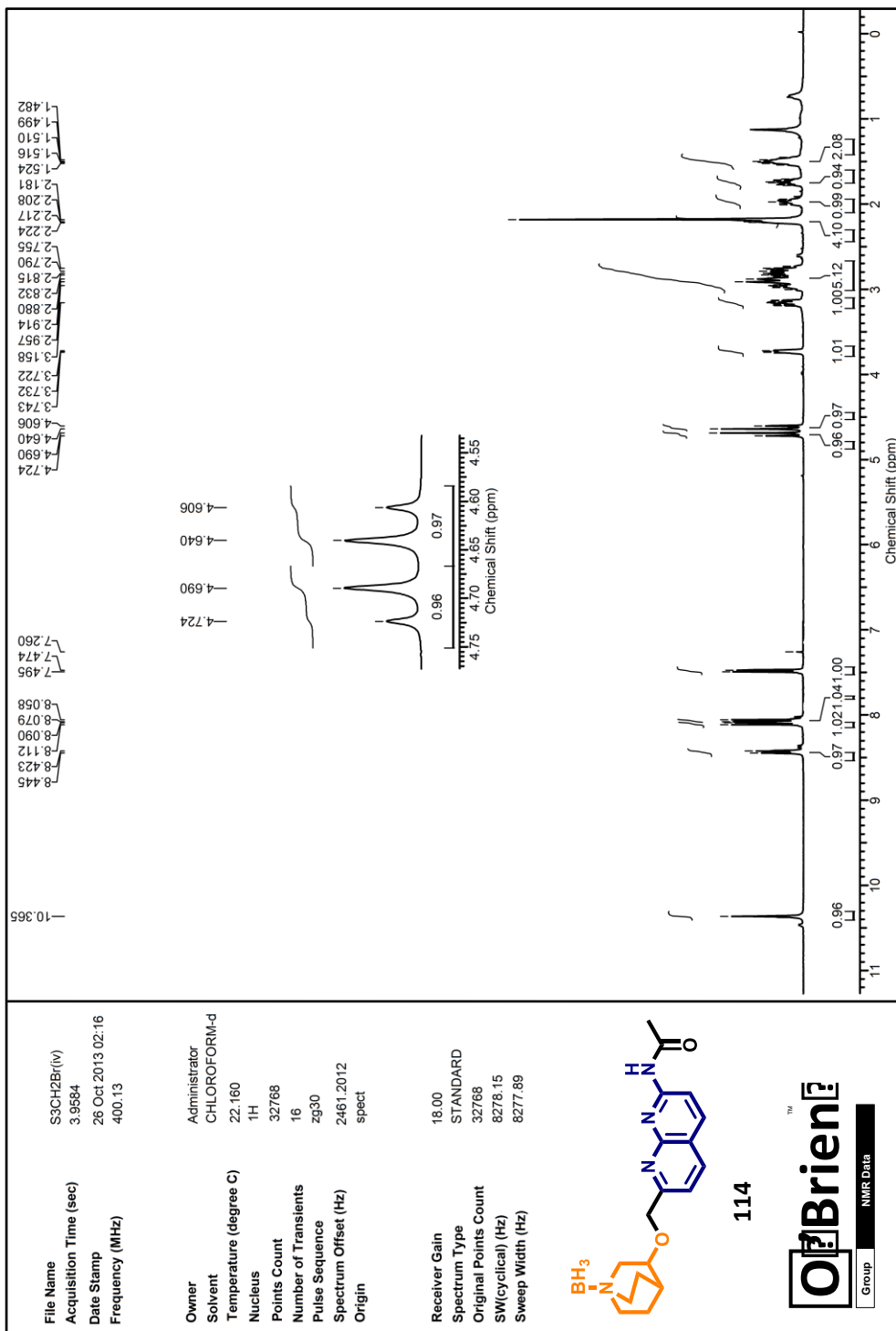


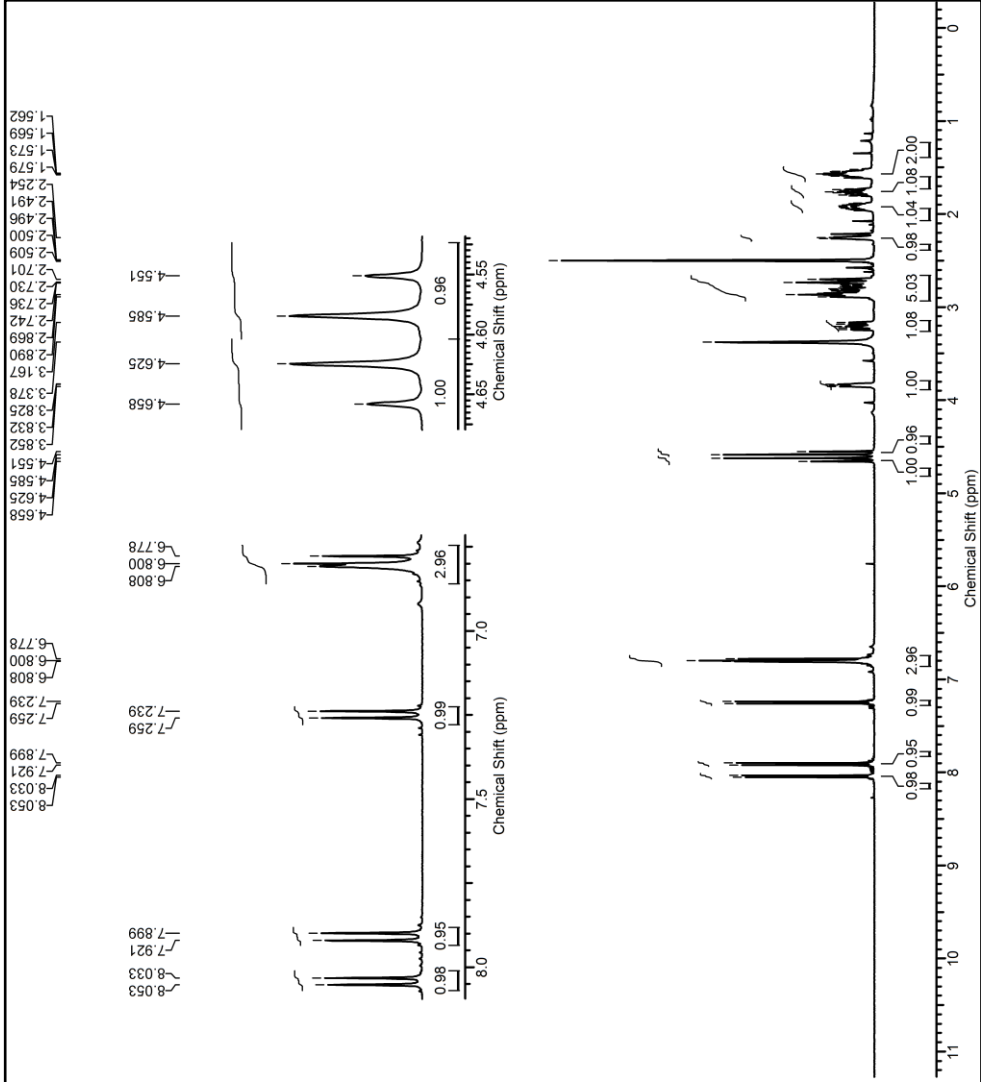








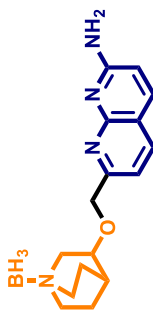





File Name S3CH2B(v)/NH2
 Acquisition Time (sec) 3.9584
 Date Stamp 08 Aug 2013 19:59
 Frequency (MHz) 400.13

Owner Administrator
 Solvent DMSO-d6
 Temperature (degree C) 20.160
 Nucleus 1H
 Points Count 32768
 Number of Transients 16
 Pulse Sequence zg30
 Spectrum Offset (Hz) 2467.9729
 Origin spect

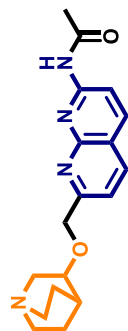
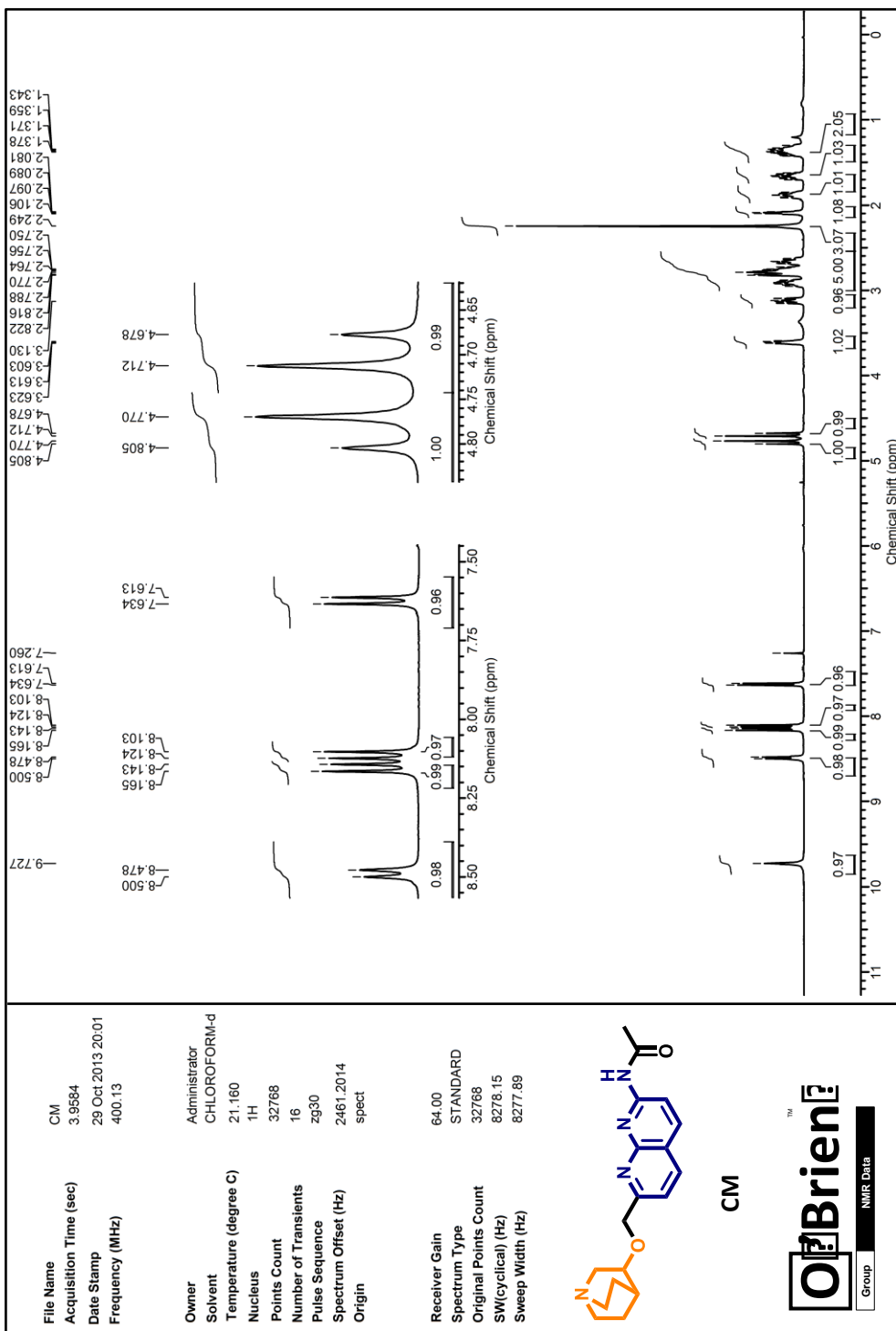
Receiver Gain 71.80
 Spectrum Type STANDARD
 Original Points Count 32768
 SW(cyclical) (Hz) 8278.15
 Sweep Width (Hz) 8277.89



123



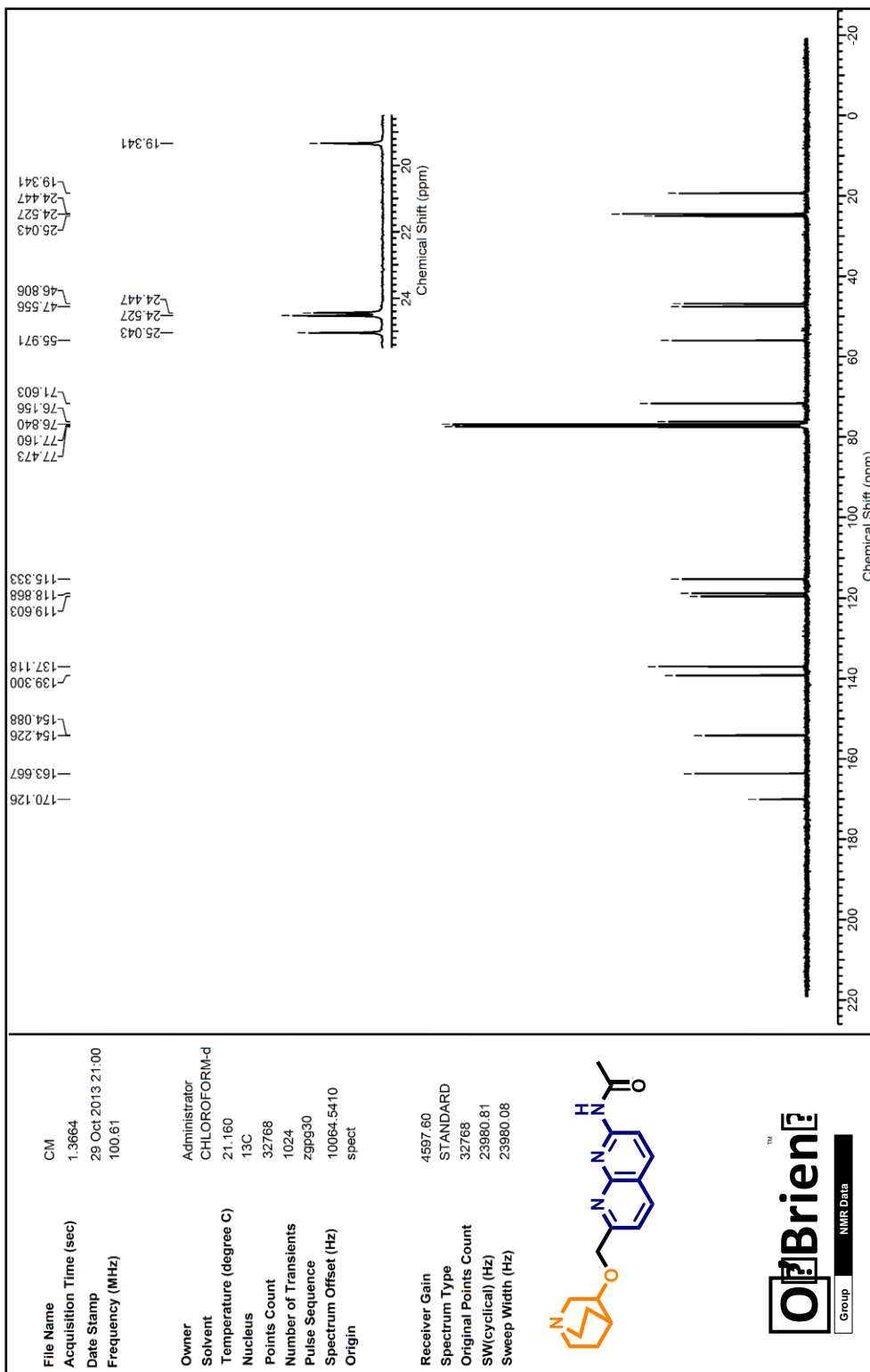
Group NMR Data

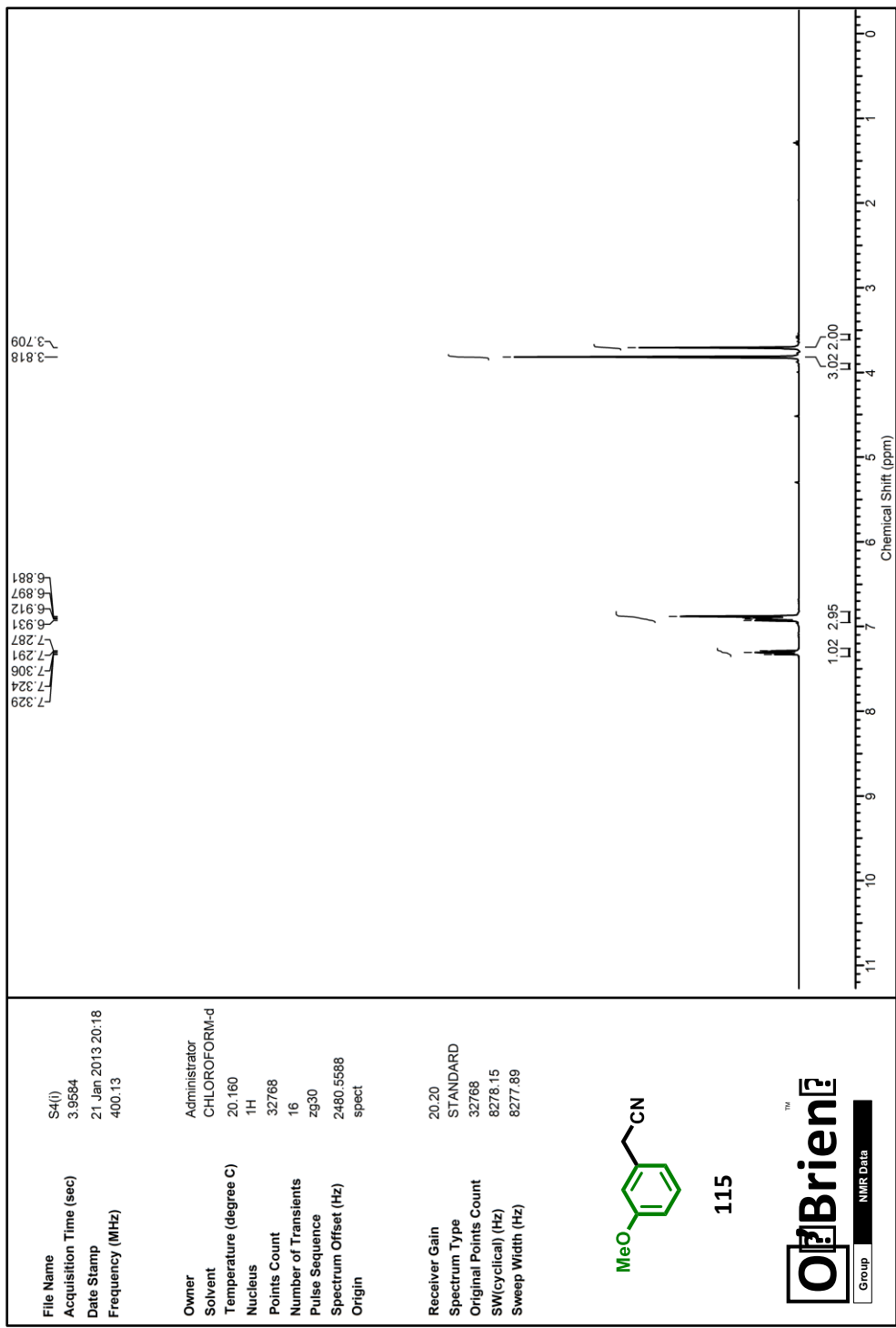


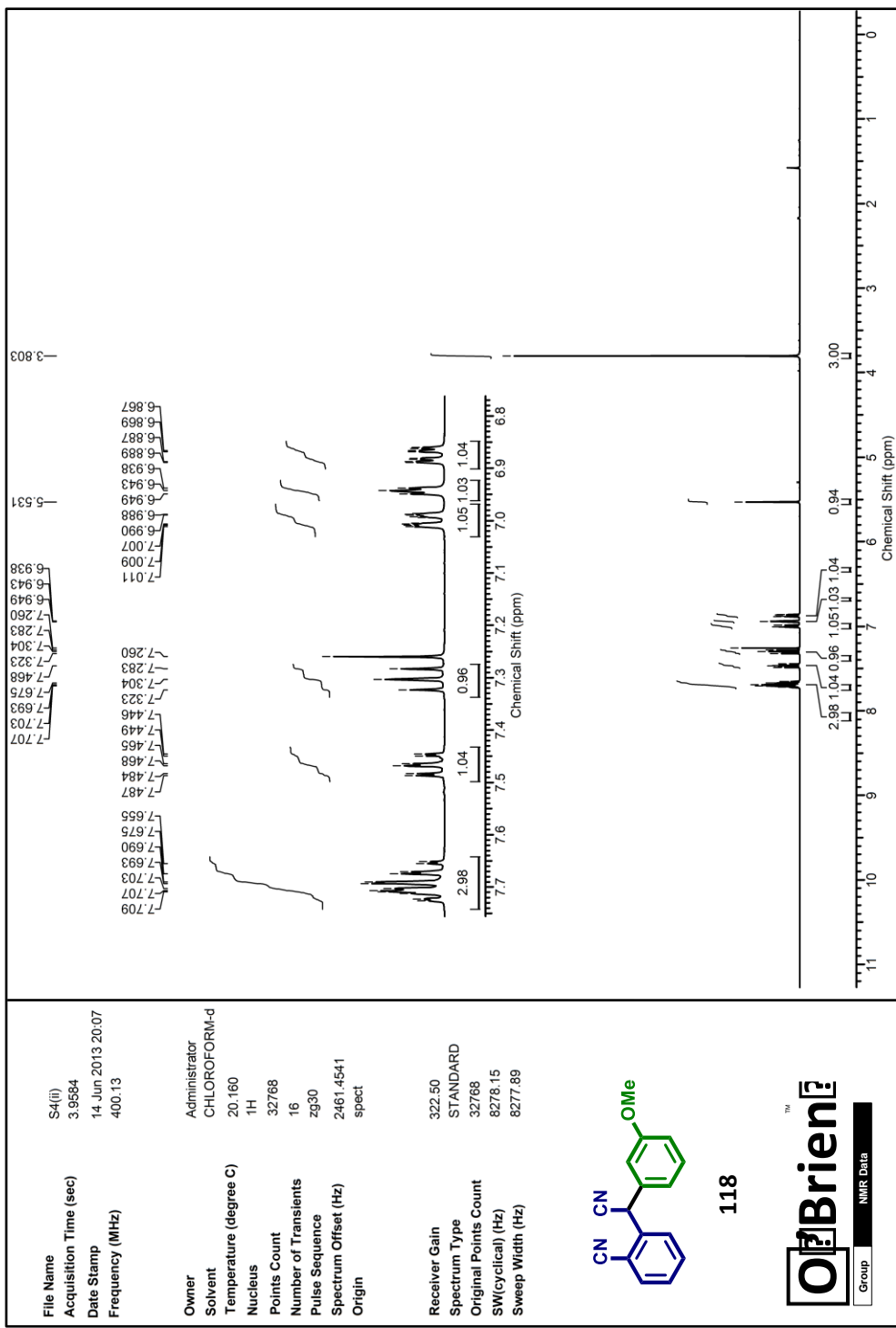
CM

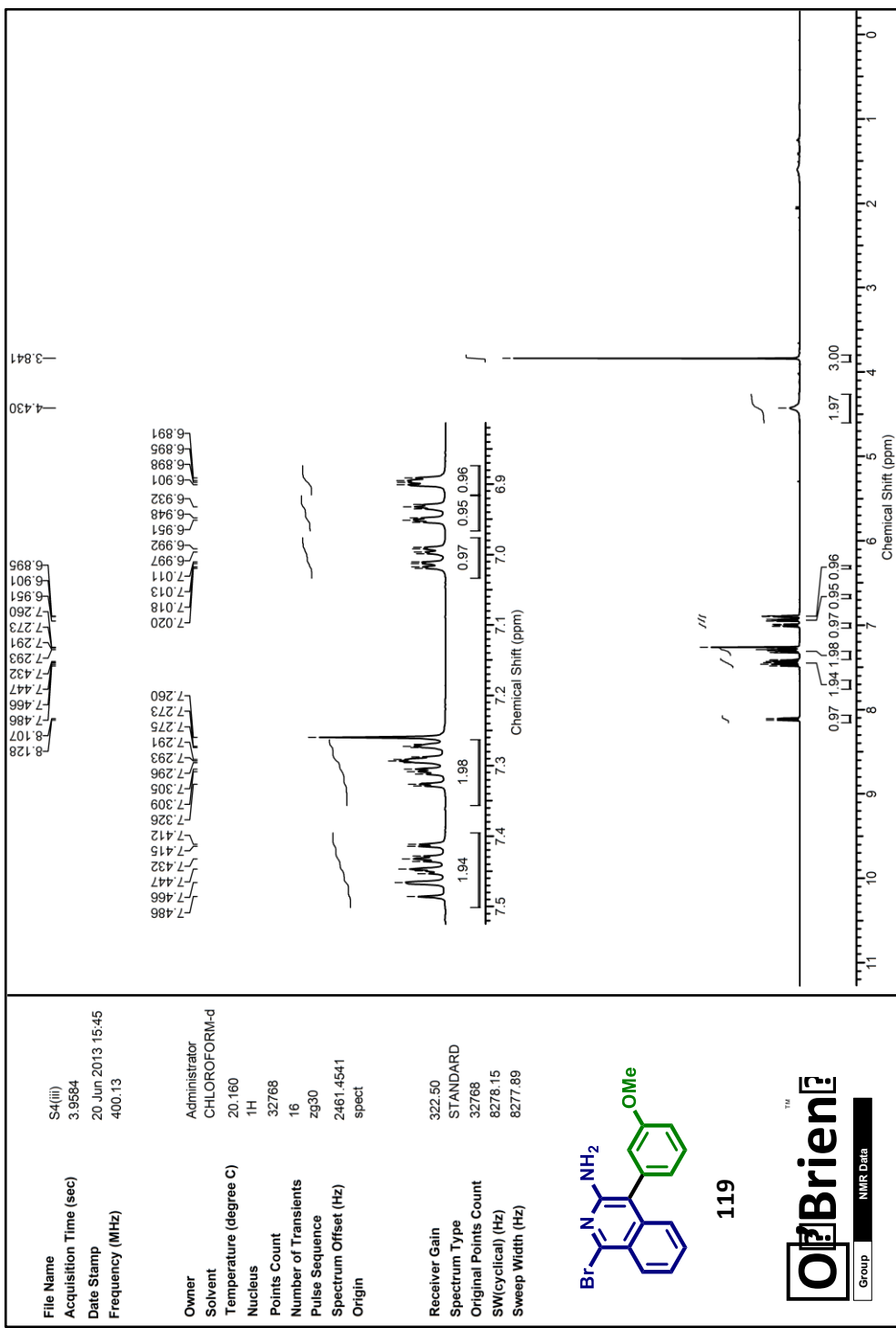
O'Brien

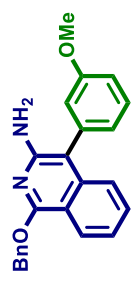
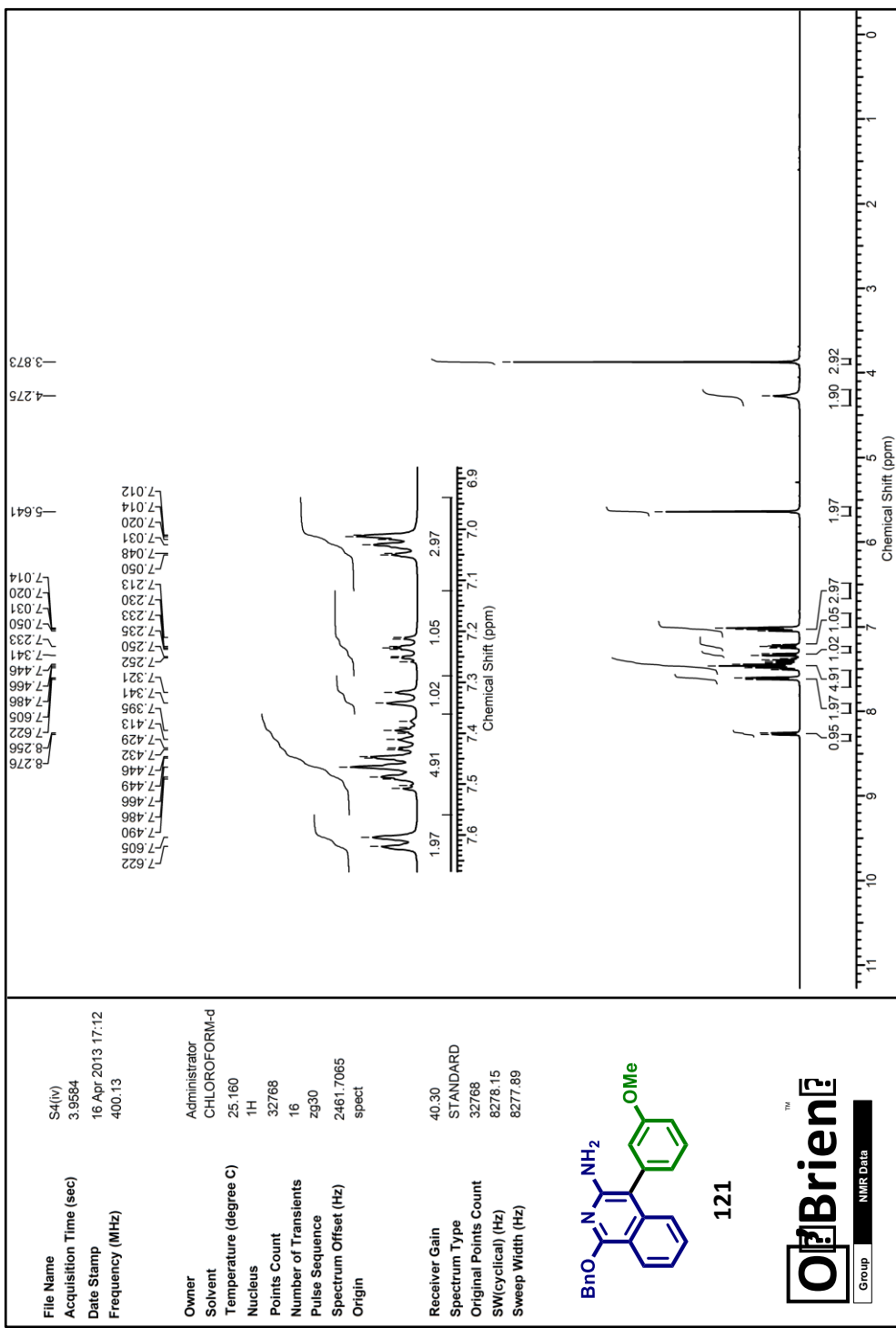
NMR Data

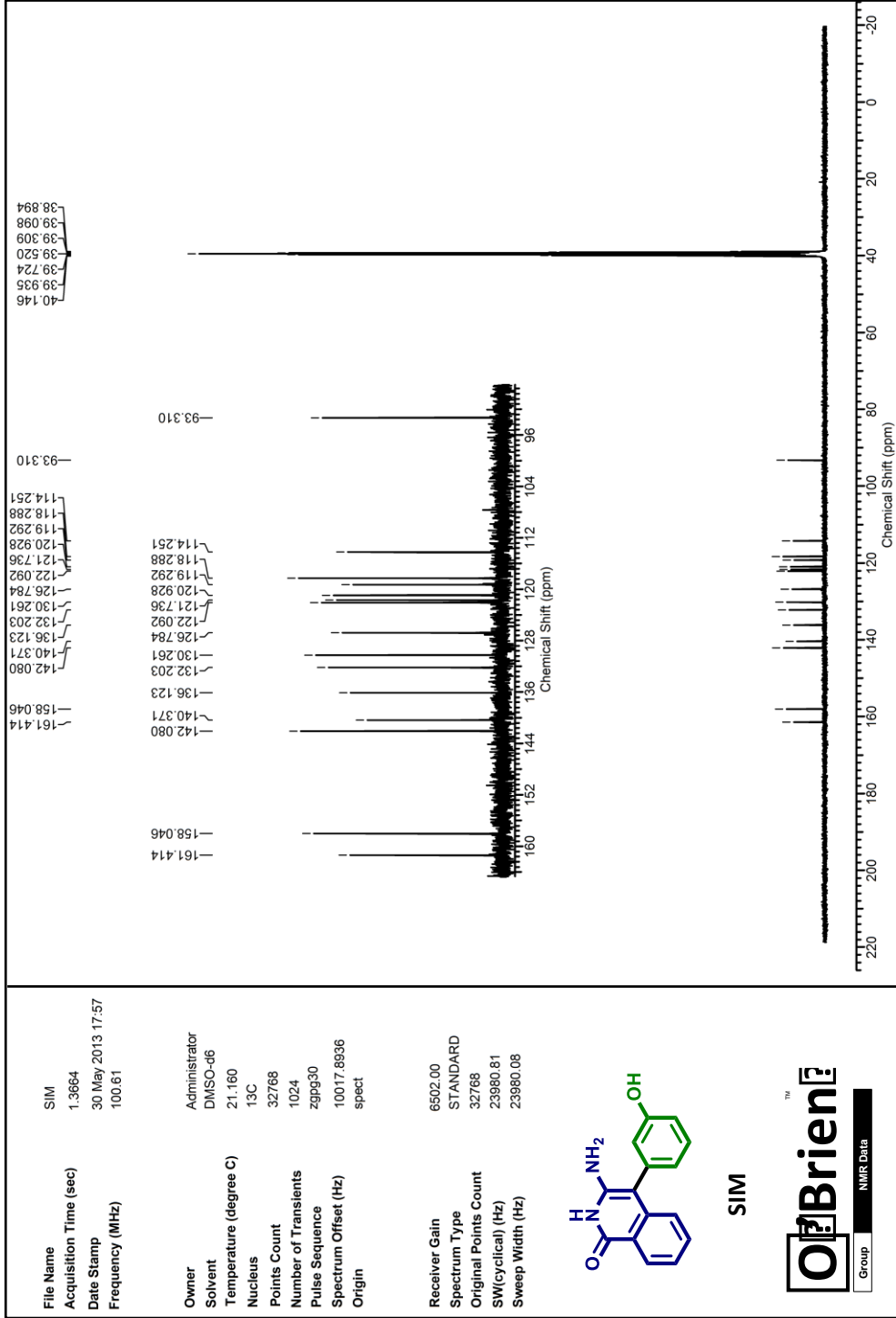


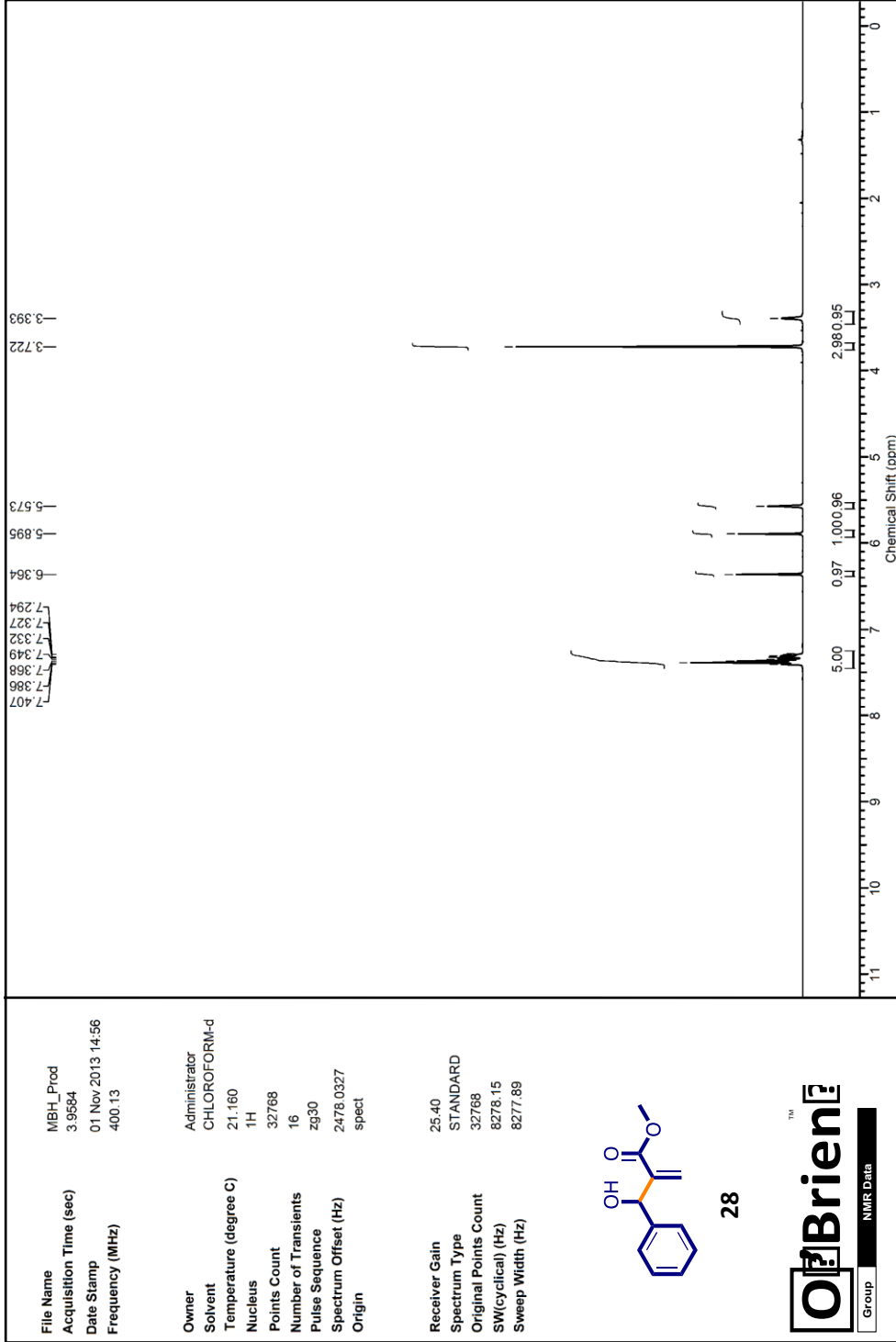












References (iii)

- [1] J. Leonard, B. Lygo and G. Procter, *Advanced Practical Organic Chemistry*, Blackie Academic & Professional: Oxford, **1995**.
- [2] L. Varadi, M. Gray, P. W. Groundwater, A. J. Hall, A. L. James, S. Orega, J. D. Perry, R. J. Anderson *Organic & Biomolecular Chemistry* **2012**, *10*, 2578-2589.
- [3] S. Goswami, R. Mukherjee, R. Mukherjee, S. Jana, A. C. Maity, A. K. Adak *Molecules* **2005**, *10*, 929-936.
- [4] T. R. Kelly, G. J. Bridger, C. Zhao *J. Am. Chem. Soc.* **1990**, *112*, 8024-8034.
- [5] B. G. Avitabile, H. Finch, J. D. Knight, A. J. Nadin, N. C. Ray *Argenta Discovery Ltd.*
- [6] L. Pignataro, M. Boghi, M. Civera, S. Carboni, U. Piarulli, C. Gennari *Chemistry-a European Journal* **2012**, *18*, 1383-1400.
- [7] Y. Wan, W. Niu, W. J. Behof, Y. Wang, P. Boyle, C. B. Gorman *Tetrahedron* **2009**, *65*, 4293-4297.
- [8] J. P. Parrish, D. B. Kastrinsky, I. Hwang, D. L. Boger *J. Org. Chem.* **2003**, *68*, 8984-8990.
- [9] Y. Akbaba, H. T. Balaydin, S. Goksu, E. Sahin, A. Menzek *Helv. Chim. Acta* **2010**, *93*, 1127-1135.
- [10] V. K. Aggarwal, I. Emme, S. Y. Fulford *J. Org. Chem.* **2003**, *68*, 692-700.